# AN ELECTRON SPIN RESONANCE STUDY OF RADICALS FORMED BY HIGH ENERGY IRRADIATION OF K<sub>2</sub>PdC1<sub>4</sub> AND K<sub>2</sub>PtC1<sub>4</sub>

THESIS FOR THE DEGREE OF PH. D. MICHIGAN STATE UNIVERSITY

THOMAS MICHAEL KRIGAS 1 9 7 1





## This is to certify that the

#### thesis entitled

An Electron Spin Resonance Study of Radicals formed by High Energy Irradiation of  ${\rm K_2PdCl_4}$  and  ${\rm K_2PtCl_4}$ 

presented by

THOMAS MICHAEL KRIGAS

has been accepted towards fulfillment of the requirements for

Ph.D. degree in Chemistry

Major professor

Date Nov. 12, 1971

O-7639

SEP 0 2 1997.

**ABSTRACT** 

6-11. 7

AN ELECTRON SPIN RESONANCE STUDY OF RADICALS FORMED BY HIGH ENERGY IRRADIATION OF K2PdCl4 and K2PtCl4

By

#### Thomas Michael Krigas

All known square-planar complexes of Pt (II) and Pd (II) are diamagnetic with  $d^8$  electron configurations and therefore cannot be studied by electron spin resonance spectroscopy. In this work serveral new paramagnetic species have been produced by high-energy irradiation of solid diamagnetic compounds to give Pt and Pd containing radicals in which one-electron oxidation or reduction has occurred. The structures of these new species have been obtained from electron spin resonance studies. The X-band electron spin resonance spectra of single crystals of  $K_2PdCl_4$  and  $K_2PtCl_4$  that were irradiated by  $\gamma$ -rays from a  $^{60}Co$  source or by 1-MeV electrons have been studied at temperatures between  $^{77}CK$  and  $^{296}CK$  with the primary purpose of elucidating the structure and bonding in species showing unusual oxidation states of palladium and platinum.

Irradiation of  $K_2Pd(II)Cl_4$  produces two identifiable paramagnetic radicals: one is shown to be  $(Pd(I)Cl_4)^{3-}$  with a  $4d^9$  electron configuration and the unpaired electron in a  $d_{x^2-y^2}$  orbital; the second radical is believed to be  $(Pd(III)Cl_5)^{2-}$  with the unpaired electron in a  $4d_{z^2}$  platinum atomic orbital.

Crystals of K<sub>2</sub>Pt(II)Cl<sub>4</sub> irradiated at 77°K show two groups of electron spin resonance lines: one belongs to a radical that shows hyperfine interaction with two equivalent platinum nuclei; the second arises from a radical showing hyperfine interaction with one platinum and three chlorine nuclei. It is suggested that these species are {(Pt(II)Cl<sub>4</sub>)(Pt(III)Cl<sub>4</sub>))<sup>3-</sup> and (Pt(I)Cl<sub>3</sub>)<sup>2-</sup>, respectively, where the metal electron configurations are 5d<sup>15</sup> and 5d<sup>9</sup>. On warming to 125°K some of the dimeric radical is converted to a new species whose spectra are consistent with those predicted for (Pt(III)Cl<sub>5</sub>)<sup>2-</sup>.

Thus, each identifiable radical contains platinum or palladium in which the original diamagnetic, low spin,  $d^8$  configuration of the metal ion M(II) (M=Pt or Pd) has been oxidized or reduced to form paramagnetic species with the metal in the unusual oxidation states M(III) or M(I). Energy level schemes for each radical are proposed based upon the electron spin resonance spectra. The nature of the metal-chlorine bonds in the new species is discussed and the extent of covalency is estimated by using a simplified molecular orbital picture.

## AN ELECTRON SPIN RESONANCE STUDY OF RADICALS FORMED BY HIGH ENERGY IRRADIATION OF K2PdCl4 and K2PtCl4

Ву

Thomas Michael Krigas

#### A THESIS

Submitted to
Michigan State University
in partial fulfillment of the requirements
for the degree of

DOCTOR OF PHILOSOPHY

Department of Chemistry

To My Wife Mary Susan Krigas

#### **ACKNOWLEDGMENTS**

To Professor Max T. Rogers under whose guidance this investigation was conducted, I wish to express my appreciation for his continued interest, counsel and assistance.

I wish to express my gratitude to Amoco Chemicals Corporation and the United States Army for their financial support of this study.

I want to thank Professor Barnett Rosenberg of the Biophysics

Department of Michigan State University for his interest and encouragement both scientifically and personally.

Of the many colleagues who have helped me in experimental and conceptual problems I want particularly to thank Professor H. A. Kuska of the University of Akron, Professor P. T. Manoharan of the Indian Institute of Technology, Kanpur, India, and Dr. V. A. Nicely of Eastman Kodak.

## TABLE OF CONTENTS

Page
INTRODUCTION
HISTORICAL
ESR Literature Reviews
ESR Studies of Platinum and Palladium Species · · · · · · ·
THEORETICAL
Introduction
Spin-Orbit Coupling
g Values
Angular Variation of the g Value • • • • • • • • • 1
Zeeman Effect
Sign of the g Shift · · · · · · · · · · · · · · · · · · ·
Sample g-Value Calculation
Hyperfine Interactions
Introduction
The Hyperfine Hamiltonian
Isotropic Hyperfine Interaction
Analysis of Metal Hyperfine Interactions
Covalency from Metal Hyperfine Splittings
Angular Variation of the Hyperfine Splitting 4
Sign of the Hyperfine Splitting
Ligand Hyperfine Interaction
Sample Calculation

																Page
EXPERIM	ENTAL		•	•		•	•	•	•	•	•	•	•	•	•	59
ESR	System		•	•		•	•	•	•	•	•	•	•	•	•	59
Samp	le Preparation		•	•		•	•	•	•	•	•	•	•	•	•	60
Crys	tal Structure of K2(Pd,Pt	)C1,	4 •	•		•		•	•	•	•	•	•	•		60
Irra	diation Methods		•	•		•	•	•	•	•	•	•	•	•	•	61
Samp	le Handling		•	•		•	•	•	•	•	•	•	•	•	•	63
Erro	r Analysis		•	•		•		•	•	•	•	•	•	•	•	64
RESULTS			•	•			•	•	•	•	•	•	•	•	•	67
K <sub>2</sub> Pt	C1 <sub>4</sub>		•	•		•	•	•	•	•	•	•	•	•	•	67
	Introduction		•	•		•	•	•	•	•	•	•	•	•	•	67
	(Pt <sub>2</sub> ) Radical		•	•		•	•	•	•	•	•	•	•	•	•	69
	UV-Photobleach Experiment		•	•		•	•	•	•	•	•	•	•	•	•	72
	(PtCl) Radical		•	•		•	•	•	•	•	•	•	•	•	•	76
	(PtCl <sub>3</sub> ) <sup>n-</sup> Radical		•	•		•	•	•	•	•	•	•	•	•	•	77
K <sub>2</sub> Pd	Cl <sub>4</sub> and (NH <sub>4</sub> ) <sub>2</sub> PdCl <sub>4</sub>		•	•			•	•	•	•	•	•	•	•	•	79
	Introduction			•			•	•	•	•		•	•	•	•	79
	Radical I			•	•		•	•	•	•	•	•	•	•	•	79
	Radical II		•	•	•		•	•	•	•	•	•	•	•	•	86
(N (C	2H5)4)2Pt2Br6		•		•		•	•	•	•	•	•	•	•	•	89
K <sub>2</sub> Pt	(CN)4.3H <sub>2</sub> O, (Pt(NH <sub>3</sub> )4)Cl <sub>2</sub>	and	K	(Pt	(NF	13)(	C1 <sub>3</sub>	3) (	н <sub>2</sub>	0	•	•		•	•	90
K <sub>2</sub> Pt	Br <sub>4</sub> , K <sub>2</sub> PdBr <sub>4</sub> and K <sub>2</sub> PtCl <sub>6</sub>	• •		•	•		•	•	•	•	•	•	•	•	•	90
DISCUSSI	ON		•	•	•		•	•		•	•	•	•	•	•	93
K <sub>2</sub> Pt	214	• •		•			•	•	•	•	•	•	•	•	•	93
	(Pt <sub>2</sub> ) Radical	• •	•	•	•		•	•	•	•	•	•	•	•	•	93
	g Values			•			•	•	•	•		•	•	•	•	93
	Pt Hyperfine Interacti	.on	•		•		•	•	•		•	•	•	•	•	98
	Linewidths				_								_			101

													Page
Structure	•	•	•	•		•	•	•	•		•	•	102
(PtCl) Radical	•		•			•	•	•	•	•	•	•	103
g and $A(^{195}Pt)$ Values	•		•			•	•	•	•			•	103
Chlorine Hyperfine Interaction	•		•	•	•	•		•	•	•	•	•	106
$(PtCl_3)^{n-}$ Radical $\cdots$	•	•	•	•	•	•		•	•	•	•	•	108
Reaction Scheme	•			•	•	•	•	•	•	•	•	•	109
$K_2$ PdC1 <sub>4</sub> · · · · · · · · · · · · · · · · · · ·	•	•	•	•	•	•	•	•	•	•	•		110
Radical I	•	•	•	•	•		•	•	•	•	•	•	110
g Values	•	•	•	•	•		•	•	•	•	•	•	110
Pd Hyperfine Interaction	•	•	•	•	•	•	•	•	•	•	•	•	110
Chlorine Hyperfine Interaction	•	•	•	•	•	•	•	•	•	•	•	•	111
Radical II	•	•	•	•	•	•	•	•	•	•	•	•	115
Reaction Scheme	•	•	•	•	•	•	•	•	•	•	•	•	116
SUMMARY	•	•	•	•	•	•	•	•	•	•	•	•	118
BIBLIOGRAPHY												•	121

## LIST OF TABLES

Table		Page
1.	g Values calculated from crystal-field theory	29
2.	Hyperfine interactions (A) calculated by the theory of Abragam and Pryce	40
3.	Comparison of calculated and experimental parameters for $(NiF_6)^{4-}$	52
4.	Representations and ESR intensities for the $(PtCl_4)_2^{3-}$ ion .	73
5.	ESR spectral parameters of radicals in irradiated crystals of $K_2PtCl_4$	74
6.	Principal values of the spin-Hamiltonian tensors of radicals in $\gamma$ -irradiated K <sub>2</sub> PdCl <sub>4</sub> and (NH <sub>4</sub> ) <sub>2</sub> PdCl <sub>4</sub>	84
7.	Calculated g Values for (Pt <sub>2</sub> )	95
8.	Hyperfine interaction parameters for platinum species by spin-unrestricted Hartree-Fock calculations	100
9.	Hyperfine fields at the nucleus $(H_n = -\kappa/2_{g_n\beta_n})$ in various platinum species	100
10.	Axial ligand spin densities	107
11.	Isotropic hyperfine fields and covalency parameters for palladium complexes	112
12.	Ligand spin densities in some σ-bonded d <sup>9</sup> square-planar complexes	115

## LIST OF FIGURES

Figure		Page
1.	Possible ordering of the five d orbitals in an octahedral field with an axially elongated tetragonal distortion increasing from A to C	9
2.	Axis system for metal $(X,Y,Z)$ and ligand $(x,y,z)$ atoms in $(PdCl_4)^{3-}$	54
3.	Crystal structure of K <sub>2</sub> PdCl <sub>4</sub> and K <sub>2</sub> PtCl <sub>4</sub> · · · · · · · ·	62
4.	The first-derivative X-band ESR spectrum of irradiated single crystals of $K_2PtCl_4$ at $77^{\circ}K$ with $H \mid   a \cdot \cdot$	68
5.	The first-derivative X-band ESR spectra of $(PtCl_5)^{2-}$ : (a) with $H \mid  c$ , (b) with $H \mid  a  \cdot \cdot$	70
6.	The first-derivative X-band spectra of $(PtCl_4)_2^{3-}$ in irradiated single crystals of $K_2PtCl_4$ : (a) with $H \mid c$ , (b) with $H \mid c$ . The feature marked X in (a) is centered at $g \approx 2.000$ and is from an unidentified species $\cdot \cdot \cdot \cdot \cdot$	71
7.	A plot of $(1/I-1/I_0)$ versus time for the photobleaching decay of $(PtCl_4)_2^{3-}$ indicates that the decay is second order in $(PtCl_4)_2^{3-}$ concentration $\cdots \cdots \cdots$	75
8.	The X-band spectra of $(PtCl_3)^{2-}$ : (a) first-derivative, $H \mid  c$ , (b) second-derivative, $H \mid (110)$ , (c) second-derivative, $H \mid  a $	78
9.	The first-derivative X-band ESR spectrum of irradiated $K_2PdCl_4$ at $77^OK$ with $H \mid \mid c$	80
10.	The X-band ESR spectra of irradiated single crystals of $K_2PdCl_4$ showing the lines from the $(PdCl_4)^{3-}$ radical ion: (top) second-derivative spectrum with $H_1 _C$ , (center) first-derivative spectrum with $H_1 _A$ , (bottom) second-derivative spectrum with $H_1 _A$ , (110)	81
11.	A plot of $\log(I/I_0)$ versus $10^3/T(^0K)$ for the $(PdCl_4)^{3-}$ radical shows two linear portions which implies two modes of decay	85

Figure		Page
12.	(a) First-derivative X-band spectrum of a single crystal of $K_2PdC1_4$ irradiated and observed at $77^{\circ}K$ with $H \mid c$ , (b) angular variation of g when the magnetic field is in the ac plane, (c) angular variation of $A(^{35}C1)$ when the magnetic field is in the ac plane. The solid curves of (b) and (c) were calculated with the parameters of Table 6	. 88
13.	The first-derivative X-band ESR spectrum of -CHCH3 in $(N(C_2H_5)_4)_2Pt_2Br_6$ at $77^0K$	. 91
14.	Possible molecular orbital energy level scheme for (PtCl <sub>4</sub> ) <sub>2</sub> <sup>3-</sup> (d orbitals only)	. 97

#### INTRODUCTION

Electron spin resonance (ESR) studies of transition metal complexes permit the identification of the paramagnetic species and provide information concerning their ground-state electronic structures and symmetries. 1 Complexes of the first-row transition metal ions in cubic, octahedral and tetrahedral crystal fields have been extensively investigated. 2 Recent work has been increasingly directed toward less common oxidation states and crystal-field symmetries and toward problems involving second- and third-row transition metal ions. 3-5 Many paramagnetic metal ions exist only as transient species and therefore are difficult to study by ESR. Thus, the stable oxidation states of platinum and palladium are diamagnetic, M(II) and M(IV), having  $\mathbf{d}^8$  and  $\mathbf{d}^6$ electronic configurations, respectively, whereas the unusual paramagnetic oxidation states of M(I) and M(III) with  $d^9$  and  $d^7$  configurations, respectively are unstable transient species. It has recently been shown that high-energy irradiation of solid materials provides a method for obtaining such unusual species and that their stability in the solid state is often adequate to permit ESR study.6,7

In this thesis, single-crystal ESR studies of several  $d^7$  and  $d^9$  complexes of platinum and palladium are reported. These species were produced by high-energy irradiation of the stable,  $d^8$  configuration, square-planar, diamagnetic compounds  $K_2PdCl_4$ ,  $(NH_4)_2PdCl_4$  and  $K_2PtCl_4$  and have been identified from their spectra. The crystal-field symmetry,

coordination, and electronic structure of each species is discussed and compared with related transition metal complexes.

#### HISTORICAL

#### ESR Literature Reviews

The literature of ESR studies of transition metal complexes has been reviewed up to 1965 in the Ph. D. thesis of H. A. Kuska, and three subsequent reviews by Kuska and Rogers<sup>2,9,10</sup> have continued the coverage up to 1971. McGarvey has written a review of theory<sup>11</sup> and Konig has presented a useful general survey of the subject. 12

A number of books on ESR have appeared including introductory surveys by Baird and Bersohn<sup>13</sup>, McMillan<sup>14</sup> and Assenheim<sup>15</sup>; there is also an excellent textbook by Carrington and McLachlan.<sup>16</sup> Experimental methods including the design and construction of spectrometers are discussed in several monographs.<sup>17-19</sup> A more advanced text by Ayscough<sup>20</sup> and a review by O'Reilly and Anderson<sup>21</sup> give up-to-date general treatments of the theory and applications of ESR spectroscopy.

A comprehensive treatment of transition metal ESR by Abragam and Bleaney $^1$  is the standard reference work on the subject, but a shorter monograph by  $Orton^{22}$  is useful because of a number of examples of typical calculations. Ligand-field theory has been treated by Figgis $^{23}$  and Watanabe. $^{24}$ 

Both the "Annual Reviews of Physical Chemistry"<sup>25-28</sup> and the "Annual Reports of the Chemical Society"<sup>29,30</sup> provide coverage of recent literature as do the proceedings of current ESR symposia.<sup>31-35</sup> Specific

topics are reviewed from time to time in the "Advances in Magnetic Resonance" series.  $^{36}$ 

#### ESR Studies of Platinum and Palladium Species

Platinum (II) and palladium (II) complexes have played a prominent role in the development of coordination chemistry. For example, the first reported organometallic compound of a transition metal was isolated over one hundred and forty years ago by Zeise. In this salt,  $K(C_2H_4PtCl_3)$ , Pt is bonded to the ethylene  $\pi$  system by both  $\sigma$  and  $\pi$  bonds. The initial accounted for the existence of two forms ( $\alpha$  and  $\beta$ ) of  $Pt(NH_3)_2Cl_2$  by postulating that the four-coordinate Pt(II) complexes were planar species and that the  $\alpha$ - and  $\beta$ -forms were the transand cis-geometrical isomers, respectively, as has since been confirmed by X-ray crystallography. The trans-effect proposed by Tscherniaev in 1926 to rationalize the results of ligand substitution reactions in Pt(II) square-planar complexes was one of the first successful attempts to formulate an inorganic reaction mechanism.

Because of this interest in Pt(II) and Pd(II) complexes, a substantial effort has been made to determine the d-orbital energy level schemes in these square-planar compounds from optical spectroscopy and by theoretical calculations. The generally accepted d-orbital sequences in  $K_2PtCl_4$  and  $K_2Pt(CN)_4$  are, in order of increasing energy,  $z^2$  xz, yz, xy,  $z^2-y^2$  for the chloride and xy, xz, yz,  $z^2$ ,  $z^2-y^2$  for the cyanide salt.

ESR provides another tool for determining the relative ordering of the d-orbital levels and at the same time provides information about

the electron spin density distribution in the ground state. Paramagnetic  $\operatorname{Pt}^{3+}(\operatorname{d}^7)$  has been observed by ESR in single crystals of  $\operatorname{Al}_2O_3$ ,  $^{45}$ ,  $^{46}$  yttrium aluminum garnet (YAIG),  $^{47}$  and  $\operatorname{BaTiO}_3$ . In each case the platinum had inadvertently been leached out of the platinum crucibles used to grow the host lattices by the high-temperature flux technique. In all three lattices, the oxygen atoms form a distorted octahedron around the metal rather than a square-planar arrangement. ESR signals centered at  $\operatorname{g}^2 2.000$  have been reported from palladium-doped silicon  $^{49}$  and palladium-doped KCl crystals  $^{50}$  but the paramagnetic species are not well defined.

The paramagnetic square-planar bis-maleonitriledithiolene (mnt) anion complexes  $^{51}$  (Pt(mnt)<sub>2</sub>)  $^{1-}$  and (Pd(mnt)<sub>2</sub>)  $^{1-}$ , and the related bischelate anion complexes (PtS<sub>4</sub>C<sub>4</sub>(CF<sub>3</sub>)<sub>4</sub>)  $^{1-}$  and (PdS<sub>4</sub>C<sub>4</sub>(CF<sub>3</sub>)<sub>4</sub>)  $^{1-}$ , have also been investigated by ESR. There has been a considerable controversy over the interpretation of the ESR and other data for these complexes,  $^{52}$  but they probably are reasonably well represented as  $^{7}$  Pt(III) and Pd(III) species, in view of the magnitude of the  $^{33}$ S ligand hyperfine interaction observed in the nickel analog,  $^{53}$  rather than as  $^{48}$ , metal-stabilized, ligand-radical systems.  $^{54}$ 

By irradiation of diamagnetic Pt and Pd compounds with  $\gamma$ -rays or high-energy electrons it should be possible to produce new M(I) and M(III) square-planar complexes in which the metal ion (M) has been reduced to a d<sup>9</sup>, or oxidized to a d<sup>7</sup>, electron configuration. Indeed, Pd(I) has apparently been produced by X-irradiation of palladium-doped powders of MgO and CaO, <sup>55</sup> and recently (Pd(I)(acac)<sub>2</sub>) <sup>1-</sup> has been detected by ESR in  $\gamma$ -irradiated palladium acetylacetonate. <sup>56</sup>

The effects of high-energy irradiation are of three main types: changes in valency, changes in the point group symmetry of the species,

and bond breaking. In a classic paper on the effects of radiation on transition metal ions substituted in LiF, NaF or KMgF3, Hall et. al. 6 noted that X-rays changed  $Fe^{2+}(d^6)$  into  $Fe^{3+}(d^5)$  and  $Fe^{1+}(d^7)$ , and in a similar manner  $Ni^{2+}(d^8)$  was converted to  $Ni^{3+}(d^7)$  and  $Ni^{1+}(d^9)$ . The scope of the irradiation method is evident in the ESR study of X-ray irradiated single crystals of  $K_3Co(CN)_6$ . Since the original  $Co^{3+}(d^6)$  ion is reduced to  $Co^{2+}(d^7)$  while one of the cyanide-metal bonds is ruptured, thereby dropping the point group symmetry of the anion from octahedral,  $O_h$ , to tetragonal,  $C_{4v}$ , all three major effects are seen in one problem.

No  $d^7$  or  $d^9$  platinum or palladium complexes showing ligand hyperfine interaction in the ESR spectra have been reported; irradiation of  $K_2PtCl_4$  and  $K_2PdCl_4$  accordingly was undertaken in an attempt to produce such species in a form sufficiently stable for study by ESR. This thesis is concerned with reporting the results of these experiments including identification of the products, a discussion of the energy levels and bonding in each new species, and some speculations on the nature of the reactions occurring.

#### THEORETICAL

#### Introduction

The solution of the many-electron problem associated with transition metal complexes has not been found exactly. Most of the important attempts to make non-empirical calculations of the eigenvalues, eigenfunctions and physical observables for a transition metal complex have centered on the  $(\text{NiF}_6)^{4-}$  cluster in  $\text{KNiF}_3^{57-59}$ , because this ion is known to have octahedral symmetry, its optical spectrum has been assigned and the fluorine hyperfine splitting has been observed by nuclear magnetic resonance  $(\text{NMR})^{61}$  and ESR.62

Most of the remaining ESR experiments on metal complexes have been interpreted by the spin-Hamiltonian method of Abragam and Pryce.  $^{63}$  In this method a phenomenological Hamiltonian is developed that is restricted to terms containing the electronic-spin and nuclear-spin operators  $\overline{S}$  and  $\overline{I}$ , respectively, which arise in a power series of the form

$$H = \sum_{n=0}^{\infty} \sum_{m=0}^{\infty} a_{nm} (\overline{S})^n (\overline{I})^m$$
 (1)

where n and m are integers. Equation (1) permits the experimentalist to interpret ESR spectra in a relatively straightforward manner. At the same time, Abragam and Pryce have shown how to estimate the coefficients

 $a_{nm}$  (usually tensor quantities) in terms of basic physical interactions such as the crystalline electric field, spin-orbit coupling, Zeeman energies, nuclear hyperfine splittings and quadrupole interactions. The basis of the calculation is to reduce the total Hamiltonian into segments according to the energy associated with each segment. Then, a sequential series of perturbations is performed in order of decreasing energy of the segments. Low<sup>64</sup> gives typical energy ranges for the specific interactions as: potential and kinetic energy  $\sim 10^5 \text{cm}^{-1}$ , spin-orbit coupling  $\sim 10^2 - 10^3 \text{cm}^{-1}$ , crystalline electric field  $\sim 10^2 - 10^4 \text{cm}^{-1}$ , electron spin-spin interaction  $\sim 1 \text{cm}^{-1}$ , nuclear hyperfine splitting  $\sim 10^{-1} - 10^{-3} \text{cm}^{-1}$  and nuclear quadrupole effects  $\sim 10^{-3} \text{cm}^{-1}$ .

In this thesis, the crystal-field approach<sup>65</sup> will be followed. The ligands will primarily establish the symmetry and magnitude of the electric field. However, the magnitude of the field will be treated as an adjustable parameter since the optical spectra of the radicals produced by irradiation were not measured. The crystal-field basis set will consist of the real metal 4d, and 5d atomic orbitals for Pd and Pt, respectively, neglecting the closed shells. The physical picture is that of a free metal ion perturbed by its nearest neighbors. Although this is only an approximation, the crystal-field technique has proven valuable in the past for determining the ground state electronic structures of paramagnetic species based upon their ESR spectra.<sup>3,6,7,66</sup>

The possible d-orbital energy level schemes in  $(PdCl_4)^{2-}$  and  $(PtCl_4)^{2-}$ , displayed in Figure 1, can be predicted by considering symmetry arguments. In a six-coordinate octahedral field, the five independent d orbitals split into a lower-energy triplet,  $t_{2g}$ , and a higher-energy doublet,  $e_g$ , where the doublet is composed of the  $d_z 2$  and

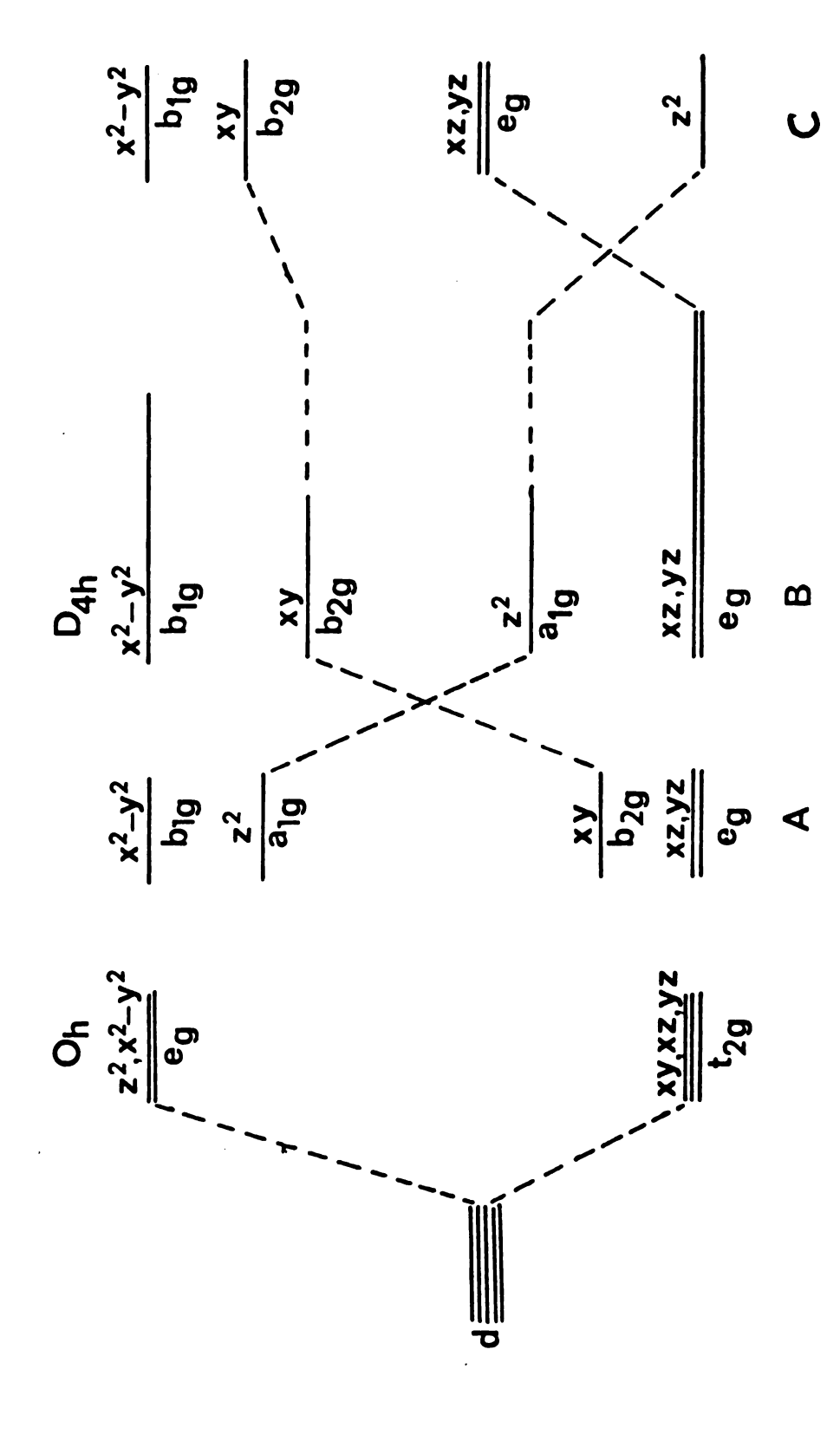


Figure 1. Possible ordering of the five d orbitals in an octahedral field with an axially elongated tetragonal distortion increasing from A to C.

 $d_{x}2_{-y}2$  orbitals whose electron density is directed at the ligands; therefore, the doublet is destabilized by electron repulsion relative to the triplet. As one mentally removes the two imaginary ions situated along the positive and negative z axis, the  $d_{z}2$  and  $d_{xz}$ ,  $d_{yz}$  orbitals are reduced in energy relative to  $d_{x}2_{-y}2$  and  $d_{xy}$ . The only point to be determined is to what extent  $d_{z}2$  and  $d_{xz}$ ,  $d_{yz}$  are stabilized. The three possibilities that result as this tetragonal field increases are shown as cases A, B and C in Figure 1. As was pointed out earlier, case C gives the correct energy-level ordering for the parent (PtCl<sub>4</sub>)<sup>2-</sup> and (PdCl<sub>4</sub>)<sup>2-</sup> ions.<sup>42</sup>

It seems probable that ESR investigations of the irradiated parent ions will usually only detect the paramagnetic species formed by a one-electron oxidation or reduction of the initial  $d^8$  configurations to produce  $d^7$  or  $d^9$ , respectively, since any other metal radicals would have to be created as a result of a less probable three-electron change. It is also expected that the strong crystal field in the Pt and Pd complexes will require that the radical species have  $S=\frac{1}{2}$ . Therefore, neglecting the small nuclear quadrupole and Zeeman terms, the spin-Hamiltonian that one would expect to apply is

$$H = \beta H \cdot \overline{g} \cdot \overline{S} + \overline{S} \cdot \overline{A}_{M} \cdot \overline{I}_{M} + \overline{S} \cdot \Sigma \overline{A}_{L} \cdot \overline{I}_{L}$$
(2)

where  $\beta$  is the electronic Bohr magneton, and the electronic Zeeman term is linear in both magnetic field and electron spin, while the electron-nuclear hyperfine interactions may be observed for both metal  $(\stackrel{=}{A_M})$  and ligand  $(\stackrel{=}{A_L})$  nuclei. Vector quantities are indicated by a single bar over the corresponding symbol while second-rank tensors are indicated by a double-bar overline throughout the thesis.

The remainder of the theoretical section will explore the crystal-field calculation of the g and  $A_M$  tensors consistent with either a  $d^7$  or  $d^9$  configuration and with the three possible axially-elongated tetragonal field energy levels of Figure 1. The ligand hyperfine interaction tensor,  $A_L$ , will be treated by the molecular orbital approach.

### Spin-Orbit Coupling

The metal ground state is subject to admixture of various excited states by spin-orbit coupling. The spin-orbit Hamiltonian is given by

$$H_{LS} = \sum_{i} \zeta_{i} \ell_{i} \cdot \bar{s}_{i}$$
 (3)

where  $\zeta_1$  is the one-electron spin-orbit coupling constant (always a positive quantity),  $\ell_1$  and  $s_1$  are the one-electron orbital and spin operators, respectively, and the sum is over the i valence electrons. The eigenfunctions of  $S^2$  and  $S_z$ , where S is the total spin of the system, are written as  $|nSm\rangle^{67}$  such that

$$S^{2}|nSm\rangle = S(S+1)|nSm\rangle$$

$$S_{z}|nSm\rangle = m|nSm\rangle$$
(4)

where m is the quantum number for the projection of S along z and n specifies information about the radial properties and the orbital angular momentum. The first-order energy correction to the ground state due to the spin-orbit coupling is

$$E_{LS} = \sum_{i} \langle OSm | \zeta_{i} \overline{\ell}_{i} \cdot \overline{s}_{i} | OSm \rangle \qquad (5)$$

where |OSm is the ground-state function prior to the spin-orbit interaction. The modified ground-state wavefunctions are

$$|\alpha OSm\rangle = |OSm\rangle + \sum_{n = m'} \sum_{i} \frac{\langle nS'm' | H_{LS} | OSm\rangle | nS'm'\rangle}{E_{O}-E_{n}}$$
 (6)

The second-order energy correction is of some considerable interest in the ESP of systems where S>1. One obtains

$$E^{2}_{LS} = \sum_{\substack{n \text{ m'i 1 1, k=x,y,z}}} \frac{\langle 0\text{Sm} | \zeta_{1}\ell_{11}\text{Si1} | n\text{S'm'} \rangle \langle n\text{S'm'} | \zeta_{1}\ell_{1k}\text{Sik} | 0\text{Sm} \rangle}{E_{0}-E_{n}}$$
(7)

which may be identified with the spin-Hamiltonian term

$$E^{2}_{LS} = \overline{S} \cdot \overline{\overline{D}} \cdot \overline{S} , \qquad (8)$$

that is, an expression, quadratic in spin, where D is a symmetric tensor. In the lower symmetry, strong crystal fields that often occur in the second— and third— row transition ion complexes, orbitally non-degenerate ground states are the rule. The electrons fill the metal orbitals with spins paired, but if there is an odd number of electrons the highest orbital will contain a single unpaired electron and the paramagnetic species will have S=1/2; thus, Equation (8) should not be needed in this thesis since D, the dipolar interaction between two unpaired electrons, is then zero.

For a centrosymmetric atom 68 the spin-orbit interaction is

$$\zeta (\mathbf{r_i}) \bar{l_i} \cdot \bar{s_i} = 2\beta^2 (\frac{1}{\mathbf{r_i}} \frac{\partial V_i}{\partial \mathbf{r_i}}) \bar{l_i} \cdot \bar{s_i}$$
 (9)

where  $V_i$  is the potential arising from the interaction of the i<sup>th</sup> electron motion with the nucleus and other electrons, and r is the interparticle distance. Although many of the common crystal fields are considerably lower in symmetry than spherical, the factor  $(\frac{1}{r_i}, \frac{\partial V_i}{\partial r_i})$  is proportional to  $Z/r_i^3$  and this latter term is large only in the region close to the nucleus where the field is nearly spherical and the simple form of Equation (3) can be used.

In complex ions the unpaired metal electrons can be found in the vicinity of the ligand nuclei, a fact confirmed by the observation of ligand hyperfine splittings. These splittings are one of the prime reasons that molecular orbital theory has been used to treat the bonding in transition metal complexes. <sup>69</sup> In this theory, molecular orbitals are constructed from metal atomic orbitals,  $|\phi_{\rm L}\rangle$ , and ligand group atomic orbitals,  $|\phi_{\rm L}\rangle$ , which transform in the same irreducible representation. The modified ground-state wavefunctions of Equation (6) will include terms having the following integrals <sup>70</sup>

$$\langle \phi_{L} | \zeta_{i} \overline{\ell}_{i} \cdot \overline{s}_{i} | \phi_{L} \rangle$$
. (10)

The  ${\rm Z/r}^3$  dependence of  $\zeta_1$  means that the ligand spin-orbit coupling constant must be used in the integrals of Equation (10). The net effect in a molecular orbital description is to introduce terms in the g value

that depend upon the ligand spin-orbit coupling constant, especially if  $\zeta_L \simeq \zeta_M$ . An extreme example of the ligand spin-orbit coupling influence on the g values can be found in the ESR study of  $(M(V)0X_5)^{2^-}$  where M=Cr, Mo and W and X=F, Cl and Br. When X is fluorine, g|| < g|, but when X is chlorine or bromine, g|| > g|. Manoharan and Rogers attribute the reversal in order of the g-tensor elements to the increased contribution of  $\zeta_L$  in the case of the heavier ligands. For the Pd and Pt radicals discussed in this thesis  $\zeta_M$  is considerably larger than  $\zeta_{C1} \simeq 550$  cm<sup>-1</sup> so neglect of the ligand contribution should not alter the relative order of the g-tensor elements.

In 1955 Owen<sup>72</sup> noted that  $\zeta_M$  for metal ions in complexes is approximately 20-30% less than the corresponding free-ion value. He ascribes the reduction in  $\zeta_M$  to the d-electron delocalization in the molecular orbitals since the  $Z/r^3$  dependence will be reduced as the electron orbital is expanded.

With  $\zeta_M \approx Z/r^3$  it is clear that a reduction in Z will also produce a reduction in  $\zeta_M$ . Murao<sup>73</sup> correctly predicted that charge donation by the ligand to the metal in the bonding molecular orbitals would lower the effective charge, Z, by partially screening the antibonding electrons from the nucleus. Such effects will be more important for the first members of a transition row because their  $\zeta_M$  values are more strongly dependent on charge. Thus the results of extended Hückel molecular orbital calculations<sup>69a</sup> carried to a self-consistent charge invariably show that substantial electron density is transferred from the ligands. As an example, a calculation of charge-transfer effects in  $(\text{CrO}_4)^{3-}$  indicates that the metal charge is closer to +2 than to the formal charge of +5.<sup>74</sup> In a similar manner, the two Hückel calculations of  $(\text{PtCl}_4)^{2-43}$  both

find that the platinum ion probably has a charge close to +1. In the absence of the correct value for the metal charge, it is difficult to decide which free-ion value of  $\zeta_M$  to use in ESR calculations.

Hazony  $^{75}$  has recently discussed the radial dependence of the 3d wave functions of iron complexes based upon Mössbauer and ESR experimental spectra. He concludes that the  $t_{2g}$  orbital triplet in octahedral symmetry undergoes radial expansion as the metal ion undergoes complex formation, whereas the  $e_g$  orbitals contract. Moreover, the degree of radial expansion or contraction is a dynamic property that depends upon the internuclear metal-ligand distance and the degree of covalency. As covalent bonding increases, the expansion of the  $t_{2g}$  orbitals becomes the dominant effect. In any event, the  $r^{-3}$  radial dependence of  $\zeta_M$  suggests that a somewhat different  $\zeta_M$  is appropriate for each separate type of d orbital in a complex.

It is common practice in the analysis of ESR data to take the free-ion value of  $\zeta_M$  corresponding to the formal oxidation state of the metal. In the case of the radicals produced in irradiated K<sub>2</sub>PdCl<sub>4</sub> and K<sub>2</sub>PtCl<sub>4</sub> one could use the free-ion  $\zeta$  values of 1416 cm<sup>-1</sup> and 3368 cm<sup>-1</sup> for Pd<sup>1+</sup> and Pt<sup>1+</sup>, respectively, since charge donation from the ligands will produce metal ions with approximate charges of +1. The above values of  $\zeta_M$  were calculated from the optical data compiled by Moore<sup>76</sup> and are based on the Russell-Saunders LS coupling scheme.<sup>69</sup> However, in this thesis  $\zeta_M$  will always appear in a perturbation coefficient of the form ( $\zeta/\Delta E$ ) where  $\Delta E$  is a d-d energy separation. Because the optical spectra of the radicals are unknown, and in view of the difficulties noted above in selecting  $\zeta$ , the ( $\zeta/\Delta E$ ) terms will be treated as adjustable parameters.

#### g Values

The spin energy of an electron with a magnetic moment,  $\bar{\mu}$ , in an external magnetic field,  $\bar{H}$ , is

$$E = -\mu \cdot H \qquad (11)$$

The fact that an electron has both spin and charge requires that the magnetic moment be proportional to the spin 16, ie.,

$$\overline{\mu} = -g\beta \overline{S} = -\gamma (h/2\pi) \overline{S} , \qquad (12)$$

where  $(h/2\pi)\overline{S}$  is the spin angular momentum,  $\beta$  is the electronic Bohr magneton ( $|e|h/4\pi mc$ ), e is the electronic charge, g is the spectroscopic splitting factor and the negative sign demonstrates that the negative charge of the electron causes the spin and magnetic moment to be oppositely directed. The quantum mechanical analogue of Equation (11), with the magnetic field in the z direction, is

$$H = g\beta H_z S_z . (13)$$

The eigenvalues of Equation (13) are

$$E = \langle S'm' | H_z | Sm \rangle = g\beta H_z m \delta_S' S \delta_m' m , \qquad (14)$$

where  $\delta_S'_S$  is the Kronecker delta;  $\delta_S'_S = 0$  if  $S' \neq S$  and  $\delta_S'_S = 1$  only if S' = S.

The resonance experiment is performed by inducing transitions between the energy states of Equation (14) by means of an oscillating microwave magnetic field which is usually oriented perpendicular to the applied static field. From time-dependent perturbation theory<sup>67</sup>, the transition probability for induced emission or absorption is proportional to the square of the matrix element of the magnetic dipole moment between the states of Equation (14). The perturbing Hamiltonian for the microwave field acting on the magnetic dipole is

$$H = -\mu_X H_X \cos \omega t , \qquad (15)$$

where t is the time and  $\omega$  is the oscillation frequency of the microwave field,  $H_X$ . If the value of  $\mu_X$  from Equation (12) is substituted into Equation (15), P, the transition probability, becomes

$$P \propto \left| \left\langle S'm' \mid g\beta H_{X} \cos \omega t \left( \frac{S++S_{-}}{2} \right) \mid Sm \right\rangle \right|^{2}$$
, (16)

where  $S_{\mathbf{X}}$  has been replaced by its equivalent ladder operator.<sup>67</sup> Then carrying out the indicated operations one obtains

$$P \propto \frac{g^2 \beta^2 H_X^2 \cos^2 \omega t}{4} \{ (S(S+1)-m(m+1)) \langle m' | m+1 \rangle + (S(S+1)-m(m-1)) \langle m' | m-1 \rangle \} .$$
(17)

Because the spin wavefunctions  $|Sm\rangle$  were chosen as an orthonormal set, one arrives at the ESR selection rule  $S' = S,m' = m\pm 1$ . Thus, magnetic resonance will be observed when the microwave frequency  $\nu$  is equal to the

energy separation between the m and the (m + 1) or (m - 1) states. The Bohr condition then gives

$$hv = E_{m\pm 1} - E_m = g\beta H$$
 . (18)

## Angular Variation of the g Value

In the most general situation the g value is a tensor quantity.

In the principal coordinate axis system of the g tensor, the magnetic dipole term becomes

$$H = \beta(g_{XX}H_{X}S_{X} + g_{YY}H_{Y}S_{Y} + g_{ZZ}H_{Z}S_{Z}) .$$
 (19)

The evaluation of the matrix elements of Equation (19) are facilitated by converting  $S_{\mathbf{x}}$  and  $S_{\mathbf{y}}$  into their corresponding ladder operators  $^{67}$  to give

$$H = \beta\{\frac{1}{2}(g_{xx}H_{x}-ig_{yy}H_{y}) S_{+} + \frac{1}{2}(g_{xx}H_{x}+ig_{yy}H_{y})S_{-} + g_{zz}H_{z}S_{z}\}$$
(20)

The secular determinant<sup>67</sup> for an S =  $\frac{1}{2}$  example where  $|m = \frac{1}{2}\rangle \equiv |\alpha\rangle$  and  $|m = -\frac{1}{2}\rangle \equiv |\beta\rangle$  is

$$|\alpha\rangle \qquad |\beta\rangle$$

$$|\alpha\rangle \qquad \frac{\beta g_{zz}H_{z}}{2} - E \qquad \frac{\beta}{2}(g_{xx}H_{x} - ig_{yy}H_{y})$$

$$|\beta\rangle \qquad \frac{\beta}{2}(g_{xx}H_{x} + ig_{yy}H_{y}) \qquad - \frac{\beta g_{zz}H_{z}}{2} - E$$

$$(21)$$

Solution of the secular determinant yields

$$E = \pm \beta/2 \left( g_{xx}^2 H_x^2 + g_{yy}^2 H_y^2 + g_{zz}^2 H_z^2 \right)^{\frac{1}{2}}$$
 (22)

If H is expressed in polar coordinates with respect to the principal g axes, then the magnetic resonance energy between the  $|\alpha\rangle$  and  $|\beta\rangle$  spin states is

$$\Delta E = g\beta H$$
 , (23)

where

$$g = (g_{xx}^2 \sin^2 \theta \cos^2 \phi + g_{yy}^2 \sin^2 \theta \sin^2 \phi + g_{zz}^2 \cos^2 \theta)^{\frac{1}{2}}$$
 (24)

Bleaney $^{77}$  has treated the angular variation problem in a slightly different fashion. Equation (20) can be written

$$H = (1_2S_+ + 1_3S_- + 1_1S_z) . (25)$$

It may be recognized that the spinor 78

$$\begin{pmatrix} 1_{1}S_{z} & 1_{2}S_{+} \\ 1_{3}S_{-} & -1_{1}S_{z} \end{pmatrix}$$
 (26)

is an Hermitian matrix operator whose coordinate axis system can be transformed by using a unitary matrix, Q, such that

$$\begin{pmatrix} 1_{1}'S_{z}' & 1_{2}'S_{+}' \\ 1_{3}'S_{-} & -1_{1}'S_{z}' \end{pmatrix} = Q \begin{pmatrix} 1_{1}S_{z} & 1_{2}S_{+} \\ 1_{3}S_{-} & -1_{1}S_{z} \end{pmatrix} Q^{\dagger}, \qquad (27)$$

where  $Q^{\dagger}$  is the adjoint of Q. Now the transformed matrix of Equation (27) is diagonalized along the magnetic field vector by forcing  $l_1' = l_2' = 0$ . The Hamiltonian of Equation (25) becomes

$$H = \beta H l_1' S_2' , \qquad (28)$$

where  $l_1$ ' is identified with g and has the same value as in Equation (24).

Even though this exercise seems redundant, it is important for two reasons: Bleaney's technique leads directly to the anisotropic transition probability<sup>79</sup> and, of greater interest, this same technique was employed by Bleaney<sup>77</sup> to find the angular variation of the hyperfine interaction tensor in the form of an analytical function.

#### Zeeman Effect

The Hamiltonian operator for the total electron magnetic dipole energy in a magnetic field is derived from the Dirac relativistic Hamiltonian.  $^{68}$  The crucial terms are

$$H = \frac{1}{2mc^2} \{e^2A^2 + 2ecA \cdot \bar{p} + 2e(h/2\pi)c\bar{\sigma} \cdot curl\bar{A}\}, \quad (29)$$

where  $mc^2$  is the electron rest energy, p is the linear momentum, A is the vector potential and  $\sigma_1$  (i = x,y,z), the components of  $\overline{\sigma}$ , are the Pauli spin matrices. The vector potential of a uniform, unidirectional external magnetic field is given by  $^{80}$ 

$$\bar{A} = -\frac{1}{2}\bar{r} \times \bar{H} \quad . \tag{30}$$

After substituting this relationship into Equation (29), the resulting expression can be simplified by vector identities to give

$$H = (eh/4\pi mc) \{ (-2\pi e/hc) (r^2 H - (\bar{r} \cdot H)\bar{r}) + \bar{\ell} + 2\bar{s} \} \cdot \bar{H} .$$
 (31)

The terms in the center brackets are the diamagnetic and paramagnetic moments induced by the external field and since they are quadratic in magnetic field strength, all of the states in the metal-ion ground term are shifted by an equal amount and, therefore, do not contribute to the spin Hamiltonian. The remaining expression is the familiar Zeeman Hamiltonian

$$H_{Z} = \beta(\bar{\ell} + 2\bar{s}) \cdot \bar{H} . \qquad (32)$$

Slichter<sup>81</sup> has shown that the orbital angular momentum is quenched for an orbitally non-degenerate ground state (orbital singlet). In other words, the expectation value of the orbital angular momentum over the ground state wavefunction,  $|\phi\rangle$ , is

$$\langle \phi | \ell_i | \phi \rangle = 0$$
 , (33)

where  $\ell_i$  is the x or y or z component of  $\overline{\ell}$ . When the resonance condition between the orbitally non-degenerate spin states  $|\alpha\rangle$  and  $|\beta\rangle$  is fulfilled one finds that

$$\Delta E = 2\beta H_z . (34)$$

Comparing this result with the basic ESR equation (Equation (23)) shows that g = 2. Indeed, most organic free radicals do exhibit g values very close to 2, whereas the g values of most paramagnetic transition metal complexes deviate substantially from 2. This fact is of paramount importance to this thesis because it will be shown that the magnitude and sign of the deviation of the g value from 2 allows one to make an assignment of the ground state wavefunction.

The goal of this section is to calculate the first-order Zeeman energies for an orbitally non-degenerate ground state using the spin-orbit augmented wavefunctions of Equation (6). Recalling the ESR selection rules  $\Delta S = 0$ ,  $\Delta m = \pm 1$ , it is obvious that one need only consider the matrix elements between the components of the ground state with different values of m. One then obtains

$$E_{z} = \langle \gamma OSm'' | H_{z} | \alpha OSm \rangle , \qquad (35)$$

which yields four terms, the first of which is

$$\sum_{k=x,y,z} \sum_{i} H_{k} \langle 0Sm'' | \ell_{ik} + 2s_{ik} | 0Sm \rangle .$$
 (36)

If Equation (36) is recast into operator form by suppressing the matrix elements of  $\mathbf{s_{ik}}$ , and remembering that the orbital angular momentum is quenched for an orbital singlet, the first term becomes

$$2\Sigma \quad \Sigma \quad H_k s_{ik}$$
 (37)  
 $k=x,y,z$  i

The second and third terms are equivalent and their sum is given by

$$2\beta\Sigma \Sigma \Sigma \Sigma \sum_{\mathbf{l},\mathbf{k}} \sum_{\mathbf{n}} \frac{\zeta_{\mathbf{i}\mathbf{1}}H_{\mathbf{k}}}{E_{\mathbf{o}}-E_{\mathbf{n}}} \left\langle \mathbf{n}S'\mathbf{m}'|\ell_{\mathbf{i}\mathbf{1}}s_{\mathbf{i}\mathbf{1}}|0Sm\right\rangle \left\langle 0Sm''|\ell_{\mathbf{i}\mathbf{k}} + 2s_{\mathbf{i}\mathbf{k}}|\mathbf{n}S'\mathbf{m}'\right\rangle . \tag{38}$$

Retaining terms to first degree in H and S, Equation (38) reduces to

$$2\beta \sum_{\substack{1,k \text{ n m'} i}} \sum_{\substack{i}} \frac{\zeta_{i1}^{H_k}}{\Delta E} \langle n | \ell_{i1} | 0 \rangle \langle S'm' | s_{i1} | Sm \rangle \langle OSm'' | \ell_{ik} | nS'm' \rangle$$
(39)

where  $\Delta E_n = E_0 - E_n$ . Equation (39) is further reduced by the orthonormality of the spin functions to

$$2\beta \sum_{\substack{1,k,n,m' \ i}} \sum_{\substack{\frac{\zeta_{i1}H_k}{\Delta E_n}}} \langle n | \ell_{i1} | 0 \rangle \langle S'm' | s_{i1} | Sm \rangle \langle 0 | \ell_{ik} | n \rangle . \quad (40)$$

Recasting Equation (40) into operator form by suppressing the matrix element  $\langle S'm'|s_{i1}|Sm \rangle$  one obtains

$$2\beta \sum_{\substack{1,k \ n \ i}} \sum_{\substack{i}} \langle 0 | \ell_{ik} | n \rangle \langle n | \ell_{i1} | 0 \rangle \frac{\zeta_{i1} H_k s_{i1}}{\Delta E_n} . \tag{41}$$

The fourth term has the form

$$\frac{H_1H_k}{(\Delta E_n)^2} \langle |\ell_{i1}+2s_{i1}| \rangle \langle |\ell_{ik}+2s_{ik}| \rangle , \qquad (42)$$

which is quadratic in magnetic field strength and will be omitted as was done in the reduction of Equation (31). When the first three terms are collected (Equations (37) and (41)) and compared with the leading term in

the spin Hamiltonian of Equation (2) the following identification may be made

$$g_{1k} = 2 \sum_{i} (\delta_{1k} + \sum_{i} \sum_{k,n} \frac{\langle 0 | \ell_{i1} | n \rangle \langle n | \ell_{ik} | 0 \rangle}{\Delta E_{n}}) , \qquad (43)$$

where  $g_{1k}$  is the lk'th element of the g tensor and  $\delta_{1k}$  is the Kronecker delta. This result was first obtained by Pryce<sup>82</sup> in 1950.

It is possible to calculate the g tensor directly from Equation (43), but in the case of strong crystal-field problems it is better to perform the sequential perturbations of spin-orbit coupling followed by the Zeeman interaction. This thesis is concerned only with  $S=\frac{1}{2}$  spin systems so, if  $|\alpha\rangle$  and  $|\beta\rangle$  are the doublet ground state wavefunctions, the principal g tensor elements of Equation (35) can be equated with the tensor elements of the phenomenological Hamiltonian of Equation (21) to give

$$g_{xx} = 2 \sum_{i} \langle \alpha | \ell_{ix} + 2s_{ix} | \beta \rangle$$

$$g_{yy} = 2i \sum_{i} \langle \alpha | \ell_{iy} + 2s_{iy} | \beta \rangle$$

$$g_{zz} = 2 \sum_{i} \langle \alpha | \ell_{iz} + 2s_{iz} | \alpha \rangle.$$
(44)

#### Sign of the g Shift

It is convenient to define a quantity known as the g shift,  $\Delta g_{\mbox{\scriptsize lk}},$  where

$$\Delta g_{1k} = (g_{1k}-2)$$
 (45)

From Equation (43)

$$\Delta g_{1k} = 2 \sum_{\substack{1,k \ n \ i}} \sum_{\substack{k \ n \ i}} \frac{\langle 0 | \ell_{i1} | n \rangle \langle n | \ell_{ik} | 0 \rangle}{\Delta E_n} . \tag{46}$$

Although this gives the prescription for calculating the magnitude of the g shift, the sign of the shift is unknown. It may be determined from the following rule:  $^{21}$  if the excited state,  $E_n$ , arises by promotion of the unpaired electron into an empty anti-bonding orbital, the g shift is negative; if the excited state arises by promotion of one of the paired electrons into the half-filled orbital, the g shift is positive.

### Sample g-Value Calculation

In the crystal-field approximation  $^{65,69}$  one needs the hydrogen-like wavefunctions

$$\psi_{n \ell m_{\ell}} = R_{n \ell}(r) Y_{\ell}^{m \ell}(\theta, \phi) , \qquad (47)$$

where, as usual, n is the principal quantum number,  $\ell$  is the orbital angular momentum quantum number,  $m_{\ell}$  is the component of  $\ell$  along the z axis, R is the radial function, and the spherical harmonics  $Y_{\ell}^{m\ell}$  describe the angular portion of the wavefunction. In considering the d orbitals ( $\ell$ =2), the radial portion  $R_{n2}$  is assumed to be the same for each. In magnetic resonance one is interested in the matrix elements of the orbital and spin angular momenta which are assumed independent of  $R_{n2}$ . Whenever a radially dependent quantity occurs, the following type of relationship is implied:

$$\zeta_{i} = \langle \zeta_{i} \rangle = \int_{0}^{\infty} R^{*}_{n\ell} \zeta_{i} R_{n\ell} r^{2} dr \qquad (48)$$

In the absence of detailed information concerning the radial wavefunctions radially dependent terms are treated as adjustable parameters to be evaluated by experiment.

In the notation for the d orbitals which will be employed in this thesis one writes

$$(z^{2})^{+} = |d_{z}^{2}, \alpha\rangle$$

$$(z^{2})^{-} = |d_{z}^{2}, \beta\rangle , \qquad (49)$$

where  $\alpha,\beta$  are the spin function and  $d_z2$  is the spatial function. The angular portions of the real d-orbitals are

$$(z^{2}) = d_{z}2 = d_{0}$$

$$(x^{2}-y^{2}) = d_{x}2-y^{2} = 1/\sqrt{2}(d_{2}+d_{-2})$$

$$(xy) = d_{xy} = 1/i\sqrt{2}(d_{2}-d_{-2})$$

$$(xz) = d_{xz} = 1/\sqrt{2}(d_{1}-d_{-1})$$

$$(yz) = d_{yz} = -1/i\sqrt{2}(d_{1}+d_{-1})$$
(50)

where

$$d_{0} = Y_{2}^{0} = \sqrt{5/16\pi} (3\cos^{2}\theta - 1)$$

$$d_{\pm 1} = Y_{2}^{\pm 1} = \sqrt{15/8\pi} \sin^{2}\theta \cos^{\pm i}\phi$$

$$d_{\pm 2} = Y_{2}^{\pm 2} = \sqrt{15/32\pi} \sin^{2}\theta e^{\pm 2i\phi}$$
(51)

and  $z^2$  and  $d_z^2$  will be used interchangeably.

As an example of a typical calculation the case of a complex with an axially symmetric g value  $(g_{zz}=g||, g_{xx}=g_{yy}=g|)$ , a  $d^7$  configuration,  $S^{-1}_2$ , the energy level scheme A of Figure 2 and the unpaired electron in  $d_z^2$  will be examined. The ground state in the hole formalism<sup>65</sup> is  $(d_x^2-y^2)^2(d_z^2)$ . The calculation is facilitated by the use of two tables; the first, the effect of the operator  $\bar{\ell} \cdot \bar{s}$  on the d-orbital set of Equations (50) is presented in Ballhausen's book<sup>69b</sup>; the second, giving the matrix elements of the orbital angular momentum within the d-orbital set is compiled in McGarvey's review<sup>11</sup>.

The zero-order Kramer's doublet is

$$|0^{+}\rangle = |(x^{2}-y^{2})^{2}(z^{2})^{+}\rangle$$
  
 $|0^{-}\rangle = |(x^{2}-y^{2})^{2}(z^{2})^{-}\rangle$  (52)

where  $|0\rangle$  refers to the ground state wavefunction. The first-order improved configurational wavefunction  $|\alpha\rangle$  obtained by introducing the spin-orbit interaction (Equation (6)) is

$$|\alpha\rangle = N | (x^{2}-y^{2})^{2}(z^{2})^{+}\rangle + ia_{1} | (x^{2}-y^{2})^{-}(xy)^{-}(z^{2})^{+}\rangle$$

$$-ia_{1} | (x^{2}-y^{2})^{+}(xy)^{-}(z^{2})^{+}\rangle \frac{-ia_{2}}{2} | (x^{2}-y^{2})^{-}(yz)^{-}(z^{2})^{+}\rangle$$

$$-ia_{4}/2 | (x^{2}-y^{2})^{+}(yz)^{+}(z^{2})^{+}\rangle \frac{+a_{2}}{2} | (x^{2}-y^{2})^{-}(xz)^{-}(z^{2})^{+}\rangle$$

$$-a_{4}/2 | (x^{2}-y^{2})^{+}(xz)^{+}(z^{2})^{+}\rangle \frac{-\sqrt{3}a_{3}}{2} | (x^{2}-y^{2})^{2}(xz)^{-}\rangle$$

$$-i\sqrt{3}a_{3}/2 | (x^{2}-y^{2})^{2}(yz)^{-}\rangle , \qquad (53)$$

where

$$a_{1} = \zeta/E(0) - E\{(x^{2}-y^{2})^{-}(xy)^{+}(z^{2})^{+}\}$$

$$a_{2} = \zeta/E(0) - E\{(x^{2}-y^{2})^{-}(e)^{-}(z^{2})^{+}\}$$

$$a_{3} = \zeta/E(0) - E\{(x^{2}-y^{2})^{2}(e)^{-}\}$$

$$a_{4} = \zeta/E(0) - E\{(x^{2}-y^{2})^{+}(e)^{+}(z^{2})^{+}\}$$
(54)

The orbital, e, can be either  $d_{XZ}$  or  $d_{YZ}$ ,  $\zeta$  is the one-electron metal spin-orbit coupling constant, N is a normalization constant and the denominators are the configurational excitation energies. Normalization gives the equation

$$\langle \alpha | \alpha \rangle = 1 = N^2 + 2a_1^2 + a_2^2/2 + a_4^2/2 + 3a_3^2/2$$
 (55)

The first-order  $|\beta\rangle$  function is found from  $|(x^2-y^2)^2(z^2)^{-}\rangle$  in a like manner. The Zeeman spin-Hamiltonian expressions of Equation (44) lead to

$$g_{\parallel} = 2N^{2} + 4a_{1}^{2} - a_{2}^{2} + 3a_{4}^{2} - 3a_{3}^{2}$$

$$g_{\perp} = 2N^{2} + 6a_{3}N + 4a_{1}^{2} + 2a_{2}a_{4} .$$
(56)

The obvious problem is that one has five unknowns and only three equations (including normalization). However, the perturbation coefficients, a<sub>i</sub>, are usually small enough (>0.1) that any product of two coefficients can be ignored. When this is done, Equations (56) become

$$g \mid | = 2N^2$$
  
 $g \mid = 2N^2 + 6a_3N$  (57)

Since the g shift  $(g_1-2)$  is due to the excitation of an electron from one of the filled orbitals  $d_{xz}$  or  $d_{yz}$  into the partially filled  $d_z^2$  orbital, its sign is positive such that  $g_1 > g_1 = 2$ . The calculated g values for the other two possible ground states of the Pt and Pd radicals reported in this thesis are shown in Table I with the normalization constant suppressed.

TABLE 1.-- g Values calculated from ligand field theory<sup>a</sup>

Configuration	Ground State (hole formalism)	8	<u>g_</u>
d <sup>7</sup>	$(d_x^2-y^2)^2(d_{xy})$	2 - 8ς/ΔE <sub>1</sub>	$2 + 2\zeta/\Delta E_2$
d <sup>7</sup>	$(d_x^2-y^2)^2(d_z^2)$	2	2 + 6ς/ΔE <sub>3</sub>
$d^9$	(d <sub>x</sub> 2 <sub>-y</sub> 2)	2 + 8ς/ΔE <sub>1</sub>	$2 + 2\zeta/\Delta E_4$

a)  $\Delta E_1 = E(x^2-y^2)-E(xy)$ ;  $\Delta E_2 = E(xz,yz)-E(xy)$ ;  $\Delta E_3 = E(xz,yz)-E(z^2)$  $\Delta E_4 = E(xz,yz)-E(x^2-y^2)$ .

If there is a low-lying excited state not coupled to the ground state by the spin-orbit interaction the resonance signal will be strongly temperature dependent because of the thermal distribution of electrons between the two orbitals. If the low-lying state is coupled to the ground state, the perturbation coefficients,  $a_1 = \zeta/\Delta E$ , will be very large. In this situation one must simultaneously diagonalize the crystal-field and spin-orbit interactions to obtain the correct ground state wavefunctions (the g shifts will still be large but calculable). Fortunately neither of these two cases occurs in the Pd radicals. But

in the Pt-containing radicals the large spin-orbit coupling constant may require a higher-order perturbation treatment. Tippens<sup>83</sup> gives analytical expressions for the second-order spin-orbit coupling correction to the g value. Atkins and Jamieson<sup>84</sup> have generalized Tippens' method to insure that the g value remains gauge invariant.

#### Hyperfine Interactions

### Introduction

When a nucleus with a non-zero nuclear magnetic moment,  $\overline{\mu}_n$ , is placed in a magnetic field,  $\overline{H}$ , the associated nuclear spin vector,  $\overline{I}$ , takes one of (2I+1) quantized values, I, (I-1), ..., -I, and the energy becomes

$$H_{N} = -\overline{\mu}_{n} \cdot \overline{H} = -g_{n}\beta_{n}\overline{H} \cdot \overline{I}$$
 (58)

where  $\beta_{\rm n}$  is the nuclear magneton, eh/4 $\pi$ Mc (M is the proton mass),  $g_{\rm n}$  is the nuclear g factor and  $\bar{\rm I}$  has all of the properties ascribed to a generalized spin angular momentum.

The hyperfine energy term  $\overline{S} \cdot \overline{A} \cdot \overline{I}$  (Equation 2) arises from the mutual interaction between the nuclear magnetic moment and the spin-plus-orbital magnetic moments of the unpaired electrons. This interaction may be viewed in two equivalent ways: either the electrons produce a magnetic field at the nucleus thereby lifting the (2I+1)-fold nuclear spin degeneracy; or, the nucleus produces a field at the electron that adds to the external magnetic field. From either point of view the magnetic field at the electron, which is being examined by the ESR experiment, has (2I+1) values. The ESR selection rules  $\Delta S=0$ ,  $\Delta m=\pm 1$  state that the quantum of

angular momentum imparted by the microwave field is used to "flip" an electron spin and as a result of the conservation of angular momentum I cannot be simultaneously changed. Thus the ESR spectrum will show (2I+1) lines of equal spacing and intensity since the nuclear energy levels are essentially equally populated. If the electron interacts with n magnetic nuclei of spin  $I_i$ , the number of lines becomes

while the relative intensities can be found by summation. Should j nuclei of spin I be magnetically equivalent, the combined nuclear spin  $\dot{j}$  vector is  $\dot{I} = \sum_{i=1}^{L} \dot{I}_{i}$  and the j nuclei produce (2jI+1) lines.

The scope and utility of the structural information from the hyperfine splitting is now apparent. One can often identify radicals by the number and intensity of the lines in the ESR spectrum. The nuclear spin of previously unexamined isotopes can be determined or, alternatively, if I is known, then the magnetic moment can be estimated from the hyperfine splitting. The extent of covalent bonding may also be judged from the magnitude of the interactions.

#### The Hyperfine Hamiltonian

The objective in this section will be to develop two expressions for the hyperfine interaction. It is desirable to have a phenomenological spin Hamiltonian (Equation 1) that will allow the spin parameters to be easily extracted from the experimental splittings. It is also desirable to have an equivalent Hamiltonian expression that is directly

related to the basic physical interactions which can then be used to give a molecular structure interpretation to the splittings. This latter expression can also be used to identify the ground state or confirm the identification made from the g values.

The relevant portion of the Dirac equation for a one-electron atom in a magnetic field is  $^{65,68}$ 

$$H_n = e/mc \{ \overline{A} \cdot \overline{p} + (h/2\pi) \ \overline{s} \cdot \overline{\nabla} \times \overline{A} \} . \qquad (60)$$

The vector potential  $\bar{A}$  for the nuclear dipole is given by 80

$$\bar{A} = \bar{\mu}_n \times \bar{r}/r^3 \tag{61}$$

where r is the distance between electron and nucleus. Substitution of Equation (61) into Equation (60) yields

$$H_{n} = g_{eg_{n}}\beta\beta_{n} \left\{ \frac{(\bar{\ell}-\bar{s})\cdot\bar{I}}{r^{3}} + \frac{3(\bar{I}\cdot\bar{r})(\bar{s}\cdot\bar{r})}{r^{5}} \right\}$$
 (62)

where as before  $\bar{\ell}$  is the orbital angular momentum for a single electron,  $\bar{s}$  is the spin angular momentum for a single electron and  $g_e = 2.000$ . This dipolar Hamiltonian integrates to zero for the spherically symmetric s orbitals which is fortunate, since a singularity develops in Equation (62) when  $r = r_0$  ( $r_0$  is the nuclear radius); yet, p, d and f electrons that do exhibit dipolar hyperfine interactions have nodes in their electron distributions at the nucleus.

The fact that s electrons show an isotropic hyperfine splitting is attributed to the Fermi contact interaction  $^{1-22}$  which may be written

$$H_f = (8\pi/3) g_e g_n \beta \beta_n | \Psi(0) |^2$$
 (63)

where  $|\Psi(0)|^2$  is the s-electron spin density evaluated at the nucleus (r=0) for the orbital  $\Psi$ . In operator form the contact term becomes

$$H_{f} = (8\pi/3) g_{e}g_{n}\beta\beta_{n} \delta(\bar{r})\bar{I}\cdot\bar{s}$$
 (64)

where the delta function requires that r=0 for the integration over the electron coordinates. The total hyperfine Hamiltonian is

$$H_h = H_n + H_f = g_e g_n \beta \beta_n \left\{ \frac{(\bar{\ell} - \bar{s})}{r^3} + \frac{3(\bar{s} \cdot \bar{r})\bar{r}}{r^5} + (8\pi/3) \delta(\bar{r})\bar{s} \right\} \cdot \bar{I}$$
 (65)

Additional unpaired electrons and/or nuclei can be included in Equation (65). If Equation (65) is expanded into its components, the result can be represented in tensor form by

$$H_{h} = \overline{s} \cdot A \cdot \overline{I} \tag{66}$$

where  $\overline{\overline{A}}$  is a symmetric tensor. Equation (66) is the phenomenological expression used to interpret experimental spectra.

Abragam and Pryce<sup>63</sup> have cast the hyperfine Hamiltonian into a form that is more convenient for computing matrix elements. Within states where L, the total orbital angular momentum, is constant, which includes the ground state and lowest-lying excited states, the Cartesian coordinates of Equation (65) can be replaced by appropriate orbital angular momentum operators. The validity of this replacement is based on the Wigner-Eckhart theorem. 81 Proper combinations of the (x,y,z)

coordinates are related (apart from a constant) to the spherical harmonics whose rotations are covered by the Wigner-Eckhart theorem. The angular momentum operator equivalent must transform in the same way as the combination of Cartesian coordinates assuming that allowance is made for the non-commutivity of  $l_x$ ,  $l_y$ , and  $l_z$ ; for example, xy transforms the same as  $\frac{l_2(l_x l_y + l_y l_x)}{l_x}$ . The constant of proportionality is determined by evaluating the same matrix element for both forms of the operator. In this manner Abragam and Pryce showed that the hyperfine Hamiltonian for a single electron is

$$H_{h} = g_{e}g_{n}\beta\beta_{n} \left\langle r^{-3} \right\rangle \left\{ \overline{\ell} \cdot \overline{1} - \kappa(\overline{s} \cdot \overline{1}) + \xi \ell(\ell+1)(\overline{s} \cdot \overline{1}) - 3\xi/2(\overline{\ell} \cdot \overline{s})(\overline{\ell} \cdot \overline{1}) - 3\xi/2(\overline{\ell} \cdot \overline{1})(\overline{\ell} \cdot \overline{s}) \right\}$$

$$(67)$$

where  $\xi=2/(2\ell+3)(2\ell-1)$  is the constant of proportionality,  $\langle r^{-3} \rangle$  is the expectation value of  $r^{-3}$  over the radial portion of  $H_h$  and  $\kappa$  is the sorbital contribution to the hyperfine interaction and is defined by

$$\kappa = \frac{(8\pi/3)\delta(\vec{r})}{\langle r^{-3} \rangle} . \tag{68}$$

The utility of Equation (67) is now apparent. The involved integrals have been replaced by simple algebraic relationships depending upon the well-known matrix elements of angular momentum operators.

# Isotropic Hyperfine Interaction

One of the most striking hyperfine interaction problems is found in the case of half-filled d-shell ions such as high-spin  ${\rm Mn}^{2+}$  (with configuration  ${\rm 3d}^5$  and ground state  ${}^6{\rm S}$ ) in an octahedral crystal field where

no hyperfine splitting would be expected. With L=0 there should be no orbital contribution to the hyperfine splitting while the spherical symmetry eliminates any dipolar contribution and the absence of halffilled s orbitals rules out splittings arising from the Fermi contact term. Yet, an appreciable splitting is observed and this splitting is attributed to core polarization 87,88 of the inner s electrons. unpaired d electron with its spin up \(^+\) will have different electrostatic repulsion and exchange interactions with inner s electrons whose spin is up ↑ than with those whose spin is down ↓ . In the conventional Hartree-Fock closed-shell calculations the spin properties of paired electrons are exactly equal, but opposed in sign, leading to a net cancellation of spin density at the nucleus due to filled s shells. The Hartree-Fock method employed by Watson and Freeman 87,88 does not have this restriction, so that electrons with the same values of the n and & quantum numbers but different values of the ms quantum number are allowed to have different radial wave functions. The result is that the s-orbital core electrons may be polarized to give a net spin at the nucleus which has a sign opposed to that produced by the unpaired d electron. Any spin density at the nucleus contributed by s electrons in the valence shell, or further removed from the nucleus than the d level, yields a core polarization term of the same sign as that of the unpaired d electron. Although these spin density differences are quite small, the contact hyperfine interaction for a single s electron is very large and produces isotropic splittings which usually dominate the observed metal hyperfine splittings.

As a measure of the core polarization, the parameter  $\chi$  is defined as the unpaired spin density at the nucleus per unpaired electron:

$$\chi = 4\pi/2S \sum_{i} \{ |\phi_{i}^{+}(0)|^{2} - |\phi_{i}^{-}(0)|^{2} \}$$
(69)

where  $|\phi_1^+(0)|^2$  is the positive spin density  $(m=+\frac{1}{2})$  in the i<sup>th</sup> s oribtal evaluated at the nucleus and S is the total spin of the system. Predictions of  $\chi$  and  $\langle r^{-3} \rangle$  by spin-unrestricted Hartree-Fock calculations 87,88 have been quite successful despite the fact that  $\chi$  is the sum of several large terms which may have opposite signs. This success is particularly surprising since the calculated metal hyperfine interaction energies are approximately  $10^{-2} \text{cm}^{-1}$ , while the total energy of the complex ions is approximately  $10^{5} \text{cm}^{-1}$ .

McGarvey<sup>89</sup> has summarized the experimental trends among values of  $\chi$ . He shows that  $\chi$  gradually decreases across a transition series from -2.0 atomic units (au) to -3.4 au as one goes from a 3d<sup>1</sup> to a 3d<sup>9</sup> configuration. Similarly  $\chi$  runs from -4.0 to -9.0 au across the 4d series and from -10 to -15 au across the 5d series. Experimentally  $\chi$  is related to  $\kappa$  by (see Equations (68) and (69))

$$\kappa \left\langle r^{-3} \right\rangle = -(2/3)\chi \quad . \tag{70}$$

A number of workers have shown that  $\kappa$  is relatively constant for a given metal ion in a variety of complexes. However, as the complexes become more covalent the unpaired electron becomes more delocalized and  $\langle r^{-3} \rangle$  decreases while  $\chi$  approaches zero, a result supported by McGarvey's <sup>89</sup> compilation. This linear correlation of  $\chi$  with covalency is observed for  $d^1$ ,  $d^3$ ,  $d^5$  and  $d^7$  configurations.

In the case of the  $d^9$  configuration, particularly  $Cu^{2+}$  complexes, the linear correlation of  $\chi$  with covalency breaks down implying that  $\kappa$  is not constant  $^{90,91}$ . Kuska et al.  $^{90,91}$  attribute the lack of correlation in copper complexes to a small admixture of 4s electron density into the

ground state. They believe that molecular vibrations reduce the symmetry restrictions which prohibits direct mixing of 4s with the  $d_{\rm X}2_{-\rm y}2$  ground state orbital. On the other hand, McGarvey<sup>89</sup> says that spin density is induced into the 4s copper orbital by exchange interaction with the ligands.

Recently McMillan<sup>92</sup> has discussed the contribution to the metal core polarization induced by unpaired spin density on the ligand nuclei which will increase with increasing covalency as one goes from the 3d to the 4d to the 5d transition series and as sigma bonding between metal and ligands increases. Therefore, ions with  $d^9$  or  $d^8$  configurations, or a strong-field  $d^7$  configuration, where the unpaired electrons are in predominately  $\sigma$ -type orbitals will experience "anomalous" core polarization and  $\chi$  cannot be easily correlated with covalency.

In certain point-group symmetries, it is possible for one of the d orbitals to belong to the totally symmetric irreducible representation as do the s orbitals. Mixing can then take place between the nd and (n+1)s orbitals and, as noted earlier, spin density in s orbitals in the valence shell (or beyond) will cause  $\chi$  to become more positive. For example, (Co(II) phthalocyanine), 65 which has a low-spin 3d7 configuration of D4h symmetry with the unpaired electron in a (3d<sub>z</sub>2 +4s) hybrid orbital, has an isotropic hyperfine field at the nucleus of  $\chi$ 2+2.2au where as the great majority of 3dn ions have negative values of  $\chi$ 2 clustered about a value of -3 au.

The reason for the extensive discussion of  $\chi$  is that in this thesis two of the three possible ground states of the Pt and Pd radicals have either d<sup>9</sup> or low-spin d<sup>7</sup> configurations. Since the molecular orbitals containing the unpaired electrons form  $\sigma$ -type bonds with the ligands, these ground states are the ones most likely to exhibit "anomalous" core polarizations. The consequences are: (1) the magnitude

and even the sign of  $\chi$  cannot be assumed to agree with that calculated from spin-unrestricted Hartree-Fock calculations for the metal ions since those are based solely on  $d^n$  core polarization; (2) the inability to interpret  $\chi$  restricts the use of hyperfine splittings to assign the ground states of the radicals; (3)  $\chi$  (or  $\kappa$ ) cannot be used to estimate the degree of covalency. Because the isotropic hyperfine splitting, as measured by  $-g_eg_n\beta\beta_n$   $\langle r^{-3}\rangle$   $\kappa$  in Equation (67), does not necessarily follow changes in  $\langle r^{-3}\rangle$ , the hyperfine Hamiltonian in this thesis will be written

$$H_{h} = -\kappa(\overline{s} \cdot \overline{1}) + P\{(\overline{\ell} \cdot \overline{1}) + \xi \ell(\ell+1)(\overline{s} \cdot \overline{1}) - 3/2\xi(\overline{\ell} \cdot \overline{1})(\overline{\ell} \cdot \overline{s})\}$$

$$(71)$$

where  $P = g_e g_n \beta \beta_n \langle r^{-3} \rangle$  and  $\kappa$  now has units of energy. In the ESR literature of transition metal complexes, energies are usually expressed in units of cm<sup>-1</sup>. To find  $\chi$  in atomic units from  $\kappa$  (cm<sup>-1</sup>) the following equation<sup>89</sup> is used:

$$\chi(au) = -3/2(hca_o^3/g_eg_n\beta\beta_n)\kappa(cm^{-1})$$
 (72)

where ao is the Bohr radius.

# Analysis of Metal Hyperfine Interactions

For transition metals Equation (71) may be transformed by putting  $\xi=2/21$  since, for d electrons,  $\ell=2$ . In the crystal-field approximation,  $r^{-3}$  is assumed to have the same value for all of the valence d electrons and one obtains

$$H_{h} = -\kappa(\bar{s}\cdot\bar{I}) + P(\bar{l} + \bar{a}/7)\cdot\bar{I}$$
 (73)

where  $\overline{a} = 4\overline{s} - (\overline{\ell} \cdot \overline{s})\overline{\ell} - \overline{\ell}(\overline{\ell} \cdot \overline{s})$ . The relationship between the experimental principal A values (Equation (66)) and the principal values of Equation (73) can be determined by examining the corresponding matrix elements between the ground state spin wavefunctions  $|\alpha\rangle$  and  $|\beta\rangle$ 

$$\langle \alpha | A_{zz} I_{zsz} | \alpha \rangle = \langle \alpha | -\kappa s_z I_z + P(\ell_z + a_z/7) I_z | \alpha \rangle$$
 (74)

and

$$A_{zz}/2 \langle \alpha | I_z | \alpha \rangle = \langle \alpha | -\kappa s_z + P(\ell_z + a_z/7) | \alpha \rangle \langle \alpha | I_z | \alpha \rangle$$
 (75)

or

$$A_{zz} = -\kappa + 2P \left\langle \alpha | \ell_z + a_z / 7 | \alpha \right\rangle$$

and similarly

$$A_{xx} = -\kappa + 2P \left\langle \alpha | \ell_x + a_x / 7 | \beta \right\rangle$$

$$A_{yy} = -\kappa + 2iP \left\langle \alpha | \ell_y + a_y / 7 | \beta \right\rangle . \tag{76}$$

The calculated hyperfine splitting values for the three possible ground states of the Pt and Pd radicals studied in this work are reported in Table 2 based upon an axially symmetric hyperfine interaction tensor  $(A_{ZZ} = A | |, A_{XX} = A_{YY} = A |)$ , where the unique axis is z). The ground state wavefunctions  $|\alpha\rangle$  and  $|\beta\rangle$  are the same spin-orbit augmented functions used earlier to calculate the g values reported in Table 1.

TABLE 2. -- Hyperfine interactions (A) calculated by the theory of Abragam and Pryce $^1$ .

T⊌	$-\kappa + P(2/7 + 11/14\Deltag)$	$-\kappa + P(-2/7 + 15/14\Delta g_{\perp})$	$-\kappa + P(2/7 + 11/14\Delta_{g})$	
A	-k + P(-4/7 + AB   + 3/7AB])	$-\kappa + P(4/7 - \Delta g / 7)$	-k + P(-4/7 + Dg   + 3/70g])	
Ground State (hole formalism)	$(d_{x}2-y^{2})^{2}(d_{xy})$	$(d_x^2-y^2)^2(d_z^2)$	$(d_{\mathbf{x}^2-\mathbf{y}^2})$	
Configuration	<sup>4</sup> 7	4 <sup>7</sup>	6 P	

where Ag|| = g|| - 2.0023 Ag| = g|| - 2.0023

# Covalency from Metal Hyperfine Splittings

 $McGarvey^{89}$  has presented the molecular orbital (MO) theory for the  $Cu^{2+}$ ,  $3d^9$ ,  $^2D$  ion in a square-planar complex of  $D_{4h}$  symmetry. The pertinent antibonding orbitals are

$$|\sigma\rangle = \alpha |d_{x}2_{-y}2\rangle - \alpha' |\phi_{L}(x^{2}-y^{2})\rangle$$

$$|\pi\rangle = \beta |d_{xy}\rangle - \beta' |\phi_{L}(xy)\rangle \qquad (77)$$

$$|\pi_{1}\rangle = \beta_{1}|d_{xz_{yz}}\rangle - \beta'_{1}|\phi_{L}(xz_{yz})\rangle$$

where the ligands lie along the  $\pm x$  and  $\pm y$  axes. The  $|\sigma\rangle$  orbital contains the unpaired electron and  $\phi_L(x^2-y^2)$ ,  $\phi_L(xy)$  etc. are the symmetry-adapted wavefunctions constructed from linear combinations of ligand atomic orbitals. The squares of the coefficients represent the electronic spin density in that atomic orbital. If  $\alpha^2 = \alpha^{12}$ , the covalency is maximized since the electron spends equal time on the metal and ligands. As  $\alpha^2 + 1$ , the electron is more nearly localized on  $Cu^{2+}$  and the bonding is more nearly ionic. The value of  $\alpha^2$  can exceed unity depending upon the value of the overlap term found on normalization, eg.,

$$1 = \alpha^2 + \alpha^{2} - 2\alpha\alpha^{3}$$
 (78)

where S is the group overlap integral.

The ESR spectra of the  $Cu^{2+}$  complexes can be fitted to the following axial spin Hamiltonian:

$$H = g | | \beta H_z S_z + g | \beta (H_x S_x + H_y S_y) + A | | I_z S_z + A | (I_x S_x + I_y S_y)$$
 (79)

which gives

$$A_{||} = -\kappa - (4/7)\alpha^{2}P + \Delta g_{||}PZ_{||} + (3/7)\Delta g_{|}PZ_{||}$$

$$A_{||} = -\kappa + (2/7)\alpha^{2}P + (11/14)\Delta g_{||}PZ_{||}$$

$$Z_{||} = \alpha \beta_{1}^{'}\{\alpha \beta_{1} - \alpha' \beta_{1}S^{-1}2\alpha' (1 - \beta_{1}^{2})^{1/2}T(n)\}$$

$$Z_{||} = \alpha \beta' \{\alpha \beta - \alpha' \beta S - (1/\sqrt{2})\alpha' (1 - \beta^{2})^{1/2}T(n)\}$$

$$S = \langle d_{x}2_{-y}2|\phi_{L}(x^{2}-y^{2})\rangle$$

$$T(n) = n - (1 - n^{2})^{1/2}a_{0}^{-1}R8(Z_{p}Z_{s})^{5/2}(Z_{s}-Z_{p})/(Z_{s}+Z_{p})^{5}$$

$$\Delta g_{||} = g_{||} - 2.0023$$

$$\Delta g_{||} = g_{||} - 2.0023$$

where  $Z_p$  and  $Z_s$  are the effective charges for p and s electrons on the ligand, R is the metal-ligand internuclear distance and  $n^2$  is the fractional p character of the ligand orbitals making up  $\phi_L(x^2-y^2)$ . Often, as in the case of the Pt and Pd radicals, there is a lack of good wave functions, information about effective charges, spin-orbit coupling constants and excitation energies which prevent one from using the complete expressions of Equations (80). McGarvey points out that by setting  $Z_{\parallel} = Z_{\parallel} = 1$  Equations (80) reduce to the much simpler pair

$$A_{\parallel} = -\kappa + P(-4/7\alpha^2 + \Delta g_{\parallel} + 3/7\Delta g_{\perp})$$

$$A_{\parallel} = -\kappa + P(2/7\alpha^2 + 11/14\Delta g_{\parallel}) . \tag{81}$$

Fortunately substitution of experimental values of A<sub>||</sub>, A<sub>|</sub>,  $\Delta g_{||}$ ,  $\Delta g_{||}$ ,

# Angular Variation of the Hyperfine Splitting 1,93,94

For a microwave frequency of  $\sim 10,000 \text{MHz}$  (X-band), the Zeeman energy is

$$E/hc \simeq 0.3cm^{-1} . ag{82}$$

Using the point-dipole approximation, the hyperfine interaction energy is about

$$E/hc \propto (\beta \beta_n/hcr^3) \simeq 0.004cm^{-1}$$
 (83)

where r is taken arbitrarily as  $0.5\text{\AA}$ . In terms of magnetic fields, the external field at X-band when g=2 is approximately 3600 Gauss at resonance. Again, within the point-dipole approximation (r=0.5 $\text{\AA}$ ), the magnetic field at the nucleus due to the electron is

$$H_n \propto \beta/r^3 \simeq 80,000 \text{ Gauss}$$
 (84)

while the field at the electron due to the nucleus is

$$H_{\rm e} \propto \beta n/r^3 \simeq 40 \text{ Gauss}$$
 (85)

These observations illustrate the so-called high-field approximation in which the larger energy Zeeman term is diagonalized with the electron spin quantized along the external field. The smaller hyperfine term is treated next with the nuclear spin quantized along the resultant magnetic field which is primarily due to the field produced by the electron.

Consider the following Hamiltonian:

$$H_{z} = \beta \overline{H} \cdot \overline{g} \cdot \overline{S} . \qquad (86)$$

If the unit vector  $\overline{n}$  along the external magnetic field direction ( $\overline{H}=H\overline{n}$ ) has direction cosines  $\cos\alpha\sin\beta$ ,  $\sin\alpha\sin\beta$ , and  $\cos\beta$  with the (x,y,z) principal axes of the g tensor, then the energy eigenvalues are

$$E = g\beta Hm \tag{87}$$

where m is the projection of S along the magnetic field direction and

$$g^{2} = (\overline{n} \cdot \overline{g}) (\overline{g} \cdot \overline{n}) = g_{xx}^{2} \cos^{2} \alpha \sin^{2} \beta + g_{yy}^{2} \sin^{2} \alpha \sin^{2} \beta + g_{zz}^{2} \cos^{2} \beta$$
 (88)

and one obtains (2S+1) equally spaced levels of interval gBH. Since the experimentally determined g tensor will always be positive and symmetric, no information is lost by dealing with the  $g^2$  tensor. The orientation of the g-tensor axes is not usually known beforehand so one chooses a right-handed Cartesian coordinate system (1,2,3) located in the crystal (often the crystallographic axes). Then the unit magnetic field vector  $\overline{\bf n}$  has direction cosines  $\cos\phi\sin\theta$ ,  $\sin\phi\sin\theta$  and  $\cos\theta$  with the chosen crystal axes and  $g^2$  becomes

$$g^{2} = \sin^{2}\theta (G_{11}\cos^{2}\phi + 2G_{12}\sin\phi\cos\phi + G_{22}\sin^{2}\phi) + 2\sin\theta\cos\theta (G_{13}\cos\phi + G_{23}\sin\phi) + G_{33}\cos^{2}\theta$$
 (89)

where the  $G_{ij}$  are the  $g^2$ -tensor elements in the (1,2,3) axis system.

To evaluate the tensor it is usual to perform three mutually perpendicular rotations of the crystal in the magnetic field and if the three rotations are made about the orthogonal crystal axes (1,2,3) one obtains

$$g^2 = G_{22}\sin^2\theta + 2G_{23}\sin\theta\cos\theta + G_{33}\cos^2\theta$$

for rotation around 1, since  $\phi = \pi/2$  and H is in the 2-3 plane;

$$g^2 = G_{11} \sin^2 \theta + 2G_{13} \sin \theta \cos \theta + G_{33} \cos^2 \theta$$
 (90)

for rotation around 2, since  $\phi$  = 0 and H is in the 1-3 plane; and

$$g^2 = G_{11}\sin^2\phi + 2G_{13}\sin\phi\cos\phi + G_{22}\sin^2\phi$$

for rotation around 3, since  $\theta = \pi/2$  and H is in the 1-2 plane. As Schonland 94 has noted each of these equations is of the form

$$g^2 = \alpha_1 + \beta_1 \cos 2\theta_1 + \gamma_1 \sin 2\theta_1 \tag{91}$$

(for rotation about axis 1)

where

$$\alpha_1 = \frac{1}{2}(G_{33} + G_{22})$$

$$\beta_1 = \frac{1}{2}(G_{33} - G_{22})$$

$$\gamma_1 = G_{23}$$

with similar results for the other two rotations. As the magnetic field makes its excursion there will be a maximum and a minimum in  $g^2$  in each of the three planes. If  $g_+^2$  and  $g_-^2$  represent the extrema in each plane, there result six equations in the six independent tensor elements  $G_{ij}$ . In each plane two unique parameters arise

$$\alpha = \frac{1}{2}(g_{+}^{2} + g_{-}^{2})$$

$$\delta = \frac{1}{2}(g_{+}^{2} - g_{-}^{2})$$
(92)

and it may be shown that the g<sup>2</sup> tensor elements are

$$G_{11} = (\alpha_2 + \alpha_3 - \alpha_1)$$

$$G_{12} = \pm \{(\delta_3 + \alpha_1 - \alpha_2)(\delta_3 - \alpha_1 - \alpha_2)\}^{\frac{1}{2}}.$$
(93)

Cyclic permutation of the indices will give the other four elements.

The  $g^2$  tensor can be diagonalized by an orthogonal (similarity) transformation to give the principal values  $g_{xx}^2$ ,  $g_{yy}^2$  and  $g_{zz}^2$  as follows:

$$\sum_{\substack{\Sigma \\ i,j=1}} (1_{ki}G_{ij}1_{jk} = g_{kk}^2\delta_{ij})$$
 (94)

where  $(l_{ki}) = (l_{ik})^{-1}$  are the orthogonal direction cosine matrices relating the experimentally chosen crystal axes (1,2,3) to the principal gaxes (x,y,z), and  $\delta_{ij}$  is the Kronecker delta.

If the Hamiltonian now includes the hyperfine interaction, and the principal axes of the hyperfine tensor coincide with those of the g tensor, then

$$H = \beta H(n_1 g_{xx} S_x + n_2 g_{yy} S_y + n_3 g_{zz} S_z)$$

$$+ A_{xx} S_x I_x + A_{yy} S_y I_y + A_{zz} S_z I_z$$
(95)

where  $\overline{H}=\overline{n}H$ . In the high-field approximation, S is quantized along  $\overline{H}$  to give

$$H = g\beta HS_{z}^{\dagger} + (1/g)(n_{1}g_{xx}A_{xx}I_{x} + n_{2}g_{yy}A_{yy}I_{y} + n_{3}g_{zz}A_{zz}I_{z})S_{z}^{\dagger}$$
 (96)

where  $g^2 = n_1^2 g_{xx}^2 + n_2^2 g_{yy}^2 + n_3^2 g_{zz}^2$ . Then I is rotated to quantize I along S to give

$$H = g\beta HS_z' + AS_z'I_z'$$
 (97)

where

$$g^{2}A^{2} = n_{1}^{2}g_{xx}^{2} A_{xx}^{2} + n_{2}^{2}g_{yy}^{2}A_{yy}^{2} + n_{3}^{2}g_{zz}^{2}A_{zz}^{2}.$$
 (98)

The important result is that to extract the principal hyperfine tensor elements the experimental tensor  $g^2A^2$  must be diagonalized and one therefore treats the  $g^2A^2$  tensor in the same manner as the  $g^2$  tensor (Equations (89)-(94)) above. Thus, following the three orthogonal rotations,  $g^2$  and  $g^2A^2$  (with A expressed in energy units) are both plotted versus the angle of rotation. From the extrema in both plots one can obtain the principal values of g and A.

When the hyperfine splitting is relatively large the off-diagonal elements in S'I' must be considered. The second-order perturbation treatment of the problem of an axially symmetric radical is very useful for interpreting the experimental results of this thesis. The solution given by Bleaney<sup>77</sup> is presented below for a radical with  $S=\frac{1}{2}$  and the selection rule  $\Delta m=\pm 1$ ,  $\Delta m_T=0$ .

$$\Delta E = hv = g\beta H + Am_{I} + (A_{||}^{2} + A_{||}^{2}) \left(\frac{A_{||}^{2}}{4A^{2}G}\right) \{I(I+1) - m_{I}^{2}\}$$

$$+ \left(\left(\frac{A_{||}^{2} - A_{||}^{2}}{8A^{2}G}\right) \left(\frac{g||g|}{g^{2}}\right) \sin^{2}2\theta \right) m_{I}^{2}$$
(99)

where

$$g^{2} = g_{\parallel}^{2} \cos^{2}\theta + g_{\perp}^{2} \sin^{2}\theta$$

$$g^{2}A^{2} = g_{\parallel}^{2} A_{\parallel}^{2} \cos^{2}\theta + g_{\perp}^{2} A_{\perp}^{2} \sin^{2}\theta$$

 $\theta$  = angle between the unique molecular axis and the magnetic field.

Although the (2I+1) hyperfine lines are no longer equally spaced, the energy difference between the  $m_{\rm I}$  and  $-m_{\rm I}$  components is simply  $2{\rm Am_{\rm I}}$ . That is, the second-order effects can be eliminated by measuring the separation between the  $\pm m_{\rm I}$  lines. The more difficult problem of non-coincident principal axes for g and A is not amenable to closed form solution, but is discussed in Abragam and Bleaney's book  $^{\rm I}$ .

# Sign of the Hyperfine Splitting

experimental hyperfine tensor elements are determined as  $A_{11}^2$ , the signs of the elements are lost. Fortman's Ph.D. thesis  $^{95}$ describes a method for establishing the signs by use of a model system in which the nucleus and unpaired electron(s) are considered to be point charges and simple magnetic dipoles. There is an easier technique to determine the signs of the hyperfine tensor elements which will be employed in the present work. As an example, if the hyperfine tensor is axially symmetric there will be two experimental principal tensor elements usually, designated  $A \mid \ |$  and  $A \mid \ |$ , either of which can be positive or negative thereby creating a total of  $2^2=4$  possible sign combinations. each of these combinations is substituted into the theoretical expressions given by Equations (76) one obtains four sets of values for  $\kappa$  and The correct sign combination will be that giving the value of P agreeing most closely in magnitude to the value of P which has been calculated for the free ion by the Hartree-Fock method, and has the correct sign. This technique for determining the signs depends upon the proven ability of the free-ion Hartree-Fock calculations to predict observables accurately, particularly  $\langle r^{-3} \rangle$  for the 3d<sup>87</sup>, 4d<sup>88</sup> and 5d<sup>96</sup> transition metal ions.

# Ligand Hyperfine Interactions 1,85

Ligand hyperfine splittings provide the most striking demonstration of covalency in transition metal compounds and also provide the best criterion for finding the extent of covalent bonding. There are two alternate theories for picturing the ligand hyperfine interaction. If one examines an isolated metal-halogen bond composed of two paired

p-electrons on the ligand and one unpaired electron on the metal, the two approaches may be compared.

In the molecular orbital (MO) approach two orbitals  $\phi_{\mbox{$A$}}$  and  $\phi_{\mbox{$B$}}$  are constructed:

$$\phi_{A} = N_{A}(d-Ap)$$
 and 
$$\phi_{B} = N_{B}(p+Bd) .$$
 (100)

The lower energy p electrons on the ligand constitute the major component of the bonding orbital  $\phi_B$  while the singly occupied antibonding orbital  $\phi_A$  is largely the metal d atomic orbital.  $N_A$  and  $N_B$  are the normalizing coefficients  $(N_A \approx N_B \approx 1)$  and A and B are small admixture constants. After bond formation the bonding orbital drops in energy below that of the original atomic p level and the antibonding orbital is raised in energy above that of the atomic d level, but the net energy of the system is lowered. Normalization gives

$$N_A = (1-2AS+A^2)^{\frac{1}{2}}$$

$$N_B = (1+2BS+B^2)^{\frac{1}{2}}$$
(101)

where  $S = \langle d | p \rangle$  . The orthogonality condition yields

$$\langle \phi_A | \phi_B \rangle = 0 = B-A+S-ABS$$
 (102)

and by neglecting the small term ABS, one obtains

$$A = B+S . (103)$$

There is a fraction  $N_B^2(B^2+BS)$  of two electrons transferred from the negatively charged ligand to the positively charged metal via the bonding function  $\phi_B$ . A fraction  $N_A^2(A^2-AS)$  of one electron is transferred in the opposite direction via the antibonding orbital to give a net electron transfer  $N_A^2(A^2-AS)$  from p to d. Since the orbitals with spin up  $\uparrow$  are each singly occupied, the only measurable electron transfer is that associated with the bonding electron with spin down  $\downarrow$ , or alternatively with the antibonding hole with spin up  $\uparrow$ . Because the hyperfine interaction drops off as  $1/r^3$  the overlap contribution is small and the fractional spin density transferred to the ligand is

$$f \simeq A^2 N_A^2 \quad . \tag{104}$$

That is, the transferred spin is just the square of the antibonding ligand coefficient.

In the configuration interaction (CI) approach the ionic nature of the complex is emphasized. The ground state is considered to be  $(M^{+n})(L^{-})$  and the wavefunction is a many-electron Slater determinant

$$\Psi g = (3)^{\frac{1}{2}} | \frac{+-+}{ppd} |$$
 (105)

where the spin is represented by the superscript + or - for  $m = \pm^{l_2}$ . A small amount of the excited state consisting of  $(M^{n-1})(L^0)$ , where the ligand has completely transferred one electron with spin down + to the metal, is admixed into the ground state by configuration interaction leading to a new wavefunction

$$\Psi g = N(\Psi g + C\Psi_{P}) \tag{106}$$

where N=1, C is small and  $\Psi_e = (3)^{\frac{1}{2}} \begin{vmatrix} +-+\\ pdd \end{vmatrix}$ . The fraction of unpaired spin on the ligand is

$$f = c^2 N^2$$
, (107)

a result that is formally analogous to the MO method.

In the past decade, the relative merits of the molecular orbital and configuration interaction methods have been explored by performing a host of non-empirical calculations on the  $(\text{NiF}_6)^{4-}$  "cluster" ion. In the "cluster" ion approximation, the remainder of the crystal is ignored except in that it creates a Madelung-type electrostatic potential at the ion. Table 3 gives a comparison of the 10Dq,  $f_{\sigma}(\%)$  and  $f_{s}(\%)$  values determined experimentally with those calculated from the crystal-field (CF), molecular orbital and configuration interaction theories. 10Dq for  $(\text{NiF}_6)^{4-}$  is defined as the energy separation between the ground  $(t^6e^2)^3A_{2g}$  state and the first excited state  $(t^5e^3)^3T_{2g}$ .

TABLE 3. -- Comparison of calculated with experimental parameters for  $(NiF_6)^{4-}$ 

Method	10Dq(cm <sup>-1</sup> )	f <sub>0</sub> (%)	f <sub>s</sub> (%)	Reference
Experiment	7250	3.8	0.5	$(1963)^{60,61}$
Calculated CF	1514			(1970) <sup>57</sup>
Calculated CF	-3572			(1971) <sup>58</sup>
Calculated MO	2800	1.0	0.3	(1964) <sup>97</sup>
Calculated CI	5400	2.9	1.0	(1966) <sup>98</sup>
Calculated MO	6089	4.8	0.4	(1970) <sup>57</sup>
Calculated MO	7210	3.3	0.4	(1971) <sup>59</sup>

The crystal-field calculation gives values of 10Dq too small and can even reverse the known energy levels. Earlier calculations seemed to favor the CI approach over the MO technique. However, larger and faster computers have allowed workers to include the closed shell orbitals, to calculate directly the energies of excited states and explicitly include three- and four-center integrals. Thus, recent MO calculations have shown good agreement with the experimental observables. The successful MO calculations are appealing to chemical intuition because complexes such as the dithiolate compounds, 53 where ~ 50% of the unpaired spin density is on the ligands, are difficult to picture in the CI framework. Also, the bulk of experimental ESR results has been analyzed by the MO technique; therefore, the MO scheme will be followed in this thesis to analyze the ligand hyperfine splittings.

#### Sample Calculation

The analysis of ligand hyperfine splittings in the complex ion  $(PdCl_4)^{3-}$  will serve an example. The ion is assumed to have the same square-planar arrangement of chlorines about the central metal atom as in the parent  $(PdCl_4)^{2-}$  ion. The ground state in  $D_{4h}$  point-group symmetry should be  $(d^9)^2B_1$  with the unpaired electron in the  $d_x2-y2$  orbital. A metal coordinate axes system (XYZ) for this radical is defined so that the Z axis is the unique  $C_4$  rotation axis. Each chlorine nucleus is assumed to have its own local right-handed Cartesian coordinate system (xyz) with each x axis directed toward the metal atom (Figure 2).

The  $b_{lg}$  antibonding orbital containing the unpaired electron is

$$|b_{1g}\rangle = \alpha |x^2 - y^2\rangle - \frac{1}{2}\alpha' |\sigma_1 - \sigma_2 + \sigma_3 - \sigma_4\rangle$$
 (108)

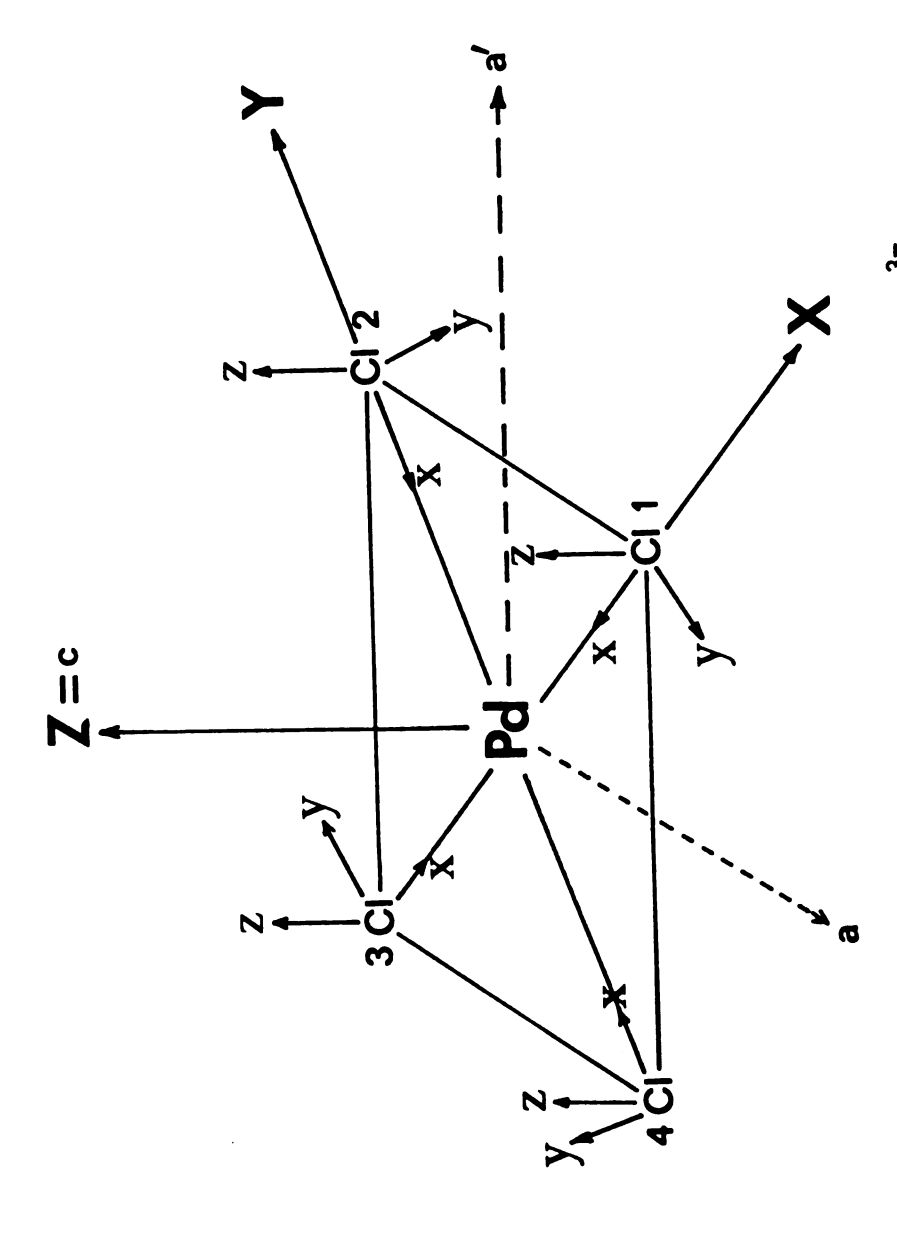


Figure 2. Axis system for metal (X,Y,Z) and ligand (x,y,z) atoms in  $(PdCl_4)^{3-}$ .

where the chlorine o orbitals are

$$|\sigma_{i}\rangle = n|3p_{x}\rangle_{i} + (1-n^{2})^{\frac{1}{2}}|3s\rangle_{i}$$
 (109)

Normalization gives

$$1 = \alpha^2 + \alpha^{\prime 2} - 4\alpha\alpha^{\prime} S \tag{110}$$

where S is the overlap integral,  $\langle x^2-y^2|\sigma_1\rangle$ .

The ligand hyperfine spin Hamiltonian for the  $\sigma$  orbitals is expected to be axially symmetric with the x axis being the unique axis:

$$H_{L} = A | |s_{x}I_{x} + A_{\perp}(s_{y}I_{y} + s_{z}I_{z}) .$$
 (111)

By symmetry, it is possible to focus attention on one of the ligands and simply multiply the spin density obtained for that ligand by four to get the total transferred spin density. The expectation value of  $H_L$  for  $b_{1g}$  retaining only those terms containing  $\sigma_1$ , is

$$\langle b_{1g} | H_{L} | b_{1g} \rangle = -\alpha \alpha' \langle x^{2} - y^{2} | H_{L} | \sigma_{1} \rangle + \frac{\alpha'}{4} \langle \sigma_{1} | H_{L} | \sigma_{1} \rangle + \frac{4}{\Sigma} \frac{\alpha'}{2} \langle \sigma_{j} | H_{L} | \sigma_{1} \rangle$$
(112)

The third term, involving integrals of Cl<sub>1</sub> with the other three chlorine nuclei, is dropped because the  $r^{-3}$  dependence of the hyperfine splitting makes the term vanishingly small. The first term would be dropped for the same reason except that the coefficient  $\alpha$  is large; that is, the majority of the unpaired electron density resides on the metal. To the ligand nucleus, the spin in  $d_{x^2-y^2}$  appears to be concentrated at the

metal nucleus and the interaction behaves as a direct dipole term which can be written

$$H_{d} = \Lambda_{d}(2s_{x}I_{x}-s_{y}I_{y}-s_{z}I_{z})$$
(113)

where  $A_d = gg_n\beta\beta_n$   $R^{-3}$  and R is the metal-ligand distance. The second term is evaluated with the hyperfine Hamiltonian of Equation (71) where  $\ell=1$ ,  $\xi=2/5$ ,  $P=g_eg_n\beta\beta_n\langle r^{-3}\rangle_{3p}$  for a chlorine 3p electron and the  $(\overline{\ell}\cdot\overline{1})$  contribution is zero for an orbital singlet. There results

$$H_{\overline{I}} = -\kappa (\overline{s} \cdot \overline{I}) - 3/5P\{-4/3(\overline{s} \cdot \overline{I}) + (\overline{\ell} \cdot \overline{s})(\overline{\ell} \cdot \overline{I}) + (\overline{\ell} \cdot \overline{I})(\overline{\ell} \cdot \overline{s})\} . \tag{114}$$

The components of the second term for  $S=\frac{1}{2}$  are

$$\langle \sigma_{1} + | (H_{L})_{x} | \sigma_{1}^{+} \rangle = \frac{\alpha'^{2}}{4} \langle \sigma_{1} + | \{ (n+1)_{\kappa} + \frac{4n^{2}}{5} P \}_{s_{x}} I_{x} | \sigma_{1}^{+} \rangle$$

$$\langle \sigma_{1} - | (H_{L})_{y} | \sigma_{1}^{+} \rangle = \frac{\alpha'^{2}}{4} \langle \sigma_{1} - | \{ (n^{2}-1)_{\kappa} - \frac{2n^{2}}{5} P \}_{s_{y}} I_{y} | \sigma_{1}^{+} \rangle$$

$$\langle \sigma_{1} - | (H_{L})_{z} | \sigma_{1}^{+} \rangle = \frac{\alpha'^{2}}{4} \langle \sigma_{1} - | \{ (n^{2}-1)_{\kappa} - \frac{2n^{2}}{5} P \}_{s_{z}} I_{z} | \sigma_{1}^{+} \rangle$$

$$\langle \sigma_{1} - | (H_{L})_{z} | \sigma_{1}^{+} \rangle = \frac{\alpha'^{2}}{4} \langle \sigma_{1} - | \{ (n^{2}-1)_{\kappa} - \frac{2n^{2}}{5} P \}_{s_{z}} I_{z} | \sigma_{1}^{+} \rangle$$

$$\langle \sigma_{1} - | (H_{L})_{z} | \sigma_{1}^{+} \rangle = \frac{\alpha'^{2}}{4} \langle \sigma_{1} - | \{ (n^{2}-1)_{\kappa} - \frac{2n^{2}}{5} P \}_{s_{z}} I_{z} | \sigma_{1}^{+} \rangle$$

If one adds the direct dipole term of Equation (113) to Equation (115) and compares corresponding elements with the phenomenological Equation (111), one finds

$$A \mid | = A_s + 2(A_p + A_d)$$
  
 $A \mid = A_s - (A_p + A_d)$ , (116)

where

$$A_{s} = \frac{\alpha^{2}^{2}}{4} (n^{2}-1)_{\kappa}$$

$$A_{p} = \frac{\alpha^{2}n^{2}}{4} (\frac{2P}{5}).$$
(117)

 $A_{||}$  and  $A_{||}$  are known experimentally, and  $A_{d}$  can be calculated if R is known, hence  $A_{s}$  and  $A_{p}$  may be computed readily.

The transferred spin densities to the first chlorine are

$$f_{S} = \frac{A_{S}}{A_{S}^{0}} = \frac{\alpha'^{2}}{4} (1-n^{2})$$

$$f_{p} = \frac{A_{p}}{A_{p}^{0}} = \frac{n^{2}\alpha'^{2}}{4} ,$$
(118)

where

$$A_s^{o}(^{35}C1) = (\frac{8\pi}{3})g_eg_n\beta\beta_n | \Psi 3s(0) |^2 = 1570 \times 10^{-4}cm^{-1}$$

$$A_p^{o}(^{35}C1) = (2/5)g_eg_n\beta\beta_n \langle r^{-3} \rangle_{3p} = 46.75 \times 10^{-4}cm^{-1}$$
(119)

are obtained from  $|\Psi_{3s}(0)|^2$  and  $\langle r^{-3} \rangle_{3p}$  which, in turn, have been taken from the Hartree-Fock calculations for free chlorine atoms with configurations (3s3p<sup>6</sup>) and (3s<sup>2</sup>3p<sup>5</sup>), respectively.<sup>99</sup> The coefficients n<sup>2</sup> and  $\alpha^{,2}$  are also obtained, as is the hybridization ratio p/s = n<sup>2</sup>/(1-n<sup>2</sup>).

The most serious approximations in the ligand hyperfine interaction are:

a) Core polarization of the chlorine 1s and 2s orbitals by the unpaired electron spin in the  $3p_{\mathbf{X}}$  orbital has been neglected

and the entire isotropic hyperfine component has been attributed to spin density in the valence shell 3s orbitals. 100

This suggests that only the anisotropic ligand term should be used to estimate spin densities and covalency just as was done in estimating covalency from the metal hyperfine splitting.

- b) Since the chlorine is essentially C1<sup>-</sup>,  $|\Psi_{38}(0)|^2$  and  $\langle r^{-3}\rangle_{3p}$  should be evaluated for the ionic species. <sup>101</sup> However, in this thesis the usual convention of taking  $|\Psi_{38}(0)|^2$  and  $\langle r^{-3}\rangle_{3p}$  from the C1<sup>o</sup> wavefunctions will be followed. This facilitates making comparisons with ESR studies in the literature.
- c) The point-dipole correction, A<sub>d</sub>, is only the leading term in a multipole expansion and is only rigorously correct for a spherical electron charge distribution on the metal 102 (<u>i.e.</u>, a half- or completely-filled shell).

#### **EXPERIMENTAL**

### ESR System

The ESR system and the techniques employed have been discussed in the Ph.D. thesis of Kuska. The measurements were performed on a Varian Associates (VA) X-band, Model V-4500-10A ESR spectrometer with 100kHz modulation and a 12-inch VA electromagnet. The magnetic field was measured with a marginal-oscillator NMR probe 103 and the resulting NMR proton frequency was counted on a Hewlett-Packard (HP) Model 524C electronic counter. The magnetic field for protons in a water sample is calculated from the following equation:

$$H(Gauss) = (2.3487465 \times 10^{-4}) \nu(Hertz).$$
 (120)

Microwave frequencies were measured by either a calibrated TS-148/UP

U. S. Navy spectrum analyzer or with a Hewlett-Packard Model 5245L

frequency counter equipped with a Hewlett-Packard Model 5257A transfer
oscillator. All of the spectra were recorded on a Moseley XY recorder.

### Sample Preparation

Samples of K<sub>2</sub>PdCl<sub>4</sub> and (NH<sub>4</sub>)<sub>2</sub>PdCl<sub>4</sub> were obtained from both Engelhard Minerals and Chemicals and the Matthey Bishop Company. K<sub>2</sub>PtCl<sub>4</sub> was prepared from platinum metal by oxidation with aqua regia<sup>104</sup> to give H<sub>2</sub>PtCl<sub>6</sub>, and K<sub>2</sub>PtCl<sub>6</sub> was then precipitated by addition of KCl. The K<sub>2</sub>PtCl<sub>6</sub> was reduced with hydrazine hydrochloride to give K<sub>2</sub>PtCl<sub>4</sub>. <sup>105</sup> All residues were saved and reworked when necessary. Single crystals were grown from slightly acidified (HCl) aqueous solutions of the salts by using seed crystals.

 $K_2Pt(CN)_4 \cdot 3H_2O$  was prepared from  $K_2PtCl_4$  in aqueous solution by addition of KCN followed by filtration and repeated recrystallizations from water solutions. Single crystals were grown by slow crystallization from water solution and had to be stored in a high-humidity atmosphere to prevent loss of water.

The bromine bridged complex, tetraethylammonium tetrabromo- $\mu\mu$ ' dibromoplatinum II,  $(N(C_2H_5)_4)Pt_2Br_6^{106a}$  was prepared by the method of Harris et al. 106b and single crystals were grown from acetone solutions of the salt.

# Crystal Structure of K<sub>2</sub>(Pd,Pt)Cl<sub>4</sub><sup>107</sup>

 $K_2PdCl_4$  and  $K_2PtCl_4$  are isostructural: the space group is  $D_{4h}^1$ -P4/mmm with Z=1 and  $a_0 = 7.04 \mbox{Å}$ ,  $c_0 = 4.10 \mbox{Å}$  for Pd and  $a_0 = 6.98 \mbox{Å}$ ,  $c_0 = 4.13 \mbox{Å}$  for Pt. Each metal atom is surrounded by four equivalent chlorines at a distance of 2.33 \mbox{Å}. These square-planar units are stacked along the c axis in alternate lamellae with the potassium cations

(Figure 3). The crystals almost always grow as rectangular needles with the c axis the needle axis and (100) and (010) forming the faces.

#### Irradiation Methods

Crystals suitable for irradiation (approximately 2 x 2 x 4 mm) were optically selected with the aid of a polarizing microscope with crossed Nicol prisms. In this manner, crystals that were twinned or had large imperfections could be discarded or cleaved perpendicular to the c axis. Crystals to be irradiated with the <sup>60</sup>Co y-ray source were placed in glass vials and immersed in a Dewar of liquid nitrogen. Dewar was placed in the center of the Michigan State University 60Co  $\gamma$ -source and subjected to 6 x  $10^6$  rads. Crystals to be irradiated by electrons were placed in Saran-wrap containers which were buoyed up by foamed polystyrene balls weighted to just float on liquid nitrogen in a Dewar. If the crystals were allowed to sink in the liquid nitrogen the electron beam was severely attenuated. The Dewar was placed approximately four inches below the tip of the 1-MeV electron source at Michigan State University and then subjected to a dose rate of  $3 \times 10^6$  rad/min for three minutes. A lower dosage gave a reduced paramagnetic signal intensity whereas doses above 3 x 10<sup>7</sup> rads produced appreciable crystal fracture and crumbling. The same crystal could be reirradiated at least twice before the physical damage was too severe to allow handling without breakage.

Experiments were conducted to measure the change in the ESR spectra of  $\gamma$ -damaged crystals upon exposure to ultraviolet irradiation. The beam of a General Electric BH6 mercury lamp was focused through the

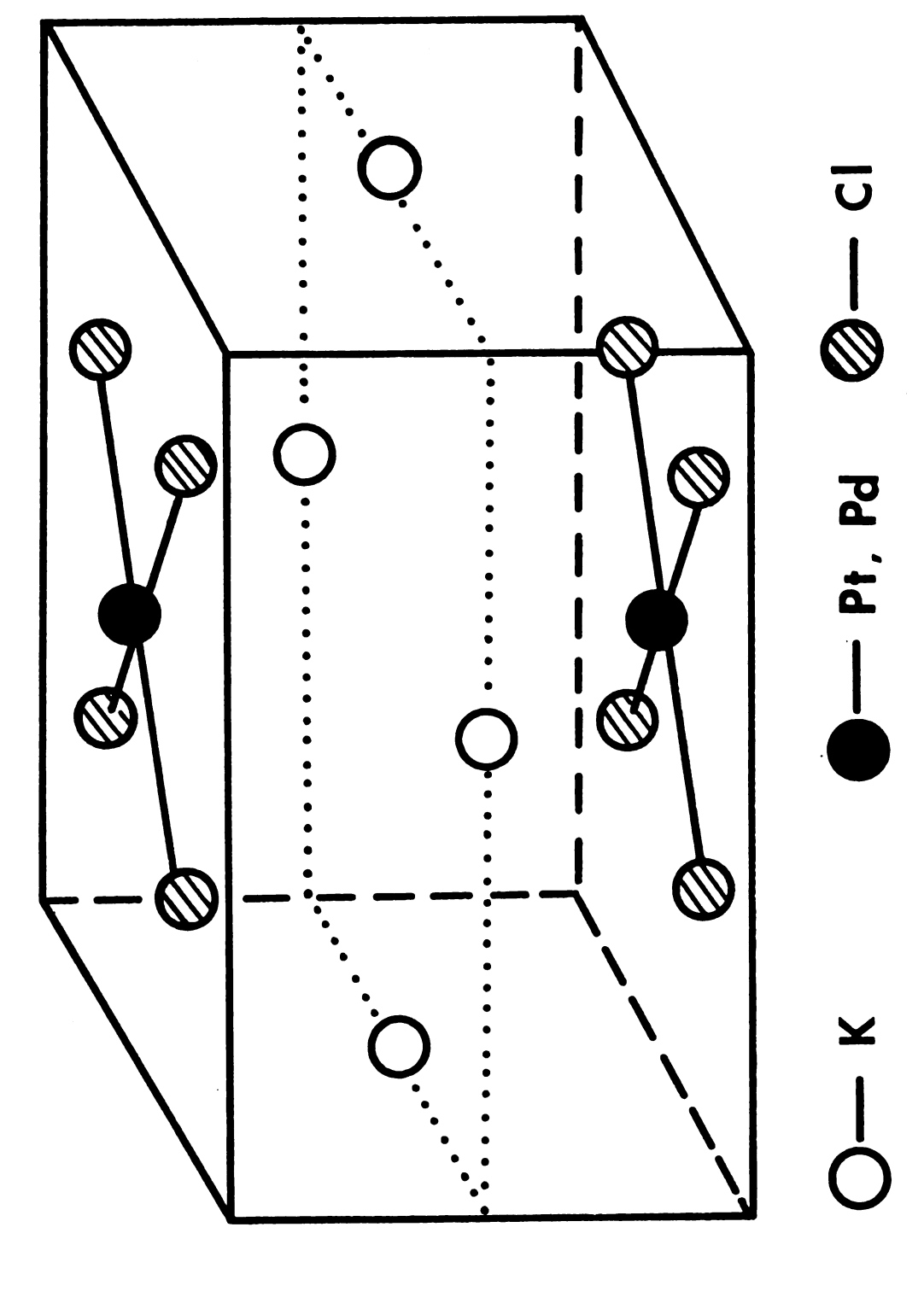


Figure 3. Crystal structure of  $\mathrm{K}_2\mathrm{PdCl}_4$  and  $\mathrm{K}_2\mathrm{PtCl}_4$ .

port of a VA Model V-4531 general purpose ESR cavity and onto the crystal which was cooled to liquid nitrogen temperature (both the lens and Dewar were quartz).

### Sample Handling

The sample handling technique was similar to that used by Kispert. 108 Because of the temperature sensitivity of the paramagnetic radicals formed in irradiated crystals of K2PtCl4 and K2PdCl4 (no radicals remain at room temperature), sample transfer, mounting and other manipulations of the crystals were all performed under liquid nitrogen. The crystals were clamped between two brass clips which were glued to the end of a quartz rod and then the entire assembly was immersed in a glass Dewar filled with liquid nitrogen. The bottom of the Dewar had a quartz finger of the proper dimensions to just fit into the Varian Associates general-purpose, T<sub>102</sub> mode, X-band cavity, Model V-4531. rod was held centered in the Dewar by a cylindrical foam insert at the top of the Dewar while the sample was centered vertically in the cavity until the signal was maximized. The initial setting of the crystal in the plane of rotation was done by visual alignment of the external crystal faces with the quartz rod. This alignment was refined by physically reorientating the sample. The oscilloscope mode of signal display was also used occasionally to refine the alignment or to find a principal axis of the radical. The angular variation in each plane of rotation was measured by either rotating the Dewar in the cavity and measuring the angle of rotation on a machined protractor or by rotating the calibrated Normally, three independent planes of rotation are employed to

obtain the magnetic tensors; however, in this case, the high degree of crystal symmetry reduced the necessary rotations to two. Accordingly, the spectra were recorded at 10° intervals with the external magnetic field in the ac and aa' planes.

## Error Analysis

The error introduced into the measured g values may be estimated by taking the total derivative of  $g = h\nu/\beta H$ 

$$dg = (\partial g/\partial H)_{\nu} dH + (\partial g/\partial \nu)_{H} d\nu \qquad (121)$$

which reduces to

$$\Delta g = \pm g(|2\Delta H/H| + |\Delta v/v|)$$
 (122)

where the factor of two arises because the magnetic field must be measured both up and down field from the center of the pattern. The proton resonance from the marginal oscillator provides an absolute field measurement limited by the precision of the fundamental constants and the accuracy of the HP 524C counter (±20 Hz). At a microwave frequency of  $10^4$  MHz and a g value of 2, the proton resonance will occur at approximately 15 MHz ±20 Hz, a very small percentage error compared to that arising from the field inhomogeneity.

Since the water probe of the marginal oscillator was located outside the cavity on the magnet pole face it was important to estimate whether the field at the sample differed from that at the NMR probe. For

this purpose a dual-probe assembly was constructed which permitted a comparison of the field at the two positions; this revealed a field difference of about 0.25 Gauss which was neglected.

The error in frequencies measured with the spectrum analyzer is less than  $\pm 0.5$  MHz. Thus, for a spectrum centered at g = 2.00 with H  $\simeq 3500$  Gauss and  $\nu$  (microwave)  $\simeq 10,000$  MHz, Equation (122) gives

$$\Delta g \approx \pm 0.0001$$
 . (123)

A larger error is introduced in the magnetic field measurement because of the finite linewidths in transition-metal ESR spectra. In a first-derivative presentation of the absorption spectrum, the point of inflection (crossover point) mid-way between the peak and valley becomes successively more difficult to determine exactly as the line width increases. Actually, in this research the limiting error is the error in crystal orientation which arises because crystals must be mounted under liquid nitrogen without the aid of a polarizing microscope or of X-ray methods for establishing the location of crystal axes. The error  $\Delta g$  in the g value of a radical with axial symmetry based upon an angular error,  $\Delta \theta$ , in orientation is

$$g = \pm \left| \left\{ \left( g_{\perp}^2 - g_{\parallel}^2 \right) / g \right\} \cos \theta \sin \theta \Delta \theta \right|$$
 (124)

where  $g^2$  is given in Equation (99). As an example, let  $\Delta\theta = 1^\circ$  or  $2^\circ$  in the data for the determination of  $g_{||}$ , where  $g_{||} = 2.500$  and  $g_{||} = 2.000$ . Then

$$\Delta\theta = 1^{\circ}, \ \Delta g = \pm 0.0035$$

$$\Delta\theta = 2^{\circ}, \ \Delta g = \pm 0.014 . \tag{125}$$

Clearly, the larger the anisotropy  $(g_1^2 - g_1^2)$ , the larger is the potential error in  $\Delta g$ . For a fixed angular error, the maximum error in  $\Delta g$  occurs with  $\theta = 45^{\circ}$ . It is difficult to assess the angular error in a single measurement by the technique described earlier; hence, to minimize and bracket the error, replicate measurements on many crystals were made. Therefore, the errors in the spin-Hamiltonian parameters are reported as standard deviations, D, given by

$$D = \begin{pmatrix} \frac{n}{\Sigma} A_{i}^{2} - (\frac{n}{\Sigma} A_{i})^{2} / n \\ \frac{i=1}{(n-1)} \end{pmatrix}^{\frac{1}{2}},$$
 (126)

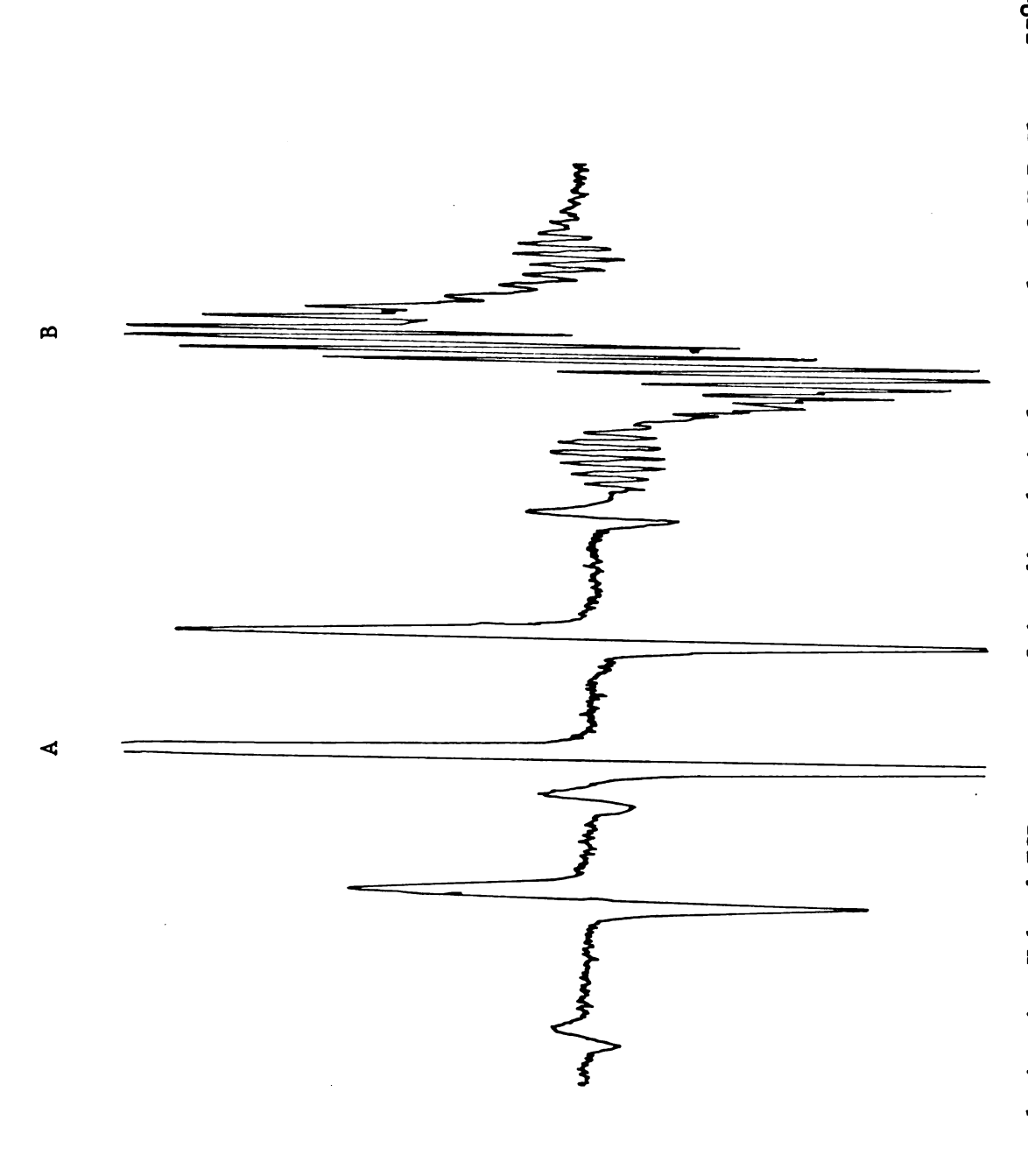
where  $A_i$  is the ith-individual observation of the n observations made. If there are less than six independent observations, the mean experimental deviation is reported.

RESULTS

K<sub>2</sub>PtC<sub>1</sub>4

### Introduction

At 77°K four distinct groups of ESR lines are observed in irradiated KoPtCl4 crystals. The two strongest sets are shown in Figure 4 with H | a. The intense group of six lines at low field (Set A) which is also seen with H | c, must belong to a radical containing two magnetically equivalent platinum nuclei; in the absence of experimental information concerning the ligands or charge, this radical will be designated as (Pt<sub>2</sub>). The second set of intense lines shown in Figure 4 at higher field (Set B) is also seen when H | c and is a triplet, each component of which shows superhyperfine splitting into ten lines. On the basis of these nuclear hyperfine interactions, this second radical is presumably (PtCl<sub>3</sub>)<sup>o</sup> or (PtCl<sub>3</sub>)<sup>2-</sup> and will, therefore, be tentatively designated (PtCl<sub>3</sub>)<sup>n-</sup>. A third set of lines of low intensity has ESR parameters essentially identical with those observed for  $(PdC1_4)^{3-}$  (see the Results and Discussion sections on K2PdCl4), but in Figure 4 the lines are obscured by the lines of Set B. This radical is attributed to palladium impurity which appears to be present in all available samples. A fourth feature of the spectrum is a weak, single line at g = 2.000 which, on warming, seems to resolve into a triplet of separation 6 Gauss; there is



The first derivative X-band ESR spectrum of irradiated single crystals of  $exttt{K}_2 exttt{PtCl}_4$  at  $77^0 exttt{K}$  with H|+a. Figure 4.

insufficient evidence to identify it and it will not be discussed further.

This fourth feature is too low in intensity to be seen under the conditions of Figure 4.

On warming the crystals from 77°K to about 108°K the (Pt<sub>2</sub>) lines slowly decrease in intensity and a new set of lines of lower intensity starts to grow in. At 125°K the (Pt<sub>2</sub>) lines are gone and the new set (Figure 5a), which shows hyperfine interaction with one platinum and one chlorine nucleus, has reached maximum intensity; this radical is tentatively designated as (PtCl) and its probable structure will be discussed later. With further warming the (PtCl<sub>3</sub>)<sup>n-</sup> lines disappear above 190°K. The (PtCl) spectrum is also gone by room temperature, where no stable radicals exist.

On irradiating the crystals at  $77^{\circ}$ K with the mercury vapor lamp the (Pt<sub>2</sub>) lines disappear rapidly and the (PtCl<sub>3</sub>)<sup>n-</sup> lines decrease in intensity slowly; the (PtCl) species was, however, never observed on illumination as it is on warming.

## (Pt<sub>2</sub>) Radical

The first-derivative spectra of the axially symmetrical radical (Pt<sub>2</sub>) are shown in the parallel (Figure 6a) and perpendicular (Figure 6b) orientations. Only a single magnetic site is observed for this radical. These spectra can be interpreted with the spin Hamiltonian of Equation (79) where  $S=\frac{1}{2}$ . Hyperfine coupling of the odd electron to two equivalent nuclei necessitates some care in constructing suitable nuclear spin wavefunctions. <sup>109</sup> In order to account for the second-order hyperfine interactions one must introduce the total nuclear spin operator  $\overline{I} = (\overline{I}_1 + \overline{I}_2)$  and associated representations  $|I, m_I\rangle$  where

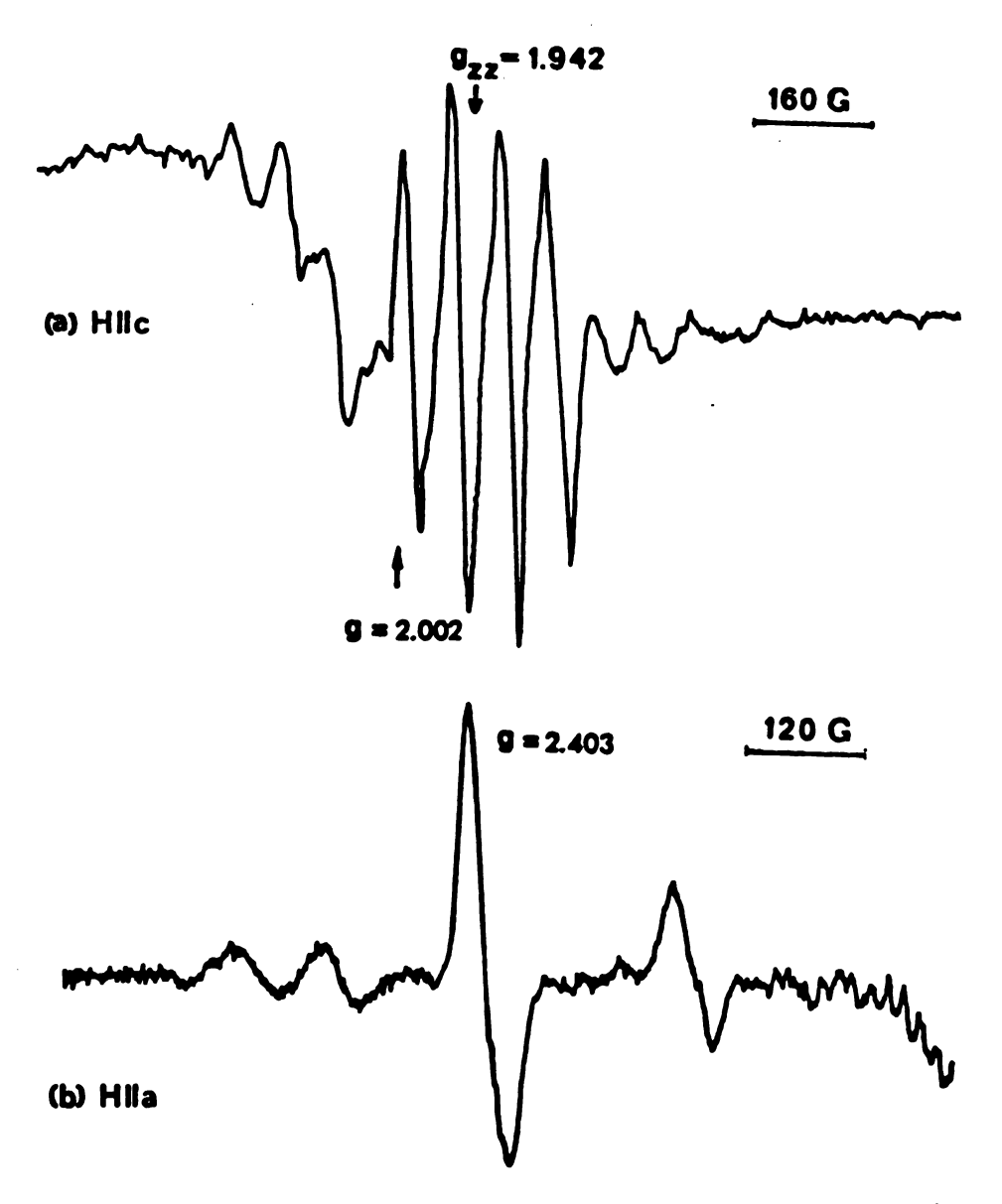


Figure 5. The first-derivative X-band ESR spectra of  $(PtCl_5)^{2-}$ :
(a) with H | | c, (b) with H | | a.

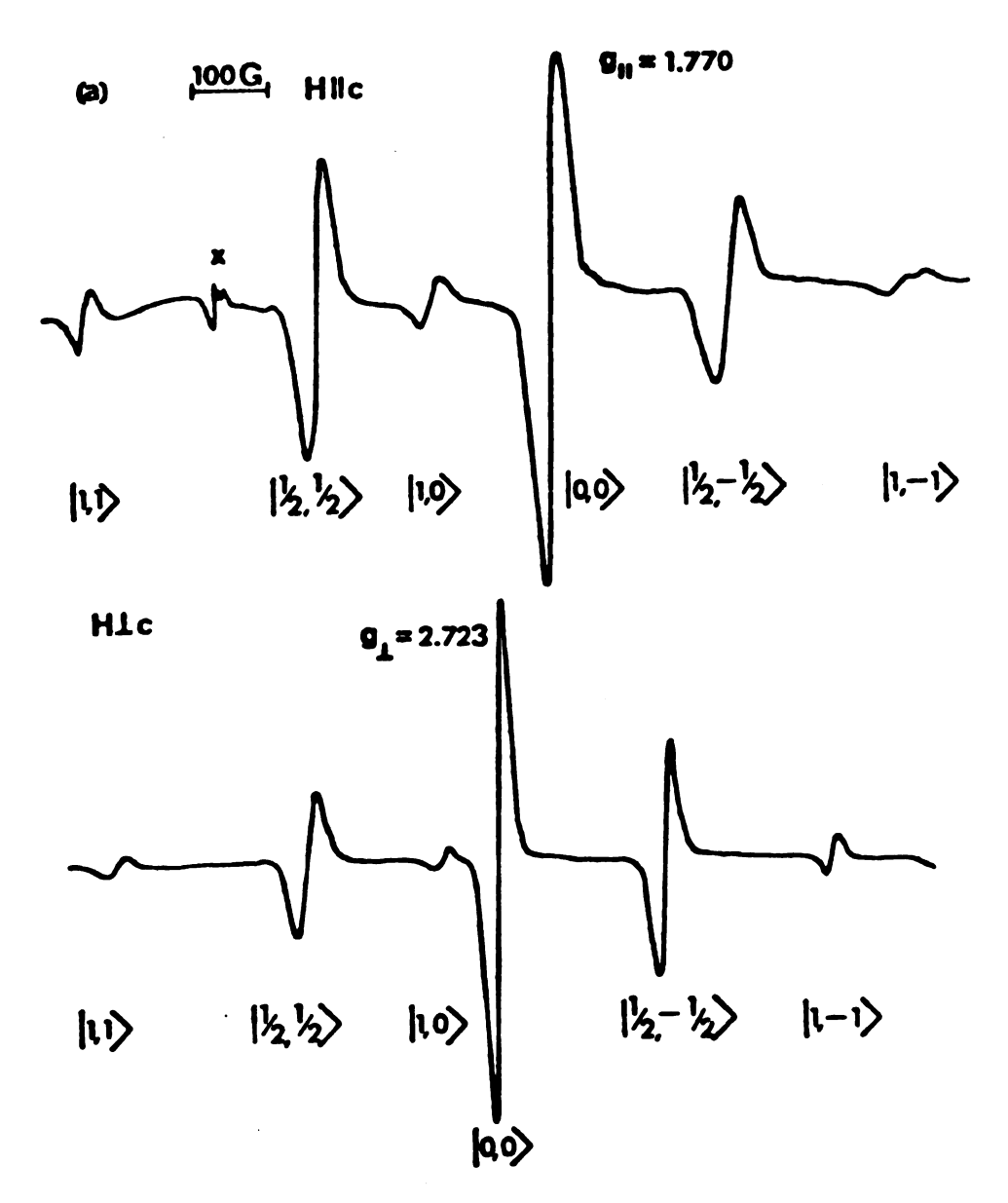


Figure 6. The first-derivative X-band spectra of  $(PtCl_4)_2^{3-}$  in irradiated single crystals of  $K_2PtCl_4$ : (a) with  $H \mid c$ , (b) with  $H \mid c$ . The feature marked X in (a) is centered at  $g \simeq 2.000$  and is from an unidentified species.

$$I = I_1 + I_2, I_1 + I_2 - 1, ..., I_1 - I_2 = 0$$
 $m_T = I, I - 1, ..., -I$ . (127)

The spin functions, representations, and degeneracies, along with the calculated and experimental relative intensities for the six-line (Pt<sub>2</sub>) radical, are given in Table 4. The line associated with the singlet product function  $(\alpha\beta-\beta\alpha)/\sqrt{2}$  is not shifted by either the first- or second-order hyperfine interaction and is therefore under the strong central line which is dominated by the radicals containing the non-magnetic platinum isotopes. The principal values of the g and A( $^{195}$ Pt) tensors that are listed in Table 5 under (Pt<sub>2</sub>) were calculated from Equations (99).

#### UV-Photobleaching Experiment

An ultraviolet (UV) photobleaching experiment was performed on  $\gamma$ -irradiated crystals of  $K_2PtCl_4$ , maintained at  $77^OK$ , with the light beam incident on the (100) face. The decrease in (Pt<sub>2</sub>) concentration was measured by recording the decrease of the ESR signal intensity as a function of UV exposure time. If the decrease in signal intensity (radical concentration) with time is assumed to be proportional to the instantaneous signal intensity (radical concentration) raised to some power, n, then

$$-dI \alpha I^{n}dt \qquad (128)$$

where I is the signal intensity and t is the time. A plot of the integral form of Equation (128) for n=2, that is  $(1/I-1/I_0)$  versus t, yields a straight line (see Figure 7) which implies that each reactive

TABLE 4. -- Representations and ESR intensities for the  $(\operatorname{PtCl}_4)_2^{3-}$  ion.

Nuclear Product Spin Functions <sup>a</sup>	Representations $ \mathtt{I.m_I}>$	Degeneracy	Calculated Relative Intensities	Experimental Relative Intensities <sup>b</sup>
α0 0α	1/2,1/2	2	7.87	7.53
80 08	1/2,-1/2	2	7.87	8.17
<b>8</b>	1,1		1.00	96.0
88	1,-1		1.00	0.97
$(\alpha\beta + \beta\alpha)/\sqrt{2}$	1,0		1.00	1.02
(ab - ba)/√2	<b>\o^*\o!</b>		16.48	16.48
00	<o.o < td=""><td>П</td><td></td><td></td></o.o <>	П		

a Here  $I_z |\alpha\rangle = 1/2 |\alpha\rangle$  and  $I_z |\beta\rangle = -1/2 |\beta\rangle$  as usual.

The relative intensity of the experimental line  $|0,0\rangle$  was chosen to be 16.48 for comparison with the calculated values. The other experimental intensities are mean values. م,

TABLE 5. -- ESR spectral parameters of radicals in irradiated crystals of  $K_2PtCl_4$ . a

Arbitrary Designation of Radical

 $(Ptc1) (PtC1) (PtC1_3)^{n-}$ 

Structure of Radical Assigned on Basis of ESR Data

(PtC1 <sub>4</sub> ) <sub>2</sub> <sup>3-</sup>	(PtCl <sub>5</sub> ) <sup>2-</sup>	(PtCl <sub>3</sub> ) <sup>2-</sup>	
g   = 1.771±0.001	$g_{zz} = 1.942 \pm 0.002$	$g_{zz} = 2.800 \pm 0.004$	
$g_{\perp} = 2.723 \pm 0.004$	$g_{XX} = 2.417 \pm 0.004$	$g_{XX} = 2.174 \pm 0.002$	
$A  (^{195}Pt) = 444\pm1$	$g_{yy} = 2.386 \pm 0.004$	$g_{zz} = 1.974 \pm 0.002$	
$A_{\perp}(^{195}Pt) = 618\pm3$	$A_{zz}(^{195}Pt) = 369\pm5$	$A(^{195}Pt) = 319\pm 4$	
	$A_{zz}(^{195}Pt) = 369\pm5$ $A_{xx}(^{195}Pt) \simeq A_{yy}(^{195}Pt) = 455\pm5$	$A(^{35,37}C1) = 15.1\pm0.1$	
	$A  (^{35,37}c1) = 56.8\pm1.0$	$A(^{195}Pt) = 360\pm 5$	
	$A_{\perp}(^{35,37}c1) = 15.6\pm2.5$	$A(^{195}Pt) = 360\pm5$ $A(^{35},^{37}C1) = 18.7\pm0.3$ H  a	

All hyperfine splittings are in units of  $10^{-4}$  cm<sup>-1</sup>. The errors listed are experimental standard deviations.

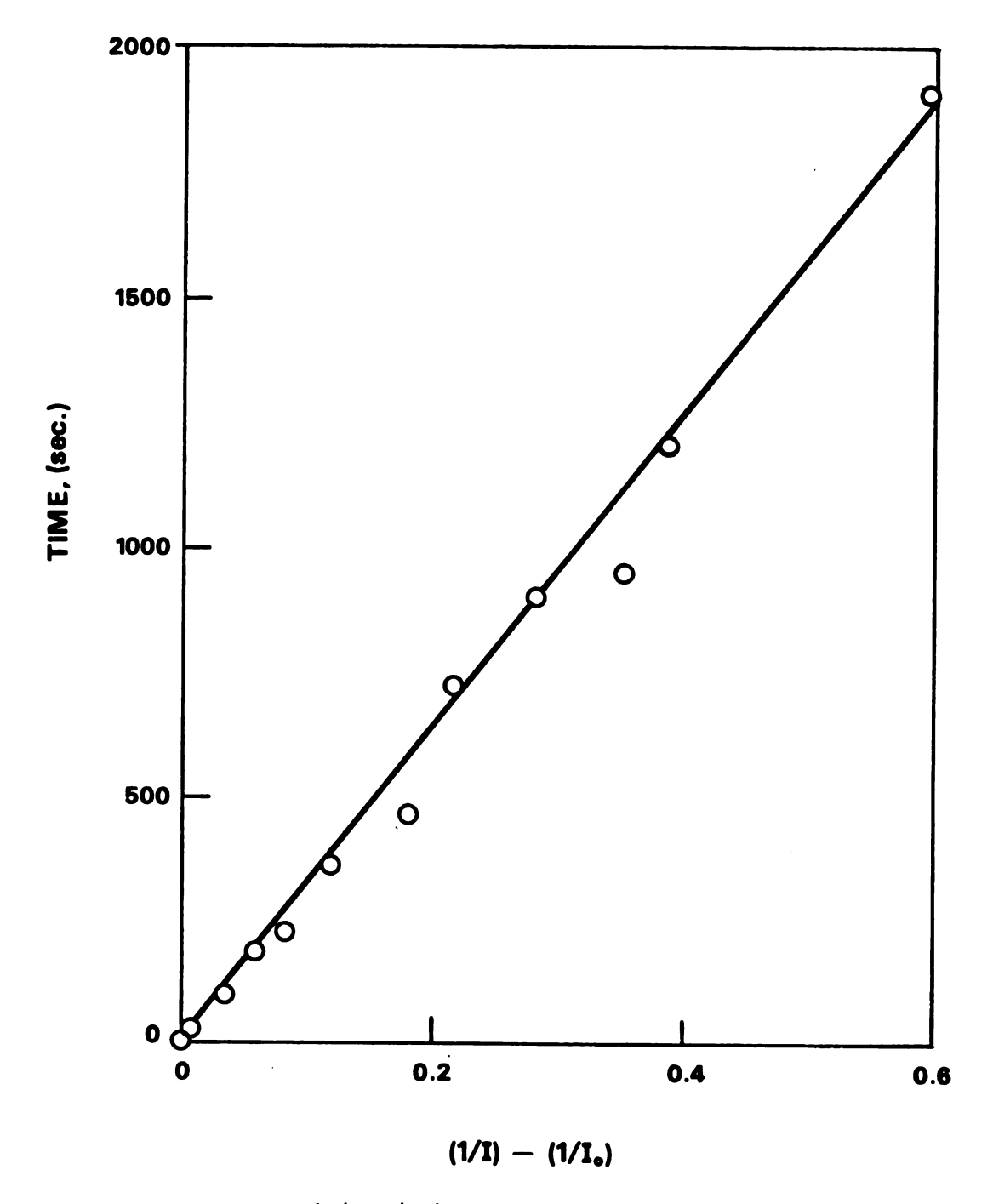


Figure 7. A plot of  $(1/I-1/I_0)$  versus time for the photobleaching decay of  $(PtCl_4)_2^{3-}$  indicates that the decay is second order in  $(PtCl_4)_2^{3-}$  concentration.

photon eliminates two (Pt<sub>2</sub>) radicals. This is apparently not a thermal effect since no new paramagnetic species appeared during or after the UV illumination unlike the warming experiments where (PtCl) is produced. The fact that two (Pt<sub>2</sub>) radicals are involved suggests that one unpaired electron is transferred through a conduction band (see Structure section below) from one (Pt<sub>2</sub>) to a second (Pt<sub>2</sub>) with the resultant production of four diamagnetic species.

## (PtCl) Radical

The first-derivative spectra of the (PtCl) radical with H||c and H||a are shown in Figures 5a and 5b, respectively. The spectrum of Figure 5a shows a central quartet plus two satellite quartets which arise from a species containing a single platinum atom; the central quartet belongs to those radicals containing the non-magnetic platinum nuclei and the satellites to those containing  $^{195}$ Pt (I= $^{1}$ 2, relative abundance 33.7%). The quartet superhyperfine splitting arises from interaction with one chlorine nucleus ( $^{35}$ Cl,  $^{37}$ Cl both I=3/2 with abundances 75.4% and 24.6%, respectively). Spectra from two magnetically nonequivalent sites are observed and these coalesce for H||c and for H||a (Figure 5). At no time could the  $^{35}$ Cl and  $^{37}$ Cl splittings be separated.

The spectra can be described by the usual spin Hamiltonian

$$H = \beta \overline{H} \cdot \overline{g} \cdot \overline{S} + \overline{S} \cdot (\overline{A} \cdot \overline{I})_{Pt} + \overline{S} \cdot (\overline{A} \cdot \overline{I})_{C1}$$
 (129)

where  $S=\frac{1}{2}$  and the smaller nuclear Zeeman and chlorine quadrupole terms are neglected.

During rotation with the external magnetic field in the ac plane the chlorine hyperfine interaction decreases from a maximum at H | c until,

at about 75° from the c axis, it disappears in the linewidth (peak-to-peak width about 37 Gauss). No chlorine splittings are observed when the magnetic field is in the aa' plane which precludes a complete determination of the principal chlorine hyperfine elements, but the symmetry of the platinum spin-Hamiltonian parameters suggests that the chlorine tensor will be nearly axial. For this reason only  $A_{\perp}(^{35},^{37}\text{Cl})$  is reported in Table 5 and it is a calculated value obtained from fitting the angular variation in the ac plane by Equations (131).

The principal values of the g,  $A(^{195}Pt)$  and  $A(^{35},^{37}C1)$  tensors are reported in Table 5. The  $g_{zz}$  element is parallel to the c axis while the  $g_{xx}$  and  $g_{yy}$  components bisect the aa' crystal axes. The two magnetically inequivalent sites are related by a  $90^\circ$  rotation about c.

# (PtCl<sub>3</sub>)<sup>n-</sup> Radical

The first-derivative spectrum of the  $(PtCl_3)^{n-}$  radical with  $H \mid c$  is shown in Figure 8a, and the second-derivative spectra with  $H \mid (110)$  and  $H \mid a$  in Figures 8b and 8c, all at X band. The g tensor has its maximum element  $g_{ZZ}$  coincident with the c axis while the  $g_{XX}$  and  $g_{YY}$  elements lie in the aa' plane at  $45^{\circ}$  to the a axis. There are two magnetically inequivalent sites related by a  $90^{\circ}$  rotation about the c axis and these become equivalent when  $H \mid a$  and  $H \mid c$ . The spectra at these two orientations consist of ten chlorine hyperfine lines with the correct intensity ratios for three equivalent chlorine nuclei. However, it has not been possible to analyze the spectra to give the complete chlorine and platinum hyperfine tensors and their direction cosines. Therefore, in Table 5, A(35,37c1) and A(195pt) are only reported for  $H \mid a$  and  $H \mid c$ .

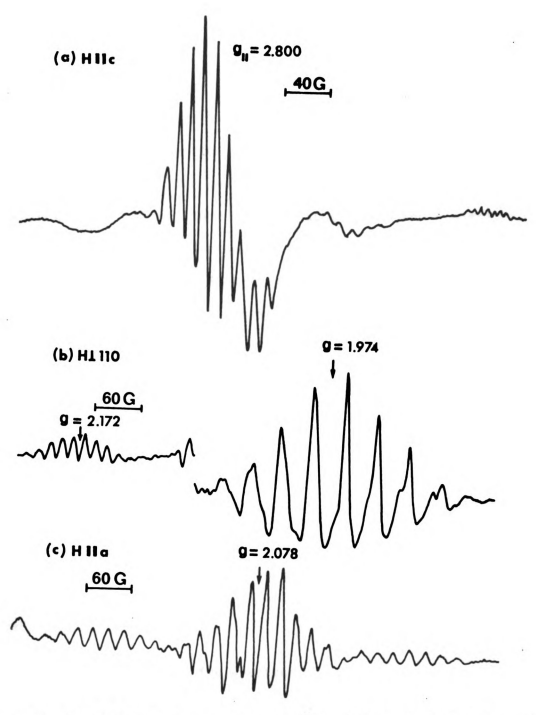


Figure 8. The X-band spectra of  $(\text{PtCl}_3)^{2^-}$ : (a) first-derivative,  $\text{H}[\cdot]c$ , (b) second-derivative,  $\text{H}[\cdot](10)$ , (c) second-derivative,  $\text{H}[\cdot]a$ .

## K<sub>2</sub>PdCl<sub>4</sub> and (NH<sub>4</sub>)<sub>2</sub>PdCl<sub>4</sub>

#### Introduction

The first-derivative ESR spectrum of irradiated single crystals of K<sub>2</sub>PdCl<sub>4</sub> shows three sets of lines when the magnetic field is parallel to the c axis (Figure 9). The set at lowest field belongs to a radical (Radical I) showing hyperfine interaction with one palladium and four equivalent chlorines. The central set of Figure 9 consists of a group of approximately twelve lines centered at g = 2.26 and appears to have two sets of hyperfine splittings (=22G. and =24G.) but these are observed only when the magnetic field is within 15° of the c axis; hence the parameters of the spin Hamiltonian could not be determined and the radical was not identified. The third set of lines (at high field) consists of four lines of equal intensity and spacing which is attributed to a radical designated as Radical II.

ESR spectra of irradiated single crystals of  $(NH_4)_2PdCl_4$ , which has the same crystal structure as  $K_2PdCl_4$ , show almost identical sets of lines as those attributed to Radical I and Radical II in  $K_2PdCl_4$ . However, the third and unidentified radical giving rise to the central set of lines in  $K_2PdCl_4$  was not observed in the ammonium salt.

#### Radical I

The second-derivative spectrum shown in Figure 10 is obtained when the external magnetic field is parallel to the c axis. The center of the spectrum is dominated by thirteen intense lines while the multiplets on either side of the central one have been recorded under a nearly fourfold greater amplification. Since palladium has only one naturally

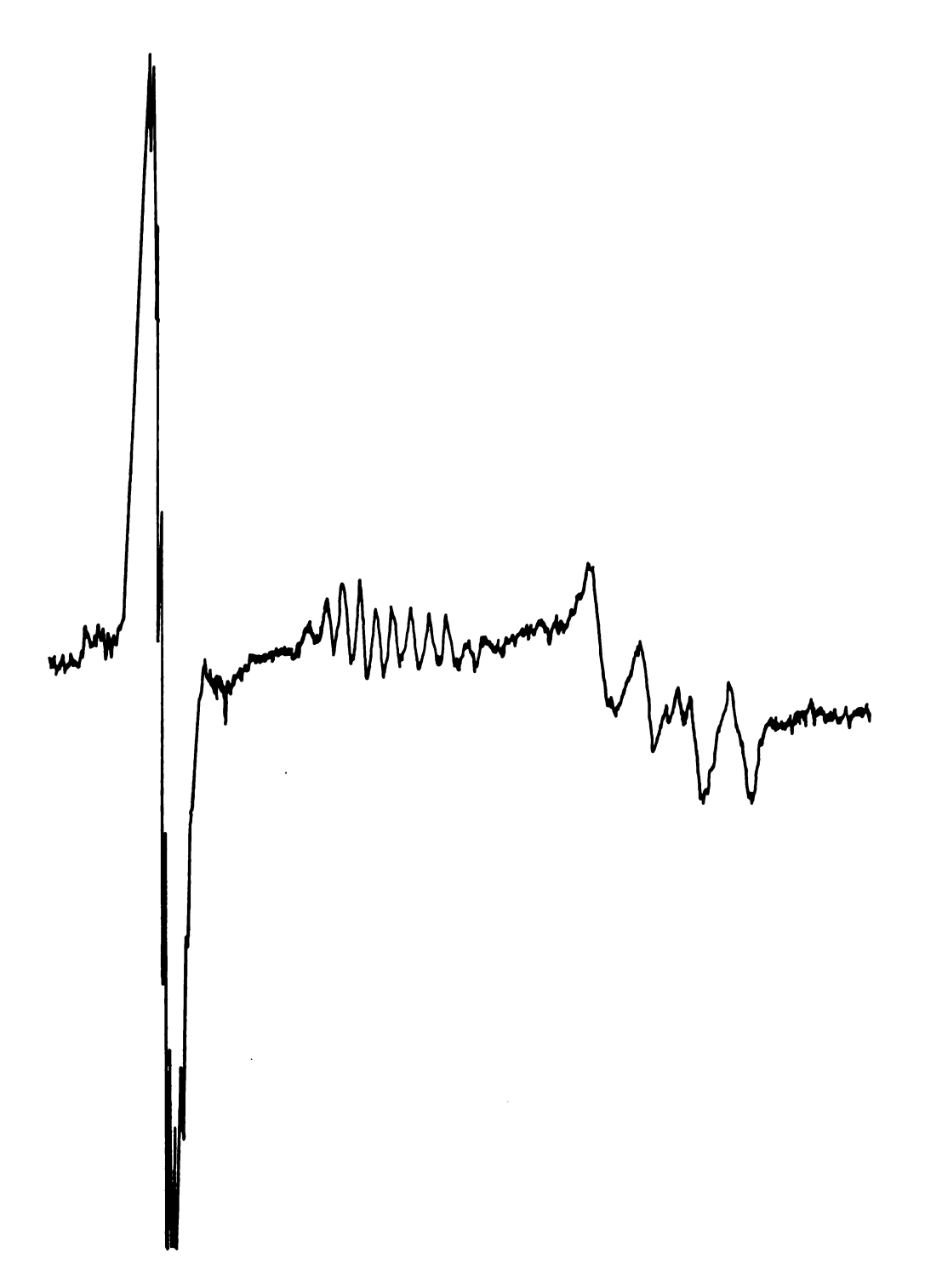


Figure 9. The first-derivative X-band ESR spectrum of irradiated  $K_2PdC1_4$  at  $77^{O}K$  with  $H\,|\,|\,c$  .

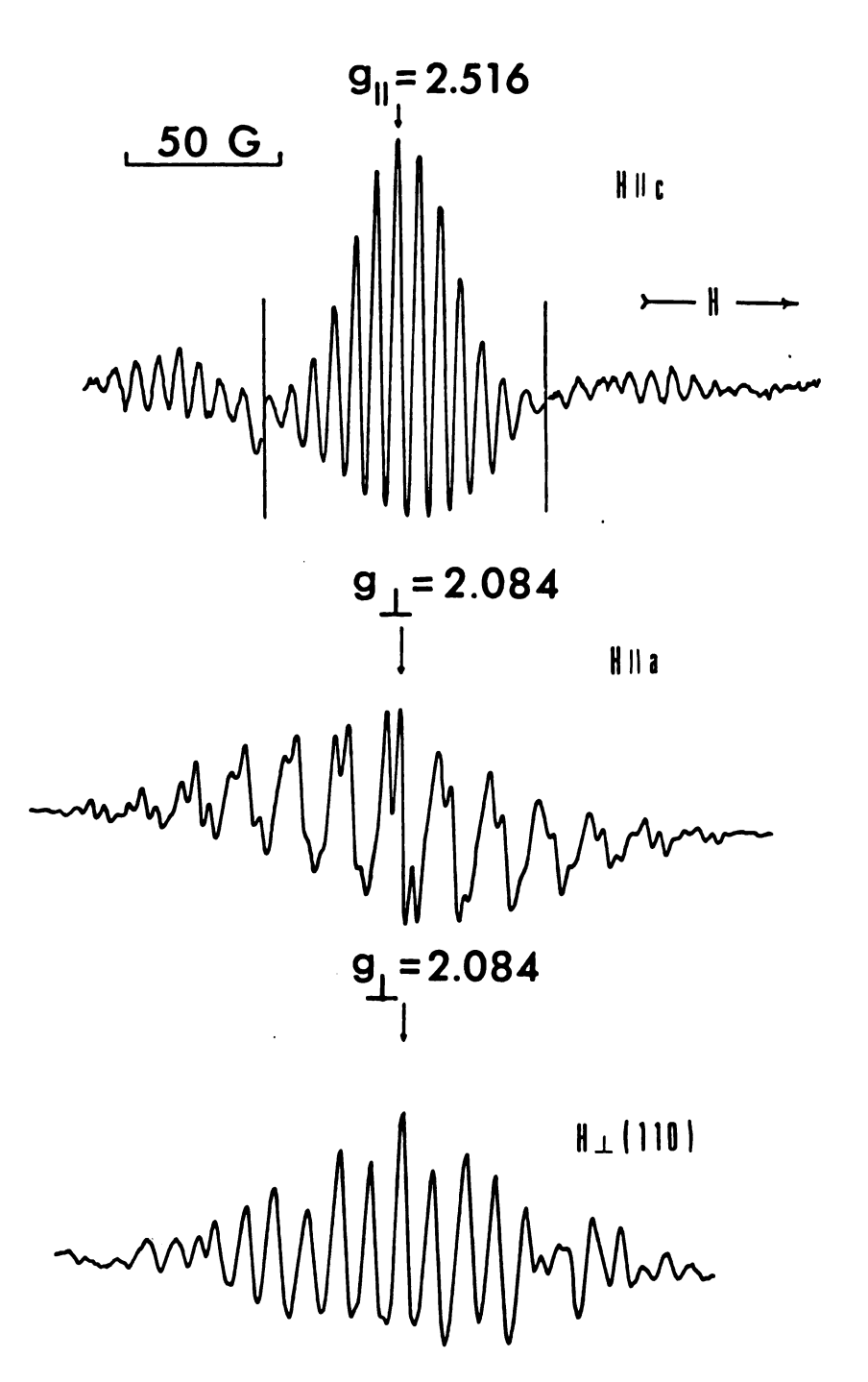


Figure 10. The X-band ESR spectra of irradiated single crystals of K<sub>2</sub>PdCl<sub>4</sub> showing the lines from the (PdCl<sub>4</sub>)<sup>3-</sup> radical ion: (top) second-derivative spectrum with H||c, (center) first-derivative spectrum with H||a, (bottom) second-derivative spectrum with H|(110).

occurring isotope with a nuclear spin ( $^{105}Pd$ ,  $^{1=5/2}$ , 22.3% relative abundance), a palladium-containing radical should show a strong central line from those species containing the palladium nuclei with even isotopes ( $^{1=0}$ ), plus six satellite lines (three on each side of the central line) each having a relative intensity 4.8% of the central line. The spectrum of Figure 10a may be interpreted on the above basis if each palladium line is split into a thirteen-line multiplet with relative intensities 1:4:10:20:31:40:44:40:31:20:10:4:1 by hyperfine interaction with four equivalent chlorine nuclei ( $^{35}$ , $^{37}$ Cl,  $^{1=3/2}$ ), and if the observable satellite multiplets are assigned to the palladium lines with  $^{105}$ Pd lines with  $^{105}$ Pd lines with  $^{105}$ Pd 2 (along with their chlorine hyperfine structure) while the  $^{105}$ Pd 1 assumed to lie buried beneath the strong central lines arising from the non-magnetic palladium nuclei. There is only one magnetic site for the ( $^{105}$ Pd)  $^{105}$ Pd  $^{105}$ 

On the basis of this analysis, the paramagnetic species is  $(PdCl_4)^{n-}$  with n=1 or 3. This assignment is strengthened by examination of the first-derivative spectrum shown in Figure 10b taken with H||a which now permits resolution of the  $^{35}$ Cl and  $^{37}$ Cl splittings. During a complete rotation of the field in the aa' plane, g and A( $^{105}$ Pd) remain constant and the spectrum repeats every  $90^{\circ}$ , thus demonstrating that the radical has retained  $D_{4h}$  symmetry and, presumably, the location of the original  $(PdCl_4)^{-2}$  anion. It will be shown below that the radical has a  $d^9$  configuration and must be identified as  $(PdCl_4)^{3-}$  so this formula will be used in the remaining discussion.

The experimental results can then be described by the spin Hamiltonian of Equation (79) for the metal (M) and the following spin Hamiltonian for the ligand (L):

$$H_{L} = A_{z}S_{z} \sum_{n=1}^{4} I_{zn} + \{A_{x}(I_{x1} + I_{x3}) + A_{y}(I_{x2} + I_{x4})\} S_{x} + \{A_{y}(I_{y1} + I_{y3}) + A_{x}(I_{y2} + I_{y4})\} S_{y}$$

$$(130)$$

where  $S=\frac{1}{2}$ , the right hand coordinate systems at palladium (X,Y,Z) and at each chlorine (x,y,z) are as in Figure 2, and the other symbols have their usual significance. Therefore, with  $H \mid |a|$  (Figure 10b) the four chlorines are equivalent and the thirteen lines are separated by  $A=\frac{1}{\sqrt{2}}(A_x^2+A_y^2)^{\frac{1}{2}}$ . When the external magnetic field is perpendicular to (110) (Figure 10c), there are two magnetically nonequivalent pairs of chlorine nuclei leading to a chlorine multiplet of forty-nine lines, simplified in this case by the accidental approximate equality  $A_x \approx 2A_y$ . The principal values of the g ,  $A(^{105}Pd)$  and  $A(^{35}C1)$  tensors are given in Table 6.

The same radical is formed in crystals of  $(NH_4)_2PdCl_4$  irradiated and observed at  $77^{\circ}K$  but the  $(PdCl_4)^{3-}$  radical in the latter crystal gives rise to broader lines (first-derivative peak-to-peak linewidths of  $\sim 6.0$  Gauss as opposed to  $\sim 2.5$  Gauss in the potassium salt), presumably as a result of interactions with the neighboring  $^{1}H$  and  $^{14}N$  nuclei.

Upon warming crystals of K<sub>2</sub>PdCl<sub>4</sub> which had been irradiated at  $77^{\circ}$ K, the lines from Radical I decay irreversibly with the decay becoming rapid at  $171^{\circ}$ K and complete at about  $200^{\circ}$ K. A plot of signal intensity  $\log(I/I_{\odot})$  versus  $1/T(^{\circ}$ K) shows two linear portions intersecting at approximately  $171^{\circ}$ K with activation energies  $\Delta E \simeq 1.4 \times 10^{2} \text{cm}^{-1}$  below  $171^{\circ}$ K and  $\Delta E \simeq 20 \times 10^{2} \text{cm}^{-1}$  above  $171^{\circ}$  (Figure 11). This implies two different modes of decay.

TABLE 6. -- Principal values of the spin-Hamiltonian tensors of radicals in γ-irradiated K<sub>2</sub>PdCl<sub>4</sub> and (NH<sub>4</sub>)<sub>2</sub>PdCl<sub>4</sub>.

Parameter	(PdC1 <sub>4</sub> ) <sup>3-</sup>	Parameter <sup>b</sup>	(PdC1 <sub>5</sub> ) <sup>2-</sup>
	K <sub>2</sub> PdC1	·4	
g	2.516±0.003	g <sub>c</sub>	2.012±0.001
g_	2.084±0.002	g <sub>a</sub>	2.149±0.004
$A  (^{105}Pd)$	35.7±0.2		
$A_{\perp}$ (105 <sub>Pd</sub> )	24.7±0.7		·
$A_{\mathbf{x}}(^{35}C1)$	(+)20.0±0.3	$A_c(^{35}C1)$	59.5±0.1
$A_y(^{35}C1)$	(+) 8.9±0.6	$A_a(^{35}C1)$	10.8±1.0
$A_z(^{35}C1)$	(+) 8.1±0.2		
	(NH <sub>4</sub> ) <sub>2</sub> Pd	C1 <sub>4</sub>	
g	2.561	gc	2.012
gŢ	2.090	A <sub>C</sub>	59.0
A     (105Pd)	32.2		
$A_{\perp}$ (105Pd)	<b>≃23.9</b>		

All hyperfine splittings are in units of  $10^{-4}$  cm<sup>-1</sup>. The errors listed are experimental standard deviations. The remaining parameters for the ammonium salt were not obtained with sufficient precision to list here but were quite similar to the corresponding values for  $K_2$ PdCl<sub>4</sub>.

The values of g and A along the a and c axes of the crystal have been written  $g_a$ ,  $A_a$  and  $g_c$ ,  $A_c$ , respectively. While  $g_c$ ,  $A_c$  are found directly experimentally the values of  $g_a$  and  $A_a$  are obtained by use of Equations (131) and the angular variation of the spectra in the ac plane.

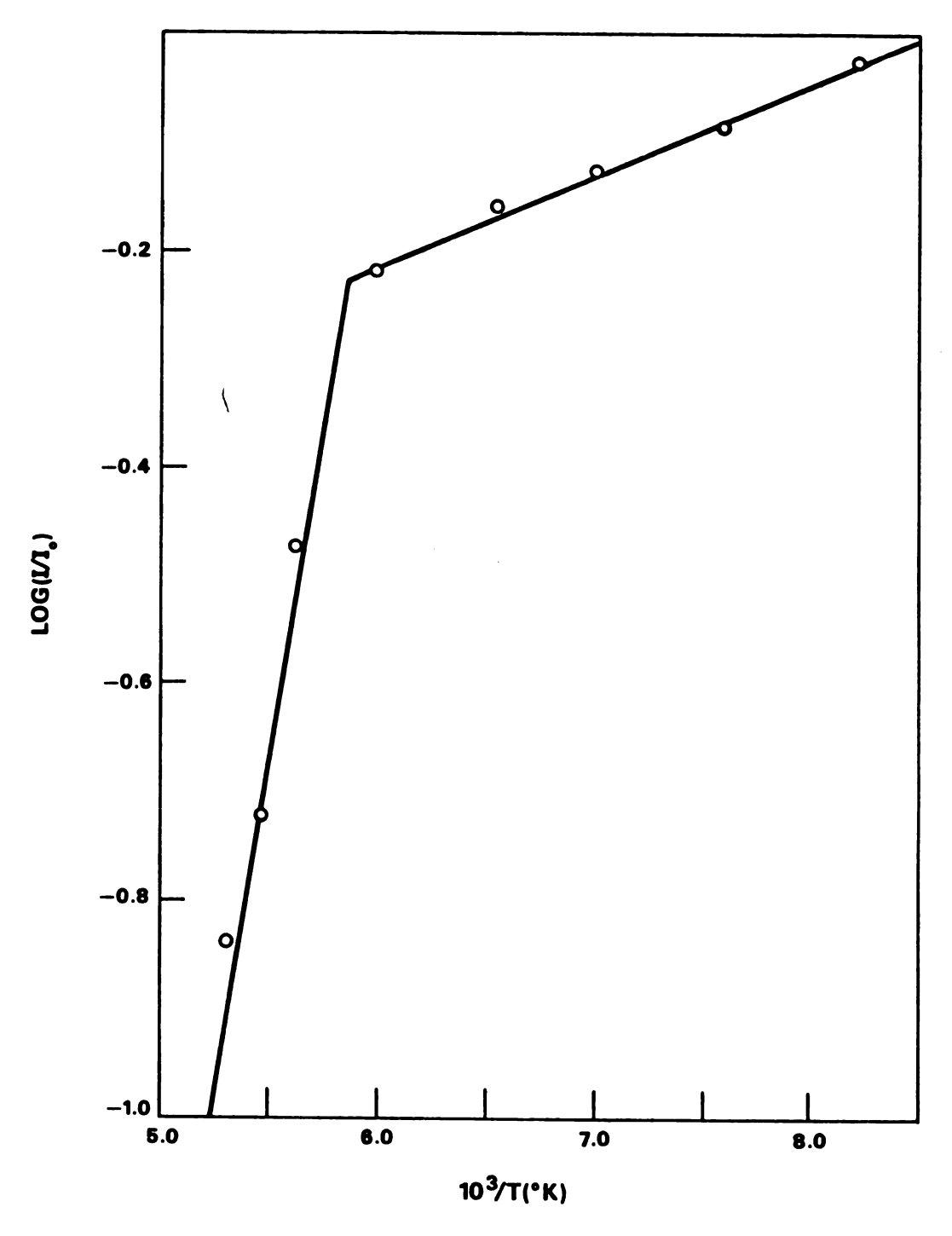


Figure 11. A plot of  $\log(I/I_0)$  versus  $10^3/T(^0\text{K})$  for the  $(\text{PdCl}_4)^{3-}$  radical shows two linear portions which implies two modes of decay.

## Radical II

A second radical is observed at  $77^{\circ}K$  in irradiated crystals of  $K_2PdCl_4$ . The spectrum consists of a four-line pattern centered at g=2.012 with a splitting of 63.4 Gauss when H||c (Figure 12a). Rotation in the ac plane allows the signal to be followed for about  $65^{\circ}$  on either side of the c axis. With the magnetic field in the aa' plane, these lines are obscured by the more intense  $(PdCl_4)^{3-}$  radical. Although the linewidth of Radical II sharpens perceptibly (from  $\sim 20$  G to  $\sim 15$  G) when the crystal is warmed slightly, both Radical I and Radical II decay at approximately the same temperature on further warming.

The large linewidths and low intensities make it difficult to determine whether the quartet arises from hyperfine interaction with chlorine or potassium, since both have nuclear spin I=3/2. An examination of the irradiated (NH<sub>4</sub>)<sub>2</sub>PdCl<sub>4</sub> crystals reveals the same radical, thus confirming that the hyperfine interaction is with chlorine. The radical does not appear to be ClO<sub>2</sub>, although the chlorine hyperfine interaction is similar, <sup>111</sup> since a crystal that was irradiated and observed in an evacuated quartz tube gave an identical spectrum.

If the nuclear quadrupole and nuclear Zeeman terms are neglected, the following tensor relationships fit the data taken with the field in the ac plane:

$$g^{2} = g_{c}^{2} \cos^{2}\theta + g_{a}^{2} \sin^{2}\theta$$

$$g^{2}A^{2} = g_{c}^{2}A_{c}^{2} \cos^{2}\theta + g_{a}^{2}A_{a}^{2} \sin^{2}\theta$$
(131)

where  $\theta$  is the angle between the c axis and the field direction. The data points are plotted in Figure 12b,c; the solid lines represent the

Figure 12. (a) First-derivative X-band spectrum of a single crystal of  $K_2PdCl_4$  irradiated and observed at  $77^{\circ}K$  with  $H \mid c$ , (b) angular variation of g when the magnetic field is in the ac plane, (c) angular variation of  $A(^{35}Cl)$  when the magnetic field is in the ac plane. The solid curves of (b) and (c) were calculated with the parameters of Table 6.

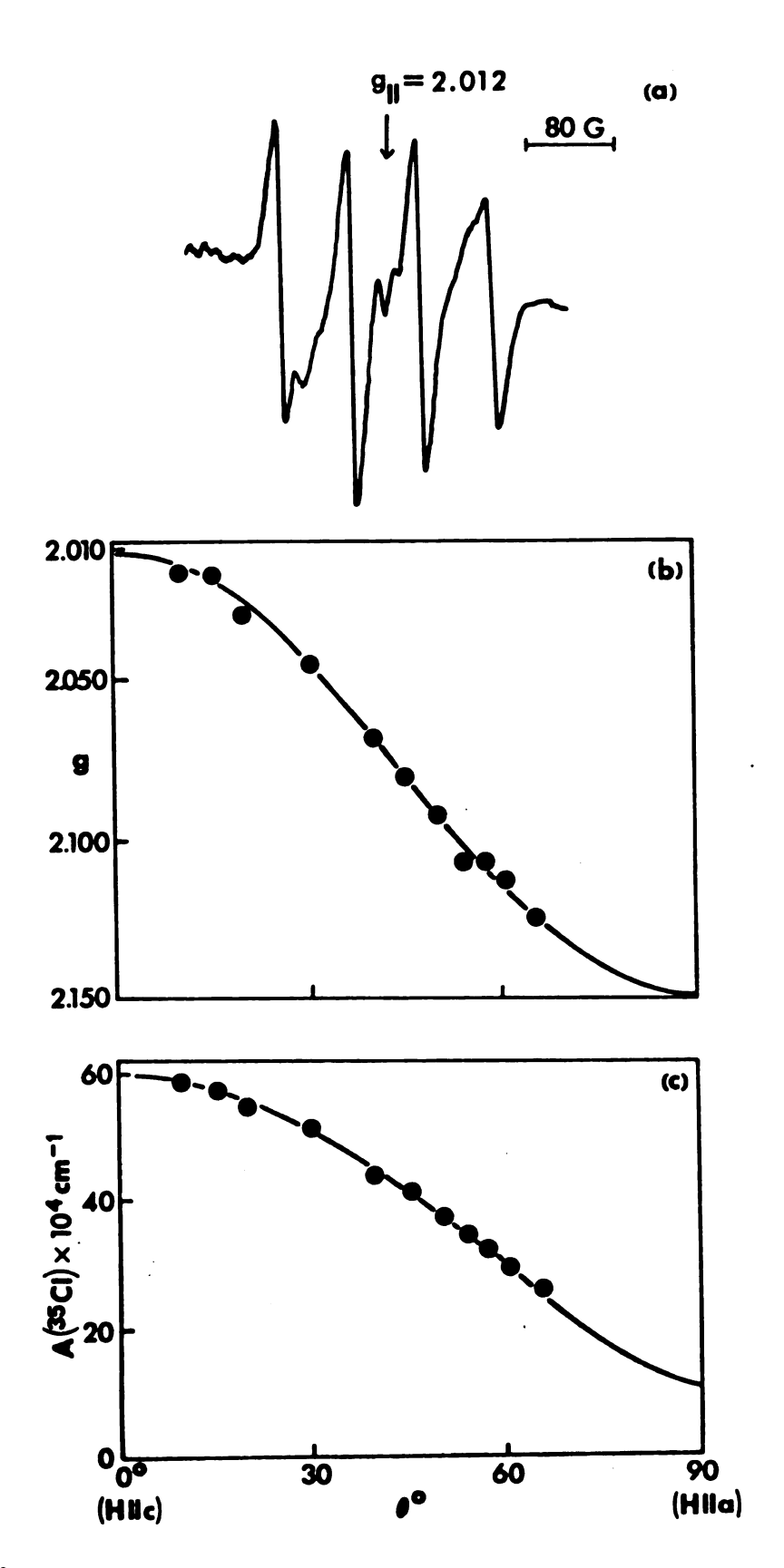


Figure 12.

values obtained by use of Equations (131) and the parameters reported in Table 6 under  $(PdC1_5)^{2-}$ .

$$(N(C_2H_5)_4)_2Pt_2Br_6$$

Since the (Pt<sub>2</sub>) radical, obtained by the irradiation of K<sub>2</sub>PtCl<sub>4</sub> in this research, may have a structure involving a bridging chlorine, irradiation of a complex known to have a bridged structure has been undertaken. The triclinic crystals <sup>106a</sup> of (N(C<sub>2</sub>H<sub>5</sub>)<sub>4</sub>)<sub>2</sub>Pt<sub>2</sub>Br<sub>6</sub> were irradiated at 77°K and the ESR spectra recorded. In this compound the bridging atoms are in the plane of the complex with one edge of the two square-planar units in common:

$$\begin{pmatrix} Br \\ Br \end{pmatrix} Pt \begin{pmatrix} Br \\ Br \end{pmatrix} Pt \begin{pmatrix} Br \\ Br \end{pmatrix}^{2-}$$

At least two radicals are formed. The spectrum of one is quite weak and consists of many lines separated by approximately 20 Gauss, in certain orientations, with the entire spectrum of this species covering nearly 800 Gauss. In most of the orientations there is considerable overlapping of these lines which apparently arises from bromine hyperfine interactions. Moreover, the center of the pattern corresponds to a g value significantly greater than 2.00, which suggests that the radical contains platinum. The poor resolution and weak signal intensity precludes making a complete study; therefore, this radical will not be discussed further.

The spectrum of the second radical is essentially isotropic with g = 2.002 and consists of five hyperfine lines nearly equally spaced with A = 28.5±1.0 Gauss (see Figure 13). The ratio of intensities for the five lines varies with angle on rotation about three mutually perpendicular axes, but remains about 1:4:6:4:1, as expected for five equivalent protons. Because power saturation of these lines tends to occur readily, unlike most transition metal spectra, the radical is believed to be the  $((C_2H_5)_3N-\dot{C}HCH_3)^+$  species obtained by removing a hydrogen atom from the tetraethylammonium cation. This assignment is supported by the magnitude of the hyperfine splittings which are just in the range between typical  $\alpha$ - and  $\beta$ - proton isotropic splittings observed for alkyl radicals in solution. The large linewidth (>10 Gauss peak-to-peak) would seem to indicate that the radical is undergoing restricted rotation at  $77^{\circ}K$  to produce a broadened but virtually isotropic spectrum.

$$K_2Pt(CN)_4 \cdot 3H_20$$
,  $(Pt(NH_3)_4)Cl_2$  and  $K(Pt(NH_3)Cl_3) \cdot H_20$ 

Irradiation of single crystals of  $K_2Pt(CN)_4 \cdot 3H_2O$  at  $77^OK$  gave no usable spectrum when examined by ESR since the fragile needles powder either on irradiation or on cooling.  $(Pt(NH_3)_4)Cl_2$  and  $K(Pt(NH_3)Cl_3) \cdot H_2O$  single crystals behaved in a similar manner and no satisfactory spectra were obtained, although there was evidence for a chlorine-containing platinum radical in the case of  $K(Pt(NH_3)Cl_3) \cdot H_2O$ .

 $K_2PtBr_4$ ,  $K_2PdBr_4$  and  $K_2PtCl_6$ 



Figure 13. The first-derivative X-band ESR spectrum of -CHCH3 in (N(C2H5)4)2Pt2Br6 at 770K.

Irradiation of single crystals of  $K_2PtBr_4$ ,  $K_2PdBr_4$  and  $K_2PtCl_6$  has been carried out at  $77^{\circ}K$  without permitting the crystals to warm up. No evidence for any platinum- or palladium-containing radicals was noted.

#### **DISCUSSION**

## K<sub>2</sub>PtC1<sub>4</sub>

## (Pt<sub>2</sub>) Radical

#### 1. g Values

Since the unique axes of the A and g tensors coincide with the c crystallographic axis, the (Pt<sub>2</sub>) radical must have a point-group symmetry no lower than  $C_{4v}$ . It is highly unlikely that any gross rearrangement of the ten nuclei that comprise the two original neighboring (PtCl<sub>4</sub>)<sup>2-</sup> anions can occur and still preserve the C<sub>4</sub> rotation axis. Therefore, it is proposed that the (Pt<sub>2</sub>) species is either  $((PtCl_4)_2)^{n-}$  or  $((PtCl_4)_1)^{n-1}$ , the latter unit having an additional bridging chlorine midway between two adjacent square-planar units along the c axis.

Since the (Pt<sub>2</sub>) radical converts on warming to the (PtCl) radical, which is believed to be (PtCl<sub>5</sub>)<sup>2-</sup>, it is tempting to postulate the presence of a bridging chlorine in the dimer unit since that would also explain why the unpaired spin is confined to two platinum nuclei rather than being further delocalized along the infinite array of (PtCl<sub>4</sub>)<sup>2-</sup> units stacked along the c axis (Figure 3). However, there is no detectable chlorine hyperfine interaction in the spectra of this species (Figure 5) to confirm the presence of a chlorine bridge; also, not all the (Pt<sub>2</sub>) radicals transform to (PtCl<sub>5</sub>)<sup>2-</sup> on warming and, on cooling, the (Pt<sub>2</sub>)

species does not reform as would be expected if a bridging chlorine were involved. Therefore, it appears more likely that the  $(Pt_2)$  radical is simply a dimer of the type  $((PtCl_4)_2)^{n-}$  in which an electron has been lost or gained from an adjacent pair of  $(PtCl_4)^{2-}$  units. On this assumption we have computed approximate values of the components of the g tensor as outlined below.

The metal orbitals that may contain the unpaired electron, and also are consistent with a  $C_4$  rotation axis parallel to c, are  $5d_z^2$ ,  $5d_{xy}$ ,  $5d_x^2-y^2$  and  $6p_z$ . The g values for these possibilities can be calculated by the crystal-field method. Starting wavefunctions are constructed from the symmetric and antisymmetric combinations of the real metal d-orbital basis set. For example,

$$|a_{1g}\rangle = |z^{2}\rangle = \{|d_{z}2\rangle_{1} + |d_{z}2\rangle_{2}\}/\sqrt{2}$$

$$|a_{2u}\rangle = |z^{2}\rangle = \{|d_{z}2\rangle_{1} - |d_{z}2\rangle_{2}\}/\sqrt{2}$$
(132)

where the functions are denoted by their symmetry under  $D_{4h}$ , the subscripts 1 and 2 refer to the two Pt nuclei, and overlap has been neglected. The g values for the four possible orbitals are given in Table 7, where only terms linear in  $\zeta$ , the one-electron spin-orbit coupling constant, are retained ( $\zeta$  is always positive). Although the exact ordering of the orbital energy levels is unknown, the relative order may be estimated from symmetry and the criterion of maximum overlap.

Experimentally one observes  $g \ge 2 > g \mid |$  which eliminates  $6p_z$  and  $5d_x 2_{-y} 2$  from further consideration. Regardless of the oxidation state of platinum,  $\zeta$  is of the order of  $^{112}$  2000 to 5000 cm $^{-1}$  which means that, in the case of  $g \mid |$  for the  $\underline{xy}$  ground state,  $E(x^2-y^2)-E(\underline{xy})$  is approximately

TABLE 7. -- Calculated g values for (Pt<sub>2</sub>)

Oribtal	ъд+	- z z -	x <sup>2</sup> -y <sup>2</sup>	χχ
<u>—</u>	2	2	$2 + \frac{8\xi}{E(xy) - E(x^2_+ - y^2)}$	$2 - \frac{8\zeta}{E(x^2 - y^2) - E(\underline{x}y)}$
<del>∞</del> 1	$2 - \frac{2\zeta}{E(p_x, p_y) - E(p_z)}$	$2 + \frac{6\zeta}{E(\underline{x}z, \underline{y}z) - E(\underline{z}^2)}$	$\frac{2\zeta}{E(p_x,p_y)-E(p_z)} = \frac{6\zeta}{\pm (xz,yz)-E(z^2)} = \frac{2\zeta}{E(xz,yz)-E(x^2-y^2)} = \frac{2\zeta}{\pm (xz,yz)-E(xy)}$	$2 + \frac{2\zeta}{E(xz,yz) - E(xy)}$
Order	8   = 2>8	g > 2 = g	8   > 8   > 2	81 > 2 > 8

70,000 to 173,000cm<sup>-1</sup>, an exceptionally large energy for one-electron,  $d \rightarrow d$  transitions. 113 Moreover, two consecutive platinum nuclei along the c axis are separated by 4.13 $^{\circ}$ A in the undamaged crystal. For this large a separation, xy would have a very small overlap and could not possibly alter the energy levels to the extent demanded by the g values. Thus  $z^2$  (Equations 132) is the only orbital consistent with the experimental evidence. Since the radical (PtC1), which is formed from the (Pt<sub>2</sub>) radical on warming, has been shown to very likely be (PtC1<sub>5</sub>)<sup>2-</sup> with  $d^7$  configuration (see below), it is reasonable to assume that an electron has been lost (rather than gained) from two (PtC1<sub>4</sub>)<sup>2-</sup> units in forming the (Pt<sub>2</sub>) species. A proposed schematic energy level diagram is shown in Figure 14.

An improved set of crystal field g values was then calculated by carrying the treatment to second order. The zero-order ground state in the hole representation is  $(x^2-y^2)^2(x^2-y^2)^2(z^2)$ . After successively applying the spin-orbit operator and the Zeeman operator over the excited states, the following g-values result: 114

$$g|_{=2N^2 - 3N^2 (\zeta/\Delta E)^2}$$
  
 $g|_{=2N^2 + 6N (\zeta/\Delta E) - 6N^2 (\zeta/\Delta E)^2}$ , (133)

where N is the normalization coefficient of the zero-order configuration in the wavefunction that arises from the spin-orbit interaction, and where  $\Delta E = E(e_u) - E(a_{2u})$ . The second-order correction terms were comuted by the method of Tippins. Substitution of the experimental g values for (Pt<sub>2</sub>) into Equations (133) yields

$$N = 0.964$$
,  $(\zeta/\Delta E) = 0.180$ .

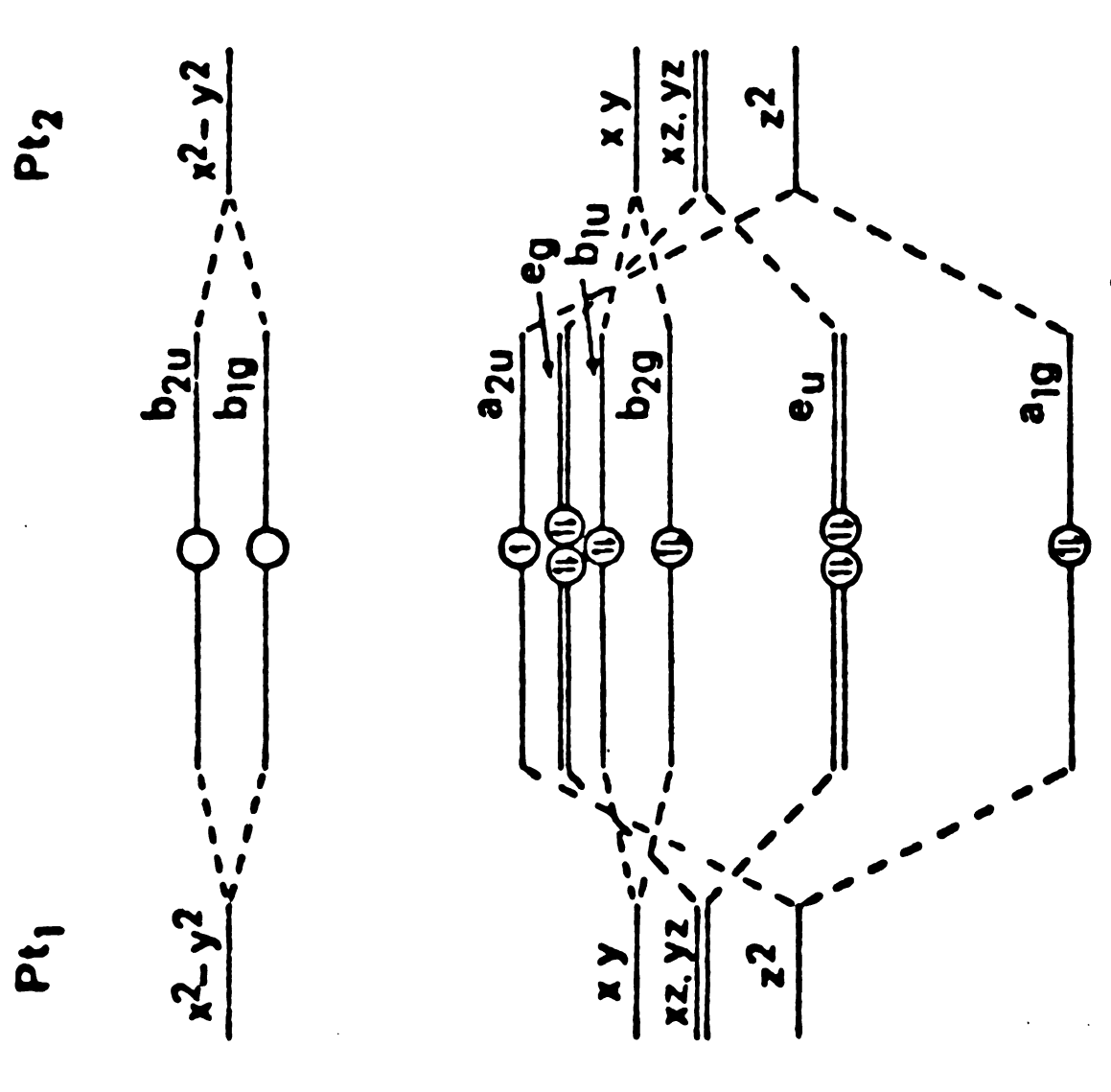


Figure 14. Possible molecular orbital energy level scheme for  $(\operatorname{PtCl}_4)_2^{3-}$  (d orbitals only).

The optical transition,  $\Delta E$ , can be estimated from the value of the spin-orbit coupling constant for  $Pt^{1+}$  ( $\zeta = 3368 \text{ cm}^{-1}$ ). If the percentage change in  $\zeta$  for platinum is similar to that exhibited by nickel in going from  $Ni^{1+}$  ( $\zeta = 565 \text{ cm}^{-1}$ ) to  $Ni^{3+}$  ( $\zeta = 705 \text{ cm}^{-1}$ ) then  $\zeta(Pt^{3+}) \sim 3368 (\frac{705}{565}) = 4203 \text{ cm}^{-1}$ . But the coupling constant in transition metal complexes is reduced by 25% to 30% from its free-ion value by covalency and charge donation by the ligands; hence it is reasonable to choose  $\zeta = 3000 \text{ cm}^{-1}$  which leads to  $\Delta E = 16,000 \text{ cm}^{-1}$ .

The ESR parameters observed for the (Pt<sub>2</sub>) radical are thus consistent with those expected for a dimer  $(PtCl_4)_2^{3-}$  with configuration  $d^{15}$  in a  $^2A_{2u}$  ground state and with the unpaired electron delocalized over two nearest-neighbor platinum ions through the interaction between their  $5d_z^2$  orbitals.

### 2. Pt Hyperfine Interaction

The crystal field platinum hyperfine tensor elements are

$$A \mid | = -\kappa + P\{4N^2\beta^2 + 12a^2 - 6aN\}/7$$

$$A \mid = -\kappa + P\{-2N^2\beta^2 - 9a^2 + 45aN\}/7$$
(134)

where  $\kappa$  is the isotropic hyperfine interaction,  $P = g_e g_n \beta_e \beta_n (r^{-3})_{5d}$ , N is as before,  $a = (\zeta/\Delta E)$  and  $\beta^2$  is the total spin density in both  $5d_z 2$  orbitals. If the covalency is ignored  $(\beta^2=1)$ , and the experimentally determined A|| and A| are assumed positive, the solution to Equations (134) results in a value for P that agrees in sign and order of magnitude with the values computed by Freeman et al. 96 by the Hartree-Fock method. The resulting parameters are

$$P = 470 \times 10^{-4} \text{ cm}^{-1}$$
  
 $\kappa = -239 \times 10^{-4} \text{ cm}^{-1}$   
 $\chi = 9.37 \text{ a.u.}$ 

where  $\chi$ , the isotropic hyperfine field at the nucleus, is obtained from  $\kappa$  by Equation (72).

The covalency can be estimated from Equations (134) if the value of P is taken from the Hartree-Fock calculations of the free ion. Using the value P =  $509 \times 10^{-4} \text{ cm}^{-1}$  for Pt<sup>3+</sup>(d<sup>7</sup>) obtained by extrapolation from the recent calculations of Freeman<sup>96</sup> (Table 8) one obtains  $\beta^2 = 1.04$ .

The fact that the hyperfine magnetic field produced at the nucleus (as measured by  $\chi$ ) is positive in (Pt<sub>2</sub>) is unusual for transition metal complexes. However, as noted earlier, positive signs for  $\chi$  have been obtained in the ESR studies of Co(II) phthalocyanine<sup>65</sup> and Co(II) in irradiated crystals of K<sub>3</sub>Co(CN)<sub>6</sub>. In both systems the Co<sup>2+</sup> ion is in a low-spin, d<sup>7</sup> configuration with the unpaired electron in an orbital composed of 3d<sub>z</sub>2 and 4s. An analogous situation appears to exist for (PtCl<sub>4</sub>)<sub>2</sub><sup>3-</sup> such that the half-filled a<sub>2u</sub> orbital (Equations 132) under D<sub>4h</sub> symmetry, where s and d<sub>z</sub>2 have the same irreducible representation, should read

$$a_{2u} = B\{(5d_z^2 + \mu 6s)_1 - (5d_z^2 + \mu 6s)_2\}$$
 (135)

where  $\mu$  is the degree of mixing and B is the normalization constant. Although it is difficult to say anything quantitative about  $\chi$ , the hyperfine fields at the nuclei in various Pt species (Table 9) indicate that Pt<sup>3+</sup> in BaTiO<sub>3</sub>, <sup>48</sup> YAlG<sup>47</sup> and particularly (PtCl<sub>4</sub>)<sub>2</sub><sup>3-</sup>, have substantial 6s character in their ground states.

TABLE 8. -- Hyperfine interaction parameters for platinum species by spin-unrestricted Hartee-Fock calculations.  $^{96}$ 

System	χ(a.u.)	⟨r <sup>-3</sup> ⟩ <sub>5d</sub> (a.u.)	P(x 10 <sup>-4</sup> cm <sup>-1</sup> )
Pt° 5d <sup>8</sup> 6s <sup>2</sup> ( <sup>3</sup> F)	-4.4	11.8	451.5
Pt <sup>o</sup> 5d <sup>9</sup> 6s( <sup>3</sup> D)	+53.6	11.1	424.7
Pt <sup>+</sup> 5d <sup>9</sup> ( <sup>2</sup> D)	-18.3	11.2	428.5
$Pt^{++} 5d^8(^3F)$	-18.1	12.2	466.8
Pt <sup>+++</sup> 5d <sup>7</sup> ( <sup>4</sup> F)	-17.9 <sup>a</sup>	13.3 <sup>a</sup>	509 <sup>a</sup>

a Values obtained in this work by linear extrapolation.

TABLE 9. -- Hyperfine fields at the Pt nucleus ( $H_n = -\kappa/2g_n\beta_n$ ) in various platinum species.

Substance	H <sub>n</sub> (kilogauss)	Ref.
(Pt(III)Cl <sub>5</sub> ) <sup>2-</sup> in K <sub>2</sub> PtCl <sub>4</sub>	-863	а
Pt <sup>3+</sup> in BaTiO <sub>3</sub>	-376	48
Pt <sup>3+</sup> in YAlG <sup>b</sup>	±124 <sup>c</sup>	47
(PtCl <sub>4</sub> ) <sub>2</sub> <sup>3-</sup> in K <sub>2</sub> PtCl <sub>4</sub>	+394	a
Pt metal	-1180	115 <sup>d</sup>
Pt <sup>3+</sup> (free ion)	<b>-</b> 754	96

a This thesis

b YAlG = yttrium aluminum garnet

 $<sup>\</sup>kappa \simeq \pm (A_{\ell} + A_{m} + A_{n})/3$ 

d Estimated from Knight shift measurements

# 3. Linewidths<sup>1</sup>

The ESR shapes for  $(PtCl_4)_2^{3-}$  are exactly Guassian and broader than those noted for most of the other species in irradiated K2PtCl4 and K<sub>2</sub>PdCl<sub>4</sub>. This broadening may be attributed to unresolved hyperfine splittings from the planar chlorine ligands. There also appears to be an anisotropic, my-dependent linewidth. In the parallel orientation (Figure 7a) the linewidth decreases from  ${\sim}45$  to  ${\sim}19$  Gauss as m $_{I}$  goes from -1 to +1, while just the opposite trend is observed in the perpendicular orientation (Figure 7b) where the linewidth increases from ∿16 to ∿30 Gauss with increase in  $m_T$ . Closer inspection reveals that the transitions at highest field in the parallel direction, and at lowest field in the perpendicular direction, are really doubled. This doubling does not seem to arise from nuclear spin flips ( $\Delta M_S=1$ ,  $\Delta m_T=\pm 1$ ) because, in that case, it should occur symmetrically about the usual transitions. For the same symmetry reason, spin-spin interactions from nearby radicals and/or splitting from two magnetically different sites should broaden the I,  $\pm m_{
m I}$  pairs to the same extent. Neither does the doubling seem to be a result of an error in orientation since a complete rotation with the magnetic field in the aa' plane gives no change in the position or intensity of the split lines. Moreover, the spectrum of irradiated K2PtCl4 powder, in which orientation effects are averaged, still shows the my-dependent linewidth. Anisotropic spin-lattice relaxation could account for the residual linewidth difference in the parallel and perpendicular orientations, but the dependence on  $m_{\text{\scriptsize I}}$  may indicate a time-dependent mechanism.

It is possible that the hole in the d manifold of  $(PtCl_4)_2^{3-}$  might migrate along the c axis but the spectra at  $77^{\circ}K$  demand that the hole be localized on just two platinum nuclei so if the hole does hop it

must do so in a time peroid slower than the reciprocal of the hyperfine splitting frequency.

#### 4. Structure

It is believed that the  $(PtCl_4)_2^{3-}$  radical is an example of a dimeric species with a one-electron metal-metal bond. It was noted many years ago that certain  $d^8$  square-planar metal complexes show evidence of metal-metal bonds. Thus, the crystal structures often show columnar stacking of the square-planar units with the metal ions in infinite chains, although such an arrangement does not permit closest possible packing of the ions,  $^{116}$  and the metal-metal distances may become quite short. The Pt-Pt distance, which is 4.13 $^{\circ}$  in K<sub>2</sub>PtCl<sub>4</sub>, is only 3.25 $^{\circ}$  in Magnus' green salt<sup>117</sup> {Pt(NH<sub>3</sub>)<sub>4</sub>}{PtCl<sub>4</sub>} and 3.09 $^{\circ}$  in Sr{Pt(CN)<sub>4</sub>}·3H<sub>2</sub>0.  $^{116}$  Also,  $\lambda_{max}$  of the absorption band polarized parallel to the metal chains increases as the Pt-Pt distance decreases in a series of platinum cyanide crystals with different cations;  $^{118}$  in solution, these are colorless.

It was suggested by Rundle, 119 and later by Miller, 120 that in the complexes with short Pt-Pt distances the nd and (n+1)p orbitals on adjacent metal ions overlap to give a pair of a<sub>2u</sub> and a pair of a<sub>1g</sub> molecular orbitals and that configuration interaction lowers the energy of the occupied (mostly nd<sub>2</sub>2) orbitals, thus accounting for the observed interaction. For a chain of metal ions, these discrete levels are replaced by energy bands and, if the metal-metal distance is small, the bands broaden and the separation between the highest occupied nd<sub>2</sub>2 band and the lowest unoccupied (n+1)s band decreases. It has indeed been shown that the d<sup>8</sup> system {(CO)<sub>2</sub>Ir(acac)} exhibits semiconductivity, with the ratio  $\sigma | |/\sigma | > 500$  for the dc conductivity parallel and perpendicular

to the chains,  $^{121}$  while the compound  $K_2Pt(CN)_4Br_{0.3}\cdot 2.3H_2O$  shows metallic conduction along the direction of the chains of metal ions.  $^{122}$ 

Monomeric  $d^8$  (PtCl<sub>4</sub>)<sup>2-</sup> units have the energy level scheme C (Figure 1). Loss of an electron from one of these units, followed perhaps by a shortening of the Pt-Pt distance to a neighboring (PtCl<sub>4</sub>)<sup>2-</sup> unit would give  $d^{15}$  dimers (PtCl<sub>4</sub>)<sub>2</sub><sup>3-</sup> with an energy level scheme as in Figure 14. The stability of this species would arise from removal of an electron from the antibonding  $a_{2u}$  orbital and configuration interaction stabilization of the  $a_{1g}$  orbital. The Pt-Pt bond could then be described as a one-electron metal-metal bond; such a bond has recently been reported 123 in the cation  $\{Fe(h^5-C_6H_5)(CO)(SR)\}_2^+$ .

## (PtCl) Radical

# 1. g and A (195Pt) Values

The g tensor for the (PtCl) radical (Table 5) is almost axial, with the unique axis parallel to the c axis of the crystal, indicating that the radical has nearly retained the tetragonal symmetry of the  $(PtCl_4)^{2-}$  ion. The magnitude of the g shifts suggests that the odd electron is largely associated with the platinum ion.

If this small deviation from axial symmetry is temporarily ignored one should be able to distinguish whether the  $Pt^{2+}(d^8)$  ion has captured an electron to form  $Pt^{1+}(d^9)$  or lost an electron to give  $Pt^{3+}(d^7)$  by comparing the experimental g values with those calculated from crystal-field theory (see Table 1). The experimental order  $g_{xx} \simeq g_{yy} > 2 > g_{zz}$  corresponds to the  $d^7$  configuration with the unpaired electron in the  $5d_z 2$  orbital.

Not only has  $Pt^{2+}$  been oxidized to  $Pt^{3+}$ , but the energy levels in the parent  $(PtCl_4)^{2-}$  anion (Case C in Figure 1) have been altered by an axial compression to the level scheme of Case A in Figure 1. Thus, the chlorine that is responsible for both the chlorine hyperfine splitting and the axial compression in the (PtCl) radical must be positioned nearly along the c axis to give  $(PtCl_5)^{2-}$ . If this chlorine were exactly parallel to the c axis the g tensor should be axial. Instead, the  $d_{xz}$ ,  $d_{yz}$  orbital pair is split in energy, presumably by a slight tipping ( $<5^{\circ}$ ) of the fifth chlorine away from the c axis in the (110) plane. The C4 rotation axis of the crystal generates four magnetically inequivalent sites, but the small tipping angle effectively reduces the inequivalence to two sites related by a  $90^{\circ}$  rotation about c. The fifth chlorine interacts with the metal  $d_z^2$  orbital to give a sigma antibonding orbital,  $\phi$ :

$$|\phi\rangle = \lambda |5d_{\mathbf{z}}2\rangle_{Pt} - \lambda' |\sigma\rangle_{C1} ,$$
where
$$|\sigma\rangle_{C1} = m|3p_{\mathbf{z}}\rangle + (1-m^2)^{\frac{1}{2}}|3s\rangle .$$
(136)

If the constraint of axial symmetry is now removed, a more accurate description of the platinum spin-Hamiltonian parameters can be calculated from crystal-field theory. Maki et al.  $^{66}$  have solved this problem for a nearly axial,  $^{7}$ , strong-field example with a  $(d_{x}2-y^{2})^{2}(d_{z}^{2})$  ground state (hole representation). In a slightly modified form the present results are:

$$g_{zz} = 2N^2$$
  
 $g_{xx} = 2N^2 + 6Na_1$   
 $g_{yy} = 2N^2 + 6Na_2$  (137)

and

$$A_{zz} = -\kappa + P\{4N^2\lambda^2 - 3N(a_1 + a_2)\}/7$$

$$A_{xx} = -\kappa + P\{-2N^2\lambda^2 + 6Na_1 + 3Na_2\}/7$$

$$A_{yy} = -\kappa + P\{-2N^2\lambda^2 + 6Na_2 + 3Na_1\}/7$$
(138)

where the symbols  $\kappa$ ,P are as before,  $a_1 = \zeta/\{E(d_{yz})-E(d_z2)\}$ ,  $a_2 = \zeta/\{E(d_{xz})-E(d_z2)\}$ ,  $\lambda$  is the MO coefficient of Equation (136), and N is the normalization coefficient of the zero-order ground state,  $(d_x2-y2)(d_z2)$ , following first-order perturbation by the spin-orbit coupling operator. Only when  $A||(^{195}Pt)$  and  $A||(^{195}Pt)$  are both negative does one obtain a magnitude and sign for the parameter P in agreement with the Hartree-Fock calculations for platinum.  $^{96}$ ,  $^{124}$  As a result of the high symmetry of the host crystal it is not possible to label  $g_{xx}$  and  $g_{yy}$  uniquely so  $g_{xx} = 2.417$  is arbitrarily chosen.

By suppressing the covalency (setting  $\lambda^2 = 1$ ) and making the approximation Alexperimental) =  $(A_{xx} + A_{yy})/2$ , Equations (137) and (138) can be solved. Substitution of the spin-Hamiltonian parameters of  $(PtC1_4)^{2-}$  yields

$$N = 0.985$$
  $P = 321 \times 10^{-4} \text{ cm}^{-1}$   
 $a_1 = 0.0805$   $\kappa = 525 \times 10^{-4} \text{ cm}^{-1}$   
 $a_2 = 0.0751$   $\chi = -20.5 \text{ a.u.}$ 

Allowing covalnecy, and using the value of P for Pt<sup>3+</sup> from Table 8, one obtains  $\lambda^2$  = 0.88 and  $\chi_{\rm exp}$  = -22.6 a.u. The relatively close agreement between  $\chi_{\rm exp}$  and the theoretical value of  $\chi$  from Table 8 implies that the hyperfine field at the Pt nucleus results mainly from

core polarization and not from any appreciable 6s involvement in the ground state, while  $\lambda^2$ <1 confirms the obvious fact that the unpaired electron is delocalized onto the ligands.

## 2. Chlorine Hyperfine Interaction

A direct measure of the covalency may be obtained from an analysis of the chlorine hyperfine interaction. The spin Hamiltonian of Equation (114) operating on the ground MO of Equations (137,138) gives

$$A_{||}(^{35,37}C1) = (1-m^2)\lambda'^2A_s^0 + 4m^2\lambda'^2P^0/5$$

$$A_{||}(^{35,37}C1) = (1-m^2)\lambda'^2A_s^0 - 2m^2\lambda'^2P^0/5.$$
(139)

The direct dipole interaction,  $A_d = g_e g_n \beta_e \beta_n R^{-3}$ , between the unpaired electron in the  $5d_z 2$  orbital of platinum and the chlorine nucleus has been neglected because the numerical value of  $A_d$  for any reasonable Pt-Cl internuclear distance, R, is less than the experimental error. Since the hyperfine splittings for  $^{35}Cl$  and  $^{37}Cl$  could not be resolved, the weighted arithmetic mean of  $A_s^0$  and  $\left\langle r^{-3} \right\rangle_{3p}$  for both isotopes was taken from the tabulated Hartree-Fock parameters. The spin densities can then be estimated as

$$f_D(\%) = \lambda^{2}m^2 \times 100 \text{ and } f_S(\%) = \lambda^{2}(1-m^2) 100$$
 (140)

Substitution of the experimental splittings into Equations (139,140) leads to

$$\lambda' = 0.57$$
  $f_8(%) = 2.0$   
 $m = 0.97$   $f_p(%) = 30.6$ 

with a hybridization ratio  $p/s = m^2/1-m^2 \approx 16$ .

Table 10 compares the axial ligand spin densities of low-spin,  $d^7$  complexes in examples where the anisotropic splittings are available. The exceptionally large spin densities on chlorine in  $(PdCl_5)^{2-}$  and  $(PtCl_5)^{2-}$  are probably a reflection of the abnormally short M-Cl distance (R<2 Å) demanded by the crystal structure. Thus, the unpaired spin in  $(PtCl_5)^{2-}$  is rather delocalized in the  $\sigma$  antibonding molecular orbital which is composed primarily of a  $5d_2$  orbital on platinum and a  $3p_2$  orbital on chlorine.

TABLE 10. -- Axial ligand spin densities.a

Substance	Nucleus	%f <sub>p</sub>	%f <sub>s</sub>	(%f <sub>p</sub> + %f <sub>s</sub> )	Reference
CoPc·Pyridine <sup>b</sup>	N(Pyridine)	2.9	2.4	5.3	125
Fe(CN) <sub>5</sub> NOH <sup>2-</sup>	N (NOH)	4.2	2.9	7.1	126
PdC1 <sub>5</sub> 2-	<b>C1</b>	34.7	1.7	36.4	c
PtC1 <sub>5</sub> 2-	<b>C1</b>	28.1	1.9	30.0	c
Rh(II)(CN) <sub>4</sub> Cl <sub>2</sub> 4-	C1	11.4	1.2	12.6	127

a Low-spin,  $d^7$  complexes with the unpaired electron in the metal  $d_z^2$  orbital.

b Pc = phthalocyanine

<sup>&</sup>lt;sup>C</sup> This thesis

# (PtCl<sub>3</sub>)<sup>n-</sup> Radical

The presence of the ten hyperfine lines characteristic of three equivalent chlorines for both H | | c and H | | a (Figure 8) indicates that three chlorine ligands lie in the aa' plane occupying three of the four chlorine positions of the  $(PtCl_4)^{=}$  ion. While the platinum need not lie in this plane the symmetry of the host lattice favors a planar species. The symmetry would then be  $D_{2h}$  and the energy levels of Figure 1, Case C, would be scrambled with  $d_{XZ}$ ,  $d_{YZ}$  split in energy;  $d_{X}2_{-Y}2$ , which is directed at the ligands, would remain highest in energy.

Consideration of the possible  $d^7$  and  $d^9$  configurations suggests that  $d^9$ ,  $(z^2)^2(xz)^2(yz)^2(xy)^2(x^2-y^2)^1$  is the only reasonably acceptable ground state. Under  $D_{2h}$  symmetry,  $d_x 2_{-y} 2$  and  $d_z 2$  transform together as  $A_1$ . Taking the ground state in the hole formalism as

$$|x^2-y^2\rangle = \alpha |d_x^2-y^2\rangle + \beta |d_z^2\rangle , \qquad (141)$$

where  $\alpha^2 + \beta^2 = 1$ , the g values are calculated to be

$$g_{zz} = 2n^{2} + 8n\alpha^{2} a_{1}$$

$$g_{xx} = 2n^{2} + 2na_{2} (\alpha + \sqrt{3}\beta)^{2}$$

$$g_{yy} = 2n^{2} + 2na_{3} (\alpha - \sqrt{3}\beta)^{2}, \qquad (142)$$

where

$$1 = N^{2} + q^{2}a_{1}^{2} + a_{2}^{2} \left(\frac{\alpha + \sqrt{3}\beta}{2}\right) + a_{3}^{2} \left(\frac{\alpha - \sqrt{3}\beta}{2}\right)^{2}$$

and

$$a_1 = \zeta/E(xy) - E(x^2-y^2)$$
  
 $a_2 = \zeta/E(yz) - E(x^2-y^2)$   
 $a_3 = \zeta/E(xz) - E(x^2-y^2)$ .

There is insufficient information to solve these equations; however, the order is predicted to be  $g_{ZZ} >> g_{XX} > g_{yy} \simeq 2$  as observed. A rough analysis of the available metal hyperfine splittings using P = 430 x  $10^{-4} \text{cm}^{-1}$  (Table 8) yields a positive value for  $\chi$  which suggests that the platinum 6s orbital contributes to the ground state as was noted in the case of the (Pt<sub>2</sub>) radical. The chlorine hyperfine interaction results from transferred spin density in the  $\sigma$  molecular orbital which is formed from a chlorine 3p orbital and the  $|x^2-y^2\rangle$  metal orbital.

## Reaction Scheme

A possible mechanism to account for the observed radicals and their decays may be given, beginning with the assumption that the initial step on  $\gamma$ -irradiation at  $77^{\circ}K$  is

$$(PtCl_4)^{2-} \rightarrow (PtCl_3)^{2-} + C1$$
.

The neutral chlorine atom could move into the potential well at the center of the unit cell (Figure 3) eventually abstracting an electron from  $(PtCl_4)^{2-}$  to form  $(PtCl_4)^{-}$ . This could then form the  $(Pt_2)$  radical by combining with a neighboring undamaged ion of the lattice

$$(PtCl_4)^{2-} + Cl \rightarrow (PtCl_4)^{-} + Cl^{-}$$
  
 $(PtCl_4)^{-} + (PtCl_4)^{2-} \rightarrow (PtCl_4)_2^{3-}$ .

On warming, the hole centered on the  $(Pt_2)$  radical could then migrate parallel to the c axis until it encounters either  $(PtCl_3)^{2-}$ , forming a diamagnetic species, or  $Cl^-$  forming  $(PtCl_5)^{2-}$ :

$$(PtCl_4)_2^{3-} + (PtCl_3)^{2-} \rightarrow 2(PtCl_4)^{2-} + (PtCl_3)^{-}$$

$$(PtCl_4)_2^{3-} + Cl^{-} \rightarrow (PtCl_4)^{2-} + (PtCl_5)^{2-}.$$

K<sub>2</sub>PdC1<sub>4</sub>

### Radical I

## 1. g Values

The ESR spectra (Figure 10) show that Radical I is  $(PdC1_4)^{n-}$  where  $n=1(d^7)$  or  $n=3(d^9)$ , corresponding to the loss or gain of an electron by the original  $(PdC1_4)^{2-}$  ion. These two possibilities are distinguished by comparing the observed g values (Table 6) with the calculated g values of Table 1. Only the  $d^9$  configuration of Table 1. is consistent with the observed order g||g|>2.

The energy separations  $\Delta E_1 \simeq 23,000~{\rm cm}^{-1}$  and  $\Delta E_4 \simeq 27,500~{\rm cm}^{-1}$  reported by Basch and  ${\rm Gray}^{43}$  for the parent  $({\rm PdCl}_4)^{2-}$  ion are based on the optical spectra of Day et al. 128 If these numbers and the value of  $\zeta_{\rm Pd} = 1416~{\rm cm}^{-1}$  are used in the theoretical expressions for g|| and g| for d<sup>9</sup> in Table 1, one obtains g|| = 2.483 and g| = 2.105; these are in fair agreement with the experiment considering the many approximations that have been made which include neglect of the change in metal charge from +2 to +1 in estimating the  $\Delta E$  values, neglect of the reduction factor in the free-ion palladium spin-orbit coupling constant, neglect of covalent bonding and other smaller terms. 85

### 2. Pd Hyperfine Interaction

The anisotropic hyperfine interaction arises from the coupling of an electron in the  $d_{\rm x}2_{-\rm y}2$  antibonding orbital with the palladium

nucleus. Only the magnitude is observed experimentally but the sign may be obtained by the method of Fortman;  $^{95}$  a positive contribution of the dipolar term with H||c is predicted. The sign of the isotropic hyperfine term is also predicted to be positive since it must arise solely from the core polarization of the s orbitals (s orbitals cannot mix with  $d_{x}2_{-y}2$  under  $D_{4h}$  symmetry in the molecular orbital treatment). Calculations of the core polarization for 4d ions with spin-polarized Hartree-Fock wavefunctions predict that the isotropic hyperfine interaction a =  $\frac{1}{3}(A_{\parallel} + 2A_{\perp})$  will be negative when the nuclear magnetic moment is positive, and vice versa. Since  $\mu$  ( $^{105}Pd$ ) =  $^{-0.639}$  nuclear magnetons,  $^{129}$  it is likely that both  $A_{\parallel}$  ( $^{105}Pd$ ) and  $A_{\parallel}$  ( $^{105}Pd$ ) are positive.

For  $(PdCl_4)^{3-}$  with the unpaired electron in a  $d_x 2_{-y} 2$  orbital one employs Equations (81) for the metal hyperfine splittings. One finds that  $P = -58.4 \times 10^{-4} \text{ cm}^{-1}$  for the Pd<sup>+</sup> ion based on an estimate of  $\langle r^{-3} \rangle_{4d}$  of 7.17 a.u. obtained by extrapolation. 87 The solution to Equations (81) shows that approximately 78% of the unpaired spin density is localized in the metal  $d_x 2_{-y} 2$  orbital. Table 11 lists the spin densities calculated in this manner for other palladium-containing species reported in the literature. On the basis of the anisotropic couplings, the acetylacetonate complex is slightly more covalent than the chloride. However, as has been observed in other  $d^9$  systems, the covalency found from the isotropic magnetic field at the nucleus per unit spin  $(\chi/\chi_0)$  bears no simple relationship to  $\alpha^2$  obtained from the anisotropic hyperfine coupling constants.

## 3. Chlorine Hyperfine Interaction

The principal values of the chlorine superhyperfine interaction tensor for  $(PdCl_4)^{3-}$  are given in Table 6 where the coordinates are

TABLE 11. -- Isotropic hyperfine fields and covalency parameters for palladium complexes.<sup>a</sup>

Substance	x	χ/χ°	α2	Reference
(PdC1 <sub>4</sub> ) <sup>3-</sup> (in K <sub>2</sub> PdC1 <sub>4</sub> )	-7.66	0.83	0.785	Ъ
$(PdC1_4)^{3-}$ (in $(NH_4)_2PdC1_4$ )	-7.55	0.82	0.78	Ъ
Pd(acac)2 (in Pd(acac)2)	-10.00	1.09	0.725	56
Pd <sup>o</sup> (in Pd metal)	-8.2	0.89		129
PdS <sub>4</sub> C <sub>4</sub> (CF <sub>3</sub> ) <sub>4</sub>	-1.58	0.17		51

a  $\chi^{0}$  = -9.2 a.u. for Pd<sup>+</sup> ion from the calculations of Watson and Freeman 87 and  $\chi$  is the experimental value.

b This thesis

defined in Figure 2. Although there are eight possible sign combinations for the principal elements, it is probable that the correct set is that with all signs positive, since only that choice is consistent with the assumptions that (a) the transferred spin density is positive (b) the  $d_{x^2-y^2}$  metal oribtal forms  $\sigma$  bonds with a hybrid of the 3s,  $3p_x$  chlorine orbitals so that  $A_y \simeq A_z$ , and (c) the isotropic chlorine hyperfine interaction should be large and sign determining because the chlorine 3s orbitals are directly involved in the bonding.

The principal elements of the chlorine hyperfine interaction tensor may be written in terms of the isotropic contribution  $A_8$ , the direct dipolar interaction  $A_d$  between the electron in the  $d_x 2_{-y} 2$  orbital of Pd and the chlorine nucleus, the dipolar interaction  $A_\sigma$  between the electron in the  $3p_x$  orbital of chlorine and the chlorine nucleus, and the dipolar interactions  $A_{\pi y}$ ,  $A_{\pi z}$  between an electron or hole in the chlorine  $p_y$  and  $p_z$  orbitals and the chlorine nucleus. As a result of the relationship between the direction cosines of the three chlorine  $p_y$  dipolar terms only two independent values  $p_y$  and  $p_z$  and  $p_z$  can be determined, such that

$$\begin{pmatrix} A_{x} & 0 & 0 \\ 0 & A_{y} & 0 \\ 0 & 0 & A_{z} \end{pmatrix} = A_{s} \begin{pmatrix} 1 & 0 & 0 \\ 0 & 1 & 0 \\ 0 & 0 & 1 \end{pmatrix} + (A_{d} + A_{\sigma} - A_{\pi x}) \begin{pmatrix} 2 & 0 & 0 \\ 0 & -1 & 0 \\ 0 & 0 & -1 \end{pmatrix}$$

$$+ (A_{\pi_{Z}} - A_{\pi y}) \begin{pmatrix} -1 & 0 & 0 \\ 0 & -1 & 0 \\ 0 & 0 & 2 \end{pmatrix} .$$
 (143)

 $A_d = 0.2 \times 10^{-4} \text{ cm}^{-1}$  is estimated from  $A_d = gg_n \beta \beta_n R^{-3}$  using the Pd-C1 distance observed for  $(PdC1_4)^{2-}$ , R = 2.33Å. The three observed

principal components lead, by the use of Equation (143), to  $A_8$  = 12.3 x  $10^{-4}$  cm<sup>-1</sup>,  $(A_{\sigma} - A_{\pi y})$  = 3.7 x  $10^{-4}$  cm<sup>-1</sup>, and  $(A_{\pi z} - A_{\pi y})$  = 0.3 x  $10^{-4}$  cm<sup>-1</sup>. Both  $A_{\pi z}$  and  $A_{\pi y}$  presumably arise from configuration interaction;  $^{130}$  that is, the approximate treatment given by the one-electron molecular orbitals should be augmented by mixing in small amounts of excited states which occur in the many-electron theory.  $^{85}$  In view of the fact that the experimental tensor is nearly axial with  $A_y(^{35}\text{Cl}) \simeq A_z(^{35}\text{Cl})$ , and the experimental error in  $A_y(^{35}\text{Cl})$  is large, one can set  $A_{\pi y} = A_{\pi z} = 0$ , in this way neglecting the small configuration interaction terms. One can then obtain information about the  $b_{1g}$  antibonding molecular orbital (Equation 108) that contains the unpaired electron. The analysis of the chlorine hyperfine interaction for  $(PdCl_4)^{3-}$  follows the sample calculation presented in the Theoretical section, Equations (108-119), and yields

$$f_8(%) = 0.78$$
  $\alpha'^2 = 0.35$   
 $f_{P_X}(%) = 7.9$   $n^2 = 0.91$ 

with a hybridization ratio p/s = 10.

Even though nitrogen-bonded ligands generally produce larger crystal fields than chlorine ligands, many of the  $d^9$  ESR studies on  $Cu^{++}$  and  $Ag^{++}$  have involved nitrogen-bonded ligands. In Table 12 we compare the spin density of Radical I with the well-characterized ESR results for Cu(II) and Ag(II) tetraphenylporphyrins.  $^{132}$  The total ligand spin density  $\{(f_8(%) + f_{P_X}(%))\}$ , which is a direct measure of the covalency of the metal-ligand bond increases in the order  $Cu^{++} < Pd^+ < Ag^{++}$ . This is the order expected qualitatively since covalency should increase in going from the

3d to the 4d series, and, in the case of Ag<sup>++</sup>, the higher metal charge will attract more electron density from the ligands resulting in a larger covalency than in the singly charged Pd complex. It should be noted that there is good agreement between the results obtained in this thesis for (PdCl<sub>4</sub>)<sup>3-</sup> and those recently reported by Fujiwara and Nakamura. <sup>131</sup>

TABLE 12. -- Ligand spin densities in some  $\sigma$ -bonded d square-planar complexes.

Complex	Configuration	f <sub>S</sub> (%)	f <sub>px</sub> (%)	(f <sub>s</sub> + f <sub>px</sub> )(%)	Reference
Cu(II)TPP <sup>a</sup>	3d <sup>9</sup>	2.5	4.6	7.1	132
Ag(II)TPP <sup>a</sup>	4d <sup>9</sup>	3.6	7.5	11.1	132
Pd(I)Cl <sub>4</sub> <sup>3-</sup>	4d <sup>9</sup>	0.8	7.9	8.7	ъ

a TPP = Tetraphenylporphyrin

#### Radical II

If Radical II were a chlorine atom in a tetragonal crystal field with the unpaired electron in a p orbital one would expect the principal anisotropic hyperfine tensor elements for  $^{35}$ Cl to be (93.5, -46.8, -46.8 x  $10^{-4}$  cm<sup>-1</sup>).  $^{99}$  Clearly only a fraction of the spin density is on the chlorine nucleus. In irradiated crystals of K<sub>2</sub>PtCl<sub>4</sub> at 77°K, the (PtCl<sub>5</sub>)<sup>2-</sup> radical has virtually the same hyperfine splitting tensors as Radical II but shows additional splitting from a platinum nucleus. Hyperfine lines from palladium in Radical II were not observed, probably

b This thesis

as a result of the weak signal intensity and large linewidths. However, by analogy with the platinum radical, it is proposed that Radical II is  $(PdCl_5)^{2-}$  (d<sup>7</sup>) formed by a chlorine atom attaching itself to  $(PdCl_4)^{2-}$  in a fifth coordination position along the fourfold axis.

The magnitude of the tetragonal field is reduced by this axial ligand to the point where the energy levels correspond to case A, Figure 1, placing the unpaired electron in the  $d_z^2$  orbital. The calculated g values given in Table 1 for a  $(d_x^2-y^2)^2(d_z^2)$  ground state show |g| > |g| = 2 as is found experimentally.

Analysis of the chlorine hyperfine interaction in  $(PdCl_5)^{2-}$ , using the same method and equations employed in the section on  $(PtCl_5)^{2-}$  (Equations 136-140), gives

$$f_s(\%) = 1.7$$
  $f_{p_{\sigma}}(\%) = 34.7$   $\lambda^2 = 0.36$   $m^2 = 0.95$   $s/p(^{35}C1)$  ratio  $\approx 20$  ,

where the sign of  $A_{||}(^{35}C1)$  is taken to be the same as the sign of  $A_{||}(^{35}C1)$  by analogy with the corresponding radical in  $K_2PtC1_4$ . Thus, Radical II also has a  $\sigma$ -bonded chlorine with a very large spin density in an almost pure  $3p_z$  orbital. It seems reasonable to assume that the large spin density of the chlorine will be accompanied by a short Pd-Cl bond distance and a large overlap.

### Reaction Scheme

For irradiated  $K_2PdCl_4$ , the first reaction is assumed to be

$$(PdC1_4)^{2-} \xrightarrow{\gamma} (PdC1_3)^- + C1 \cdot + e^-$$
.

The electron could then react with one of the original  $(PdC1_4)^{2-}$  complex ions to produce Radical I

$$(PdC1_4)^{2-} + e^- \rightarrow (PdC1_4)^{3-}$$
.

By analogy with the proposed platinum reaction scheme, the chlorine atom could then move into the potential well at the center of the unit cell. At  $77^{\circ}$ K the overlap between adjacent Pd atoms is apparently too small to stabilize the palladium analogue of (Pt<sub>2</sub>); therefore, the chlorine atom may react directly with an undamaged (PdCl<sub>4</sub>)<sup>2-</sup> ion to give Radical II

$$(PdC1_4)^{2-} + C1 \cdot \rightarrow (PdC1_5)^{2-}$$
.

#### SUMMARY

- 1. Paramagnetic species produced by irradiation of diamagnetic squareplanar complexes of Pt(II) and Pd(II) have been studied by electron
  spin resonance spectroscopy. The ESR spectra have, in each case, been
  obtained as a function of magnetic field orientation and the results
  analyzed by the spin-Hamiltonian method. The spin-Hamiltonian parameters have been determined and nearly complete g and hyperfine
  splitting tensors reported. An attempt has been made to identify
  each radical with the aid of this information.
- 2. It has been shown that irradiation produces both Pt(I), Pd(I) and Pt(III), Pd(III) species resulting from one-electron reduction or oxidation, respectively. The results of irradiation by  $\gamma$ -rays from a  $^{60}$ Co source and by 1 Mev electrons from a G. E. Resonant Transformer are identical.
- 3. The ESR spectra have been followed, for each crystal studied, as a function of temperature, and the regions of stability for each species investigated. The reactions of the various radical species have been studied and some postulates concerning the mechanisms made.
- 4. Single crystals of K<sub>2</sub>PdCl<sub>4</sub> and (NH<sub>4</sub>)<sub>2</sub>PdCl<sub>4</sub> have been irradiated at 77°K, the ESR spectra analyzed, and the radicals shown to be {Pd(I)Cl<sub>4</sub>}<sup>3-</sup> and {Pd(III)Cl<sub>5</sub>}<sup>2-</sup> in both crystals. On warming, these radicals decay to diamagnetic products and at room temperature no ESR signal can be observed.

- have been analyzed. The two radical species produced have been shown to most probably be {(Pt,(II,III)Cl<sub>4</sub>)<sub>2</sub>}<sup>3-</sup> and {Pt(I)Cl<sub>3</sub>}<sup>2-</sup>. On warming to about 125°K the former reacts with other species in the crystal to produce a new radical which the ESR results indicate is {Pt(III)Cl<sub>5</sub>}<sup>2-</sup>. On warming to 190°K the (PtCl<sub>3</sub>)<sup>2-</sup> radical decays to diamagnetic products and at room temperature no ESR spectrum is observed.
- 6. The species  $(PtCl_4)_2^{3-}$  appears to be an example of a complex containing a metal-metal bond. In the species  $(PtCl_4)_2^{3-}$  the entire spin density is shared by two equivalent platinum atoms. This is consistent with a structure in which there is a metal-metal bond between the platinum atoms.
- 7. Energy level schemes have been proposed for each radical species and the nature of the chemical bonding in each has been discussed.
- 8. A number of other diamagnetic complexes of platinum and palladium have been irradiated. None gives interpretable ESR spectra under the experimental conditions employed.

**BIBLIOGRAPHY** 

#### **BIBLIOGRAPHY**

- 1. A. Abragam and B. Bleaney, "Election Paramagnetic Resonance of Transition Ions," Oxford University Press, London, 1970.
- 2. H. A. Kuska and M. T. Rogers, "Radical Ions," edited by E. T. Kaiser and L. Devan, Interscience Publishers, New York, 1968.
- 3. B. R. McGarvey, Inorg. Chem. 5, 476 (1966).
- 4. R. G. Hayes, J. Chem. Phys. 44, 2210 (1966).
- 5. T. Halpern, S. M. McKoskey and J. A. McMillan, J. Chem. Phys. <u>52</u>, 3526 (1970).
- 6. T. H. P. Hall, W. Hayes, R. W. H. Stevenson and J. Wilkens, J. Chem. Phys. <u>39</u>, 35 (1963).
- 7. W. C. Lin, C. A. McDowell, and D. J. Ward, J. Chem. Phys. <u>49</u>, 2883 (1968).
- 8. H. A. Kuska, Ph. D. Thesis, Michigan State University, 1965.
- 9. H. A. Kuska and M. T. Rogers, "Spectroscopy in Inorganic Chemistry," edited by J. R. Ferraro and C. N. R. Rao, Academic Press, New York, 1971.
- 10. H. A. Kuska and M. T. Rogers, "Coordination Chemistry," edited by A. E. Martell, Reinhold, New York, 1971.
- B. R. McGarvey, "Transition Metal Chemistry," R. L. Carlin, Ed., Marcel Dekker, Inc., New York, 1966.
- 12. E. König, "Physical Methods in Advanced Inorganic Chemistry," edited by H. A. O. Hill and P. Day, Interscience Publishers, New York, 1968.
- 13. M. Bersohn and J. C. Baird, "An Introduction to Electron Paramagnetic Resonance," W. A. Benjamin, Inc., New York, 1966.
- 14. J. A. McMillan, "Electron Paramagnetism," Reinhold Publishing Co., New York, 1968.
- 15. H. M. Assenheim "Introduction to Electron Spin Resonance," Hilger and Watts, London, 1966.
- 16. A. Carrington and A. D. McLachlan, "Introduction to Magnetic Resonance," Harper and Row Publishers, New York, 1967.

- 17. T. H. Wilmshurst, "Electron Spin Resonance Spectrometers," Hilger and Watts, London, 1967.
- 18. C. P. Poole, Jr., "Electron Spin Resonance," Interscience Publishers, New York, 1967.
- 19. R. S. Alger, "Electron Paramagnetic Resonance," Interscience Publishers, New York, 1968.
- 20. P. B. Ayscough, "Electron Spin Resonance in Chemistry," Methuen & Co., London, 1967.
- 21. D. E. O'Reilly and J. H. Anderson, "Physics and Chemistry of the Organic Solid State," edited by D. Fox, M. M. Labes and A. Weissberger, John Wiley and Sons, New York, 1965.
- 22. J. W. Orton, "Electron Paramagnetic Resonance," Iliffe Books, London, 1968.
- 23. B. N. Figgis, "Introduction to Ligand Fields," Interscience Publishers, New York, 1966.
- 24. H. Watanabe, "Operator Methods in Ligand Field Theory," Prentice-Hall, Englewood Cliffs, New Jersey, 1966.
- 25. M. T. Jones and W. D. Phillips, Ann. Rev. Phys. Chem. 17, 323 (1966).
- 26. A. H. Maki, Ann. Rev. Phys. Chem. 18, 9 (1967).
- 27. M. C. R. Symons, Ann. Rev. Phys. Chem. 20, 219 (1969).
- 28. A. Carrington and G. R. Luckhurst, Ann. Rev. Phys. Chem. 19, 31 (1968).
- 29. N. M. Atherton, A. J. Parker and H. Steiner, Chem. Soc. Ann. Repts. 63, 62 (1966).
- 30. G. R. Luckhurst, Chem. Soc. Ann. Repts. 66A, 37 (1969).
- 31. Symposium of Electron Spin Resonance, East Lansing, Michigan, 1-3 August, 1966. (See also the first issue of J. Phys. Chem. 71, (1967).)
- 32. Fifth Annual George H. Hudson Symposium, Plattsburg, New York, 20-22 October, 1969.
- 33. Second ESR Conference, Athens, Georgia, December, 1970.
- 34. T. F. Yen, "Electron Spin Resonance of Metal Complexes," Plenum Press, .
  New York, 1969.
- 35. "Magnetic Resonance" (Proceedings of the International Symposium on Electron and Nuclear Magnetic Resonance, Melbourne, Australia,

- 11-15 August, 1969), edited by C. K. Coogan, N. S. Ham, S. N. Stuart, J. R. Pilbrow and G. V. H. Wilson, Plenum Press, New York, 1970.
- 36. "Advances in Magnetic Resonance," edited by J. Waugh, Academic Press, New York 1, (1965), 2, (1966), 3, (1968), and 4, (1970).
- 37. J. A. Wunderlich and D. P. Mellor, Acta Cryst. <u>7</u>, 130 (1954); <u>ibid</u>. <u>8</u>, 57 (1955).
- 38. A. Werner, A. Anorg. Allgem. Chem. 3, 267 (1893).
- 39. B. N. Dickinson, Z. Krist, 88, 281 (1934).
- 40. G. B. Bokii, Proc. Inst. Cryst. Acad. Sci. USSR 10, 214 (1954).
- 41. I. I. Tscherniaev, Ann. Inst. Platine 4, 243 (1926).
- 42. A. J. McCaffery, P. N. Schatz and P. J. Stephens, J. Am. Chem. Soc. 90, 5730 (1968), and references therin.
- 43. H. Basch and H. B. Gray, Inorg. Chem. <u>6</u>, 365 (1967); F. A. Cotton and C. B. Harris, <u>1bid</u>. <u>6</u>, 369 (1967), and references therein.
- 44. S. B. Piepho, P. N. Schatz, and A. J. McCaffery, J. Am. Chem. Soc. 91, 5994 (1969).
- 45. S. Geschwind and J. P. Remeika, J. Appl, Phys. Suppl. 33, 370 (1962).
- 46. R. Lacrox, V. Hochli, and K. A. Muller, Helv. Phys. Acta. <u>37</u>, 627 (1964).
- 47. J. A. Hodges, R. A. Serway and S. A. Marshall, Phys. Rev. <u>151</u>, 196 (1966).
- 48. E. Simanek, Z. Sroubek, K. Zdansky, J. Kaczer and L. Novak, Phys. Status Solidi 14, 333 (1966).
- 49. H. H. Woodbury and G. W. Ludwig, Phys, Rev. <u>126</u>, 466 (1961).
- 50. S. C. Jain, S. K. Argarwal, G. D. Sootha and R. Chander, J. Phys. <u>C3</u>, 1343 (1970).
- 51. A. Davison, N. Edelstein, R. H. Holm and A. H. Maki, J. Am. Chem. Soc. <u>85</u>, 2029 (1963); Inorg. Chem. <u>2</u>, 1227 (1963); <u>ibid</u>. <u>3</u>, 814 (1964).
- 52. F. Lalor, M. F. Hawthorne, A. H. Maki, K. Darlington, A. Davison, H. B. Gray, Z. Dori, and E. I. Steifel, J. Am. Chem. Soc. 89, 2278 (1967), and references therein.
- 53. R. D. Schmitt and A. H. Maki, J. Am. Chem. Soc. <u>90</u>, 2288 (1968).

- 54. E. J. Steifel, J. H. Waters, E. Billig and H. G. Gray, J. Am. Chem. Soc. 87, 3016 (1965); S. I. Shupak, E. Billig, R. F. H. Clark, R. Williams, and H. B. Gray, ibid. 86, 4595 (1964).
- 55. P. Auzins, J. W. Orton and J. E. Wertz, "Paramagnetic Resonance," edited by W. Low, Academic Press, New York, Vol. 1, 1963.
- 56. S. Fujiwara and M. Nakamura, J. Chem. Phys. 52, 6299 (1970).
- 57. J. W. Moskowitz, C. Hollister, C. J. Hornback, and H. Basch, J. Chem. Phys. 53, 2570 (1970), and references therein.
- 58. B. Kleinman and M. Karplus, Phys. Rev. B 3, 24 (1971), and references therein.
- 59. T. F. Soules, J. W. Richardson and D. M. Vaught, Phys. Rev. B 3, 2186 (1971), and references therein.
- 60. a) R. G. Shulman and S. Sugano, Phys. Rev. <u>130</u>, 506 (1963); (b) K. Knox, R. G. Shulman and S. Sugano, Pjys. Rev. 130, 512 (1963).
- 61. R. G. Shulman and K. Knox, Phys. Rev. Letters 4, 603 (1960).
- 62. M. Tinkham, Proc. Roy. Soc. (London) A236, 535 and 549 (1956).
- 63. A. Abragam and H. M. L. Pryce, Proc. Roy. Soc (London) <u>A205</u>, 135 (1951).
- 64. W. Low, "Solid State Physics," Suppl. 2, Academic Press, New York, 1960.
- 65. J. S. Griffith, "Theory of Transition Metal Ions," Cambridge University Press, Cambridge, 1961.
- 66. A. H. Maki, N. Edelstein, A. Davison and R. H. Holm, J. Am. Chem. Soc. <u>86</u>, 4580 (1964).
- 67. H. Eyring, J. Walter and G. E. Kimball, "Quantum Chemistry," John Wiley and Sons, New York, 1944.
- 68. H. S. Jarrett, "Solid State Physics," 14, Academic Press, New York, 1963.
- 69. a) C. J. Ballhausen and H. B. Gray, "Molecular Orbital Theory," W. A. Benjamin, Inc., New York, 1965; (b) C. J. Ballhausen, "Introduction to Ligand Field Theory," McGraw-Hill, New York, 1962.
- 70. A. A. Misetich and T. Buch, J. Chem. Phys. 41, 2524 (1964).
- 71. P. T. Manoharan and M. T. Rogers, J. Chem. Phys. 49, 5510 (1968).
- 72. J. Owen, Proc. Roy. Soc. (London) <u>A227</u>, 183 (1955).

- 73. T. Murao, Prog. Theoret. Phys. (Kyoto) 21, 657 (1959).
- 74. B. R. McGarvey, "ESR of Metal Chelates," edited by T. F. Yen, Plenum Press, New York, 1969.
- 75. Y. Hazony. Phys. Rev. B 3, 711 (1971).
- 76. C. E. Moore, Natl. Bur. Std. (U.S.), Circ. 467, Vol. 3 (1958).
- 77. B. Bleaney, Phil. Mag. (7) 42, 441 (1951).
- 78. H. Goldstein, "Classical Mechanics," Addison-Wesley, Cambridge, Mass., 1950.
- 79. J. R. Pilbrow, Mol. Phys. <u>16</u>, 307 (1968).
- 80. J. R. Reitz and F. J. Milford, "Foundations of Electromagnetic Theory," Addison-Wesley, Reading, Mass., 1960.
- 81. C. P. Slichter, "Principles of Magnetic Resonance," Harper and Row, Publishers, New York, 1963.
- 82. M. H. L. Pryce, Proc. Phys. Soc. A, 63, 25 (1950).
- 83. H. H. Tippins, Phys. Rev. 160, 343 (1967).
- 84. P. W. Atkins and A. M. Jamieson, Mol. Phys. 14, 425 (1967).
- 85. J. Owen and J. H. M. Thornley, Rept. Progr. Phys. <u>29</u> (II) (1966).
- 86. B. Bleaney, "Hyperfine Interactions," edited by A. J. Freeman and R. B. Frankel, Academic Press, New York, 1967.
- 87. A. J. Freeman and R. E. Watson, "Magnetism," Vol. IIA, edited by G. T. Rado and H. Suhl, Academic Press, New York, 1965.
- 88. R. E. Watson and A. J. Freeman, "Hyperfine Interactions," edited by A. J. Freeman and R. B. Frankel, Academic Press, New York, 1967.
- 89. B. R. McGarvey, J. Phys. Chem. 71, 51 (1967).
- 90. H. A. Kuska and M. T. Rogers, J. Chem. Phys. 43, 1744 (1965).
- 91. H. A. Kuska, M. T. Rogers and R. E. Drullinger, J. Phys. Chem. <u>71</u>, 109 (1967).
- 92. J. A. McMillan, J. Chem. Phys. 55, 33 (1971).
- 93. J. A. Weil and J. H. Anderson, J. Chem. Phys. 28, 864 (1958).
- 94. D. S. Schonland, Proc. Phys. Soc. (London) 73, 788 (1959).

- 95. J. J. Fortman, Ph. D. Thesis, University of Notre Dame, Notre Dame Indiana, 1965.
- 96. A. J. Freeman, private communication; see also A. J. Freeman, J. V. Mallow and P. S. Bagus, J. Appl. Phys. 41, 1321 (1970).
- 97. R. E. Watson and A. J. Freeman, Phys. Rev. 134, A1526 (1964).
- 98. J. Hubbard, D. E. Rimmer and F. R. A. Hopgood, Proc. Phys. Soc. (London) 88, 13 (1966).
- 99. P. W. Atkins and M. C. R. Symons, "The Structure of Inorganic Radicals," Elsevier Publishing Co., New York, 1967.
- 100. A. J. Freeman and R. E. Watson, Phys. Rev. Letters 6, 343 (1961).
- 101. S. Sugano and Y. Tanabe, J. Phys. Soc. Japan 20, 1155 (1965).
- 102. W. Marshall, "Paramagnetic Resonance," edited by W. Low, Vol. 1, Academic Press, New York, 1963.
- 103. L. Buss and L. Bogart, Rev. Sci. Instr. 31, 204 (1960).
- 104 D. C. Giedt and C. J. Nyman, Inorganic Synthesis, 8, 239 (1966).
- 105. G. B. Kauffman and D. O. Cowan, Inorganic Synthesis, 7, 240 (1963).
- 106. a) N. C. Stephenson, Acta Cryst. <u>17</u>, 587 (1964); (b) C. M. Harris, S. E. Livingstone and N. C. Stephenson, J. Chem. Soc. 3697 (1958).
- 107. a) R. J. Dickenson, J. Am. Chem. Soc. <u>44</u>, 2404 (1922); (b) W. Theilacker, Z. Anorg. Allgem Chem. 234, 161 (1937).
- 108. L. Kispert, Ph. D. Thesis, Michigan State University, East Lansing, Michigan, 1966.
- R. W. Fessenden, J. Chem. Phys. <u>37</u>, 747 (1962); D. Schoemaker, Phys. Rev. <u>174</u>, 1060 (1968).
- 110. H. Kon and N. E. Sharpless, J. Phys. Chem. 70, 105 (1966).
- 111. J. R. Byberg, S. J. K. Jensen and L. T. Muus, J. Chem. Phys. 46, 131 (1967).
- 112. B. N. Figgis, "Introduction to Ligand Fields," Interscience Publishers, New York, 1966.
- 113. C. K. Jorgensen, "Absorption Spectra and Chemical Bonding in Complexes," Pergamon Press, New York, 1962.
- 114. J. M. Assour, J. Chem. Phys. 43, 2477 (1965).
- 115. A. M. Clogston, V. Jaccarino and Y. Yafet, Phys. Rev. <u>134A</u>, 650 (1964).

- 116. K. Krogmann and D. Stephan, Z. Anorg. Allgem. Chem. <u>262</u>, 301 (1968).
- 117. M. Atoji, J. W. Richardson and R. W. Rundle, J. Am. Chem. Soc. <u>79</u>, 3017 (1957).
- 118. S. Yamada, Bull. Chem. Soc. Japan 24, 125 (1951).
- 119. R. E. Rundle, J. Phys. Chem. 61, 45 (1957).
- 120. J. R. Miller, J. Chem. Soc. 713 (1965).
- C. G. Pitt, L. K. Monteith, L. F. Ballard, J. P. Collman, J. C. Morrow, W. R. Roper and D. Ulku, J. Am. Chem. Soc. <u>88</u>, 4286 (1966).
- 122. M. J. Minot and J. H. Perlstein, Phys. Rev. Letters <u>26</u>, 371 (1971).
- 123. N. G. Connelly and L. F. Dahl, J. Am. Chem. Soc. 92, 7472 (1970).
- 124. C. Froese, "Hartree-Fock Parameters for the Atoms Helium to Radon," Department of Mathematics, University of British Columbia, Vancouver, B. C., 1966.
- 125. J. M. Assour, J. Am. Chem. Soc. 87, 4701 (1965).
- 126. J. D. W. van Voorst and P. Hemmerich, J. Chem. Phys. <u>45</u>, 3914 (1966).
- 127. R. P. A. Muniz, N. V. Vugman and J. Danon, J. Chem. Phys. <u>54</u>, 1284 (1971).
- 128. P. Day, A. F. Orchard, A. J. Thomson and R. J. P. Williams, J. Chem. Phys. 42, 1973 (1965).
- 129. J. A. Seitchik, A. C. Grossard and V. Jaccarino, Phys. Rev. <u>136A</u>, 1119 (1964).
- 130. D. Kivelson and S. K. Lee, J. Chem. Phys. 41, 1896 (1964).
- 131. S. Fujiwara and M. Nakamura, J. Chem. Phys. 54, 3378 (1971).
- 132. P. T. Manoharan and M. T. Rogers, "ESR of Metal Chelates," edited by T. F. Yen, Plenum Press, New York, 1969.

MICHIGAN STATE UNIV. LIBRARIES
31293010934606